MAP-RIVIERA PROJECT

http://www.iac.ethz.ch/en/research/map_riviera/index.html

META DATA REPORT

Meta Data Report

1 Introduction

The MAP-Riviera project has been realised in connection with the Mesoscale Alpine Programme (MAP), a major research initiative to investigate atmospheric and hydrological processes over the alpine ridge. According to the MAP science plan (http://www.map.ethz.ch/splan/spindex.htm), one of the objectives of this programme is the investigation of boundary layer (BL) processes in complex topography. The specific objectives with respect to boundary layer processes of MAP may be summarised as follows:

- Description, characteristics and parameterisation of effective vertical turbulent fluxes of momentum, heat, moisture, and other atmospheric constituents over complex terrain. The knowledge of physically consistent area-averaged turbulent fluxes is mandatory for numerical models over wide range of scales.
- Development of mixing height (including its definition) in the alpine region as well as upstream and downstream of the Alps. Determination of the vertical extent of the BL and the spatial/temporal distribution of turbulence statistics within the BL.
- Interaction between local winds and (valley) BLs/ Erosion of (valley) BLs by Foehn. Ambient winds have an effect on the development of thermally forced local wind systems. Their influence is certainly instrumental and depends on the characteristics (stability, forcing) of both systems.
- Exchange of air masses and atmospheric constituents between the BL and the lower free troposphere. The preceding points highlight possible modifications of the BL over complex terrain as compared to flat, homogeneous surfaces. Consequently, also the exchange processes at the BL's top are likely to be enhanced (or at least different) with respect to current understanding.
- The impact of boundary layer, through momentum, moisture and heat exchanges, on the formation of heavy orographic precipitation, distribution of precipitation particles, upstream flow blocking, lower tropospheric wave breaking, and PV banners.

For the investigation of some of these open questions, a collaboration was established between the Swiss Federal Institute of Technology (ETH – co-ordination), the University of Basle (MCR-LAB), the University of British Columbia (UBC) and European Joint Research Centre (JRC) at Ispra, Italy. Further collaboration in numerical modelling is foreseen with the University Joseph Fourier (UJF), Grenoble.

It was decided to concentrate the joint efforts to one valley in order to obtain a maximum of spatial coverage from the available instrumentation. This means, however, that characteristics like valley size, orientation (with respect to synoptic wind direction), aspect ratio etc. cannot be investigated in depth from the present observations.

The valley was selected according to following criteria:

- *Valley structure:* as unobstructed as possible, i.e. more or less symmetric (approximately equal height and slopes on both sides, few side valleys), more or less straight.
- *Infrastructure*: availability of suitable experimental sites on the slope(s) and also possibilities to reach them.
- *Valley size*: a small valley would be desirable with respect to optimal spatial resolution in the measurements. However, it is felt that a valley of the size of today's operational model resolution ('Schweiz Modell': 14 km) is preferable: for a global model it is clearly subgrid scale, and still so for today's operational tools. On the other hand, non-hydrostatic models at 1-3 km horizontal resolution (what may soon become operational) can resolve, at least broadly, such a valley, similar to a LES model which is intended to be used in a detailed modelling study within the present project. Note that a small valley would be subgrid scale for all but LES models, thus offering a narrower range of application.

According to these criteria the Riviera valley in Southern Switzerland was selected as a test site (Section 2).

A number of **permanent sites** were selected, where towers were instrumented with typically several levels of turbulence probes up to 30 m from the ground (sonic anemometers, fast response hygrometers), profiles of mean meteorological variables, the radiation balance and precipitation probes (Section 2.1). In addition, some of these sites were equipped with hydrological instrumentation (soil moisture, temperature profiles into the ground). The layout of these sites was chosen in such a way that a cross–section through the valley resulted in order to investigate the near-surface exchange processes. These instruments were operated continuously from roughly the beginning of August to the beginning of October 1999.

Additional ('special') **instrumentation** with a lager need for maintenance (a radio sounding system, two scintillometers, a tethered balloon system, two SODARs and a temperature profiler, see Section 2.2) was deployed at specific sites and operated only during periods of intensive operation (Section 6). These periods are referred to as '**Flight days**' in the following. During these days, also a research aircraft (the light research aircraft DIMONA of MetAir, Section 3) was available, with which the turbulence (and, of course, mean meteorological) characteristics within the bulk of the valley atmosphere (and above) were investigated. A total of eight such Flight days could be realised within two preselected periods (August 15 to 31 and September, 20 to October, 8 1999, respectively). These two periods will be referred to as R-IOP's (Riviera Intensive Observation Periods) and do not necessarily correspond to the so-called IOPs of MAP.

Finally, two **tracer release experiments** could be performed, one during one of the above mentioned Flight days and another one after the last Flight day (Sections 4 and 6.9, respectively).

2 Location, sites and instrumentation

The test site is in the Lago Maggiore target area of MAP (Ref to implementation plan). The chosen **Riviera valley** constitutes the part of the Ticino valley (Fig. 2.1) between the towns of Biasca and Bellinzona. This section has an overall length of about 20km. The Riviera valley is an approximately straight, u-shaped valley, ranging from about 250m above sea level (valley ground) up to about 2500 m (a.s.l.) on both sides (Fig. 2.2). The ‘width’ of the valley is about 1.5 km at the ground and the slopes (at the height of the instrumented cross-section, i.e. near the village of Claro – Fig. 2.3) are about 30° (eastern slope) and 35° (western slope). Within the Riviera valley, two major tributary valleys (one on each side) are present.

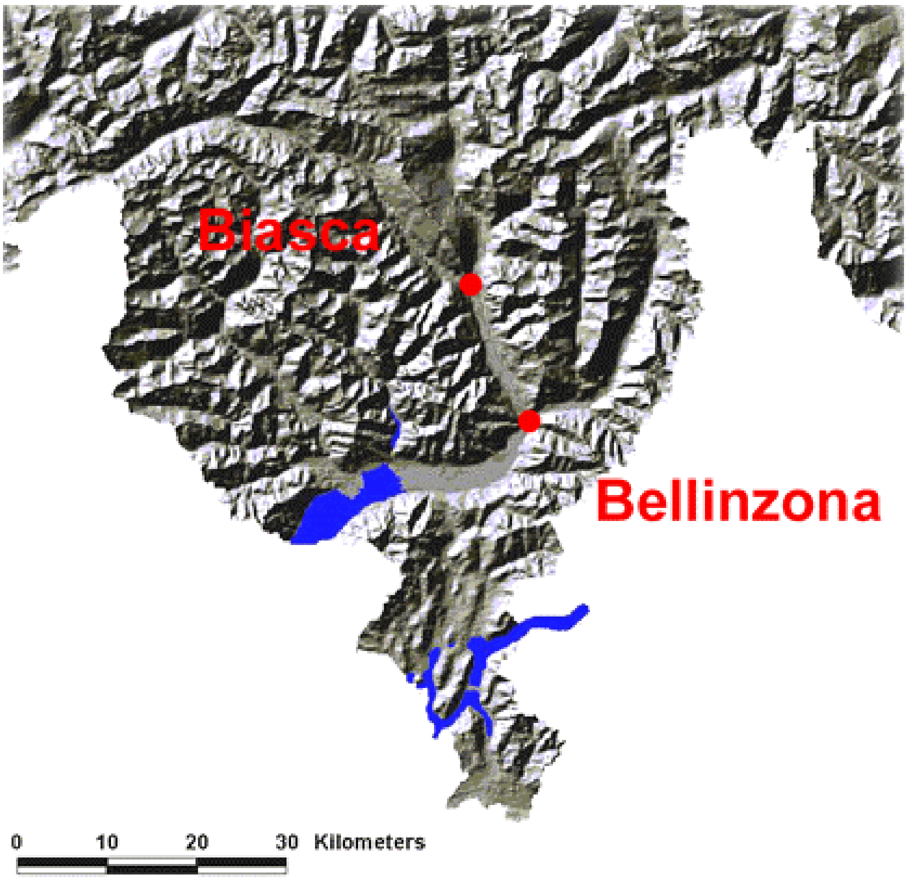

Fig. 2.1 Topography of southern Switzerland showing the Riviera valley between the towns of Biasca and Bellinzona (© Bundesamt fuer Landestopographie 2000 (JD002102).

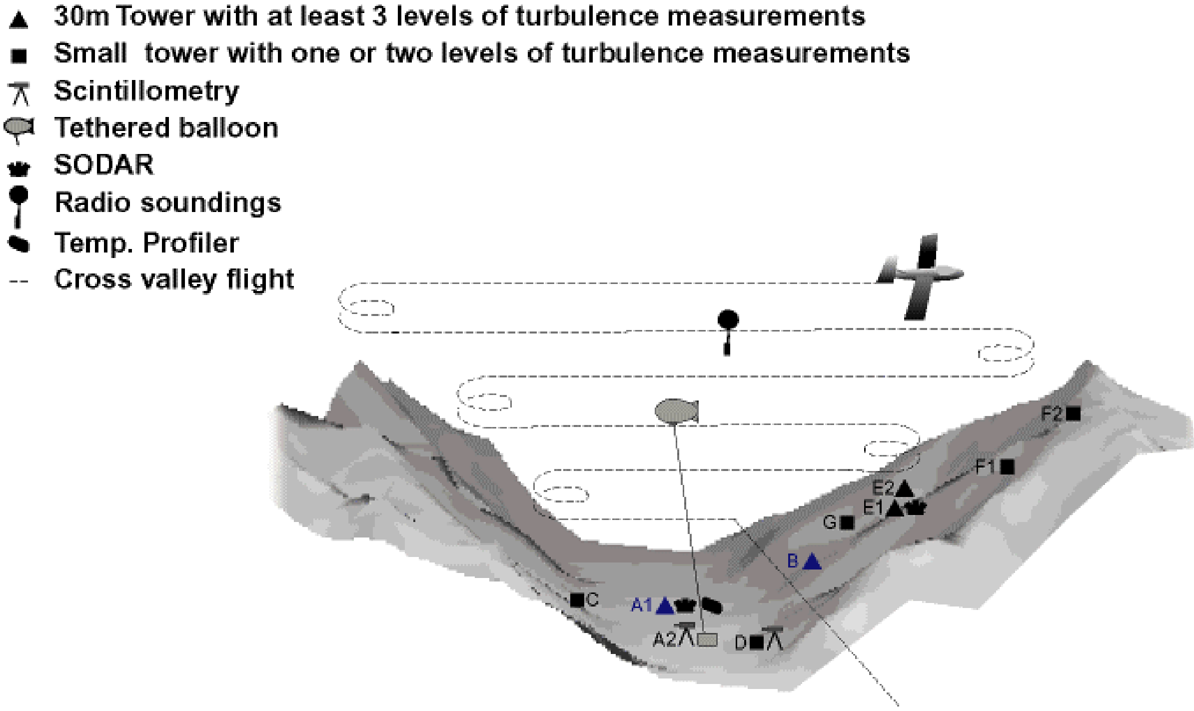

Fig. 2.2 Cross section through the Riviera valley at the height of Claro (see Fig. 2.3). Symbols refer to the various observational systems as indicated in the inlet.

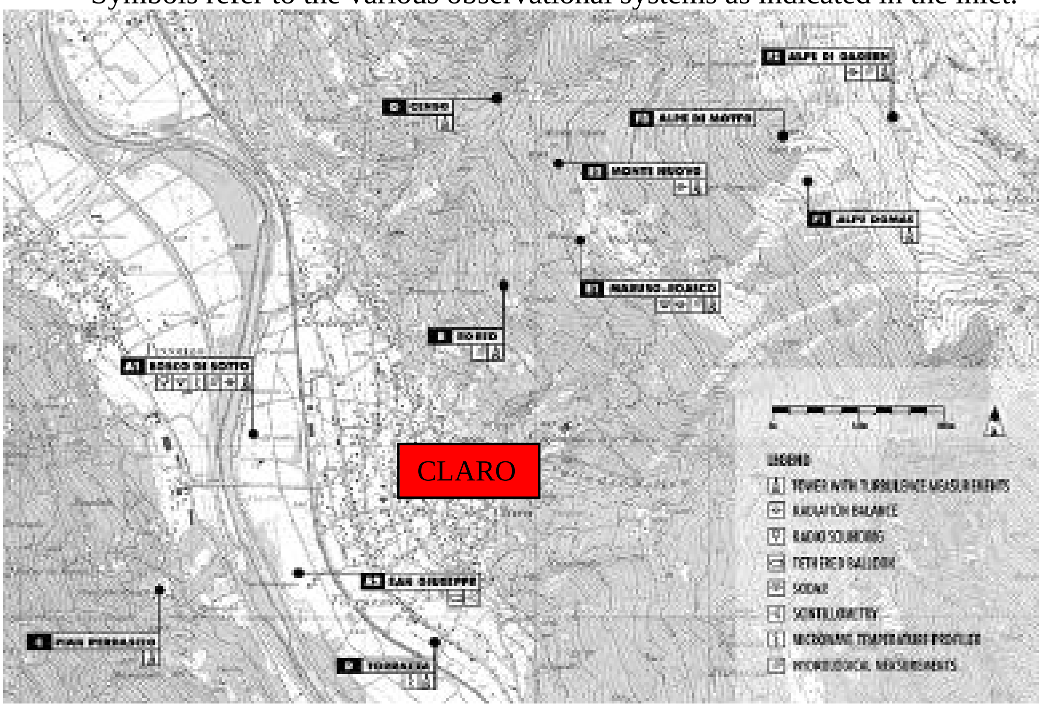

Fig. 2.3 Topographical map of the various sites together with their names and activities in the Riviera valley. [© Bundesamt fuer Landestopographie 2000 (JD002102)].

The valley ground consists of agricultural land (grass, corn, hedges and groups of trees) and a number of villages and isolated farm houses. A highway, the railroad and the river Ticino all run more or less straight along the valley. The slopes are mainly covered with forest (chestnut, some regions of birch) with an average height of approximately 10–15 meters. Above roughly 1000m (a.s.l.) meadows are intersected with rocks and areas of rubble.

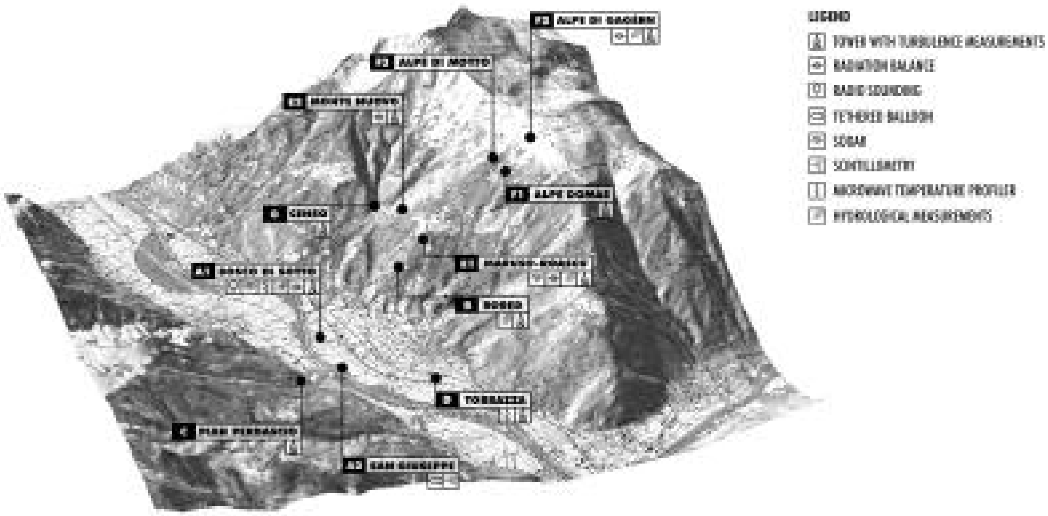

Fig. 2.4 Names and positions of the various sites within the Riviera valley. The inlet legend indicates the activities at the respective sites. [© Bundesamt fuer Landestopographie 2000 (JD002102)]

3.1 Sites A-D: run by ETH Zürich

A series of micrometeorological measurements were carried out at four sites located on the bottom and lower part of the valley cross-section (see Tab. 3.1-I and Fig. 2-X) during August to October 1999. An overview of the availability of the different data can be seen on Fig.3.1-1. The different locations, the instrumentation and the measured variables are presented in detail for each site.

Tab. 3.1-I: Coordinates and heights of sites A-D.

Site	Name	Height a.s.l. [m]	Latitude	Longitude
A1	Bosco di Sotto	250	$46^0$15’17” N	$09^0$00’42” E
A2	San Giuseppe	250	$46^0$14’52” N	$09^0$00’52” E
B	Rored	760	$46^0$15’47” N	$09^0$01’51” E
C	Pian Perdascio	340	46^0 14’17” N	$09^0$00’17” E
D	Torrazza	256	46^0 14’39” N	$09^0$01’33” E

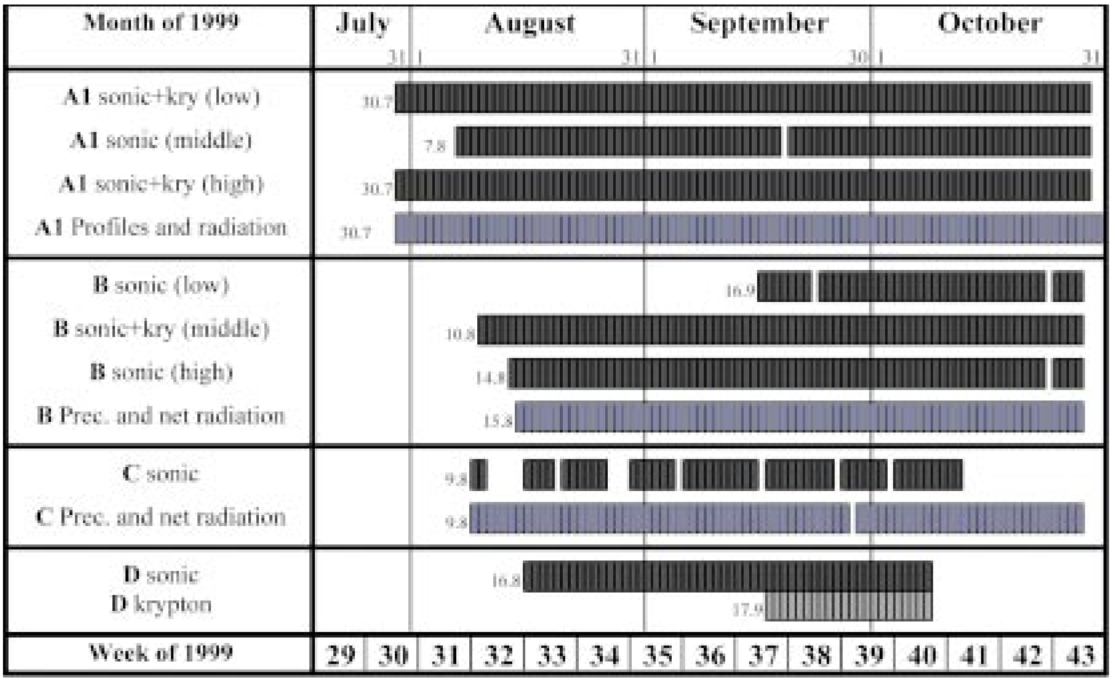

Fig. 3.1-1: Data availability at sites A- D.

3.1.1 Site A1: Bosco di Sotto

Main ETH site located at the center of the valley, east of the town of Claro. Consists mainly of a guyed lattice tower with an height of 28m (Fig. 3.1-2). The tower was instrumented with sonic anemometers at 3 levels, combined with krypton fast-response hygrometers at the upper and lower level (Table 3.1-II). Profile measurements of wind speed, aspirated temperature and relative humidity were taken at six levels. Two-meter booms were used to support the instruments. For the sonic measurements screening by the mast body occurs when mean flow direction is 280^0-290^0. Wind direction, precipitation, net radiation, and global radiation were also measured. Hydrological observations were performed around the base of the tower, for a detailed description see section 3.3.

Fig.3.1-2: View of the tower at Bosco di Sotto (A1).

The tower is located at the northern end of the town‘s soccer field, which lies in a flat rural area called Bosco and Campagna nuova further south (Fig. 3.1-3). This area borders

eastward on the railway and westward on the Ticino river. The primary ground cover is maize fields and meadows (each approximately 40% of the land use). The remaining 20% is composed of groups of trees and in a smaller amount roads and farms. Both maize and grass fields have a mean extension of 100m in east-west direction and about 200-300m in north-south direction, separated by trees or small roads). Maize plants had an height of 2.60-2.90m, and started to dry out at the beginning of September. They were harvested at the end of October. The maize field close to the tower was harvested the 27th of October. Grass was harvested several times during the operational phase when it reached about 0.4m.
Being placed at the northeast corner of the soccer field the close fetch going from west to south is given by the grass of the soccer field. For the remaining sector (south-east-north-west) the tower is surrounded by a maize field. The maize fields extend at least 500m to the north and reaches the railway to the east (200m). Further north is a small forest (10-15m high trees). The town of Claro lies east of this site, at the foot of the west facing mountain ridge. The town itself begins east of the railway and consists mostly of a sequence of small streets and two- to three-story houses.
The Ticino river lies 50m westward of the site. It is surrounded by trees on both sides. At this location the river flows roughly from north to south. Further west is the highway which runs parallel to the river. After a meadow and some industrial buildings begins the forest that covers most of the western mountain ridge.
South of the tower, at the end of the soccer field (150m), the fetch crosses a small road followed by a farm. Going further south, after a 200m long grass field, the bottom of the valley is crossed by an elevated road. The road lies 15m above the ground level. The Campagna nuova area southern of the farm consist of mostly meadows with only a few maize fields for about 800m. Further south were mostly maize fields.

Tab.3.1-II: Measurements and instrumentation at Bosco di Sotto (A1).

Variable	Nominal height [m]	Instrument (serial number)	Sampling [Hz]	Averaging period	Output signal	Calibration	Person responsible
u, v, w, t	3.56	Gill R2A (0068)	20.8	raw data, calibrated	[m s^{-1}], [K]	manufac-turer and relative	Andretta
	15.58	Gill R2A (0069)	20.8	raw data, calibrated	[m s^{-1}], [K]	manufac-turer and relative	Andretta
	27.63	Gill R2A (0047)	20.8	raw data, calibrated	[m s^{-1}], [K]	manufac-turer and relative	Andretta
Water vapor density fluct.	3.56	Krypton KH2O (1299)	20.8	raw data	[g m^{-3}]	manufac-turer and relative	Andretta

Variable	Nominal height [m]	Instrument (serial number)	Sampling [Hz]	Averaging period	Output signal	Calibration	Person responsible
	27.63	Krypton KH2O (1299)	20.8	raw data	[g m^{-3}]	manufac-turer and relative	Andretta
Temp./ Humid-ity vent.	1.77 / 2.82 / 5.85 / 11.91 / 18.99 / 27.39	VAISALA AMP45DSP (1-6)	0.07	30 [min]	[K], [%]	relative	Schroff
Wind Speed	1.77 / 2.82 / 5.85 / 11.91 / 18.99 / 27.67	Aanderaa 2740 (1-6)	0.07	30 [min]	[m s^{-1}]	manufac-turer	Schroff
Wind Direc-tion	5.85	Aanderaa 2750 (1474)	0.07	30 [min]	[deg] N=N+70 0	manufac-turer.	Schroff
Pressure	0.2		0.07	30 [min]	[hPa]	manufac-turer	Schroff
Precipi-tation	2.28	Tognini Raingauge (1005)	0.07	30 [min], 2 [min]	[mm]	manufac-turer.	Schroff
Global sw radi-ation	1.54	Davos PD1 (TS 7101)	0.07	30 [min], 2 [min]	[W m^{-2}]	manufac-turer.	Schroff
Reflected sw rad.	1.50	Davos PD1 (TS 7105)	0.07	30 [min], 2 [min]	[W m^{-2}]	manufac-turer.	Schroff
lw in	1.52	Eppley PIR (29441F3)	0.07	30 [min], 2 [min]	[W m^{-2}]	manufac-turer.	Schroff
lw out	1.50	Eppley PIR (32555F3)	0.07	30 [min], 2 [min]	[W m^{-2}]	manufac-turer.	Schroff
Net radia-tion	1.59]	Swisstech S-1 (8170)	0.07	30 [min], 2 [min]	[W m^{-2}]	manufac-turer.	Schroff
PC's		Digital 486					Andretta
Logger		Campbell 21X					Schroff
		Campbell Multiplex			analog + digital		Schroff

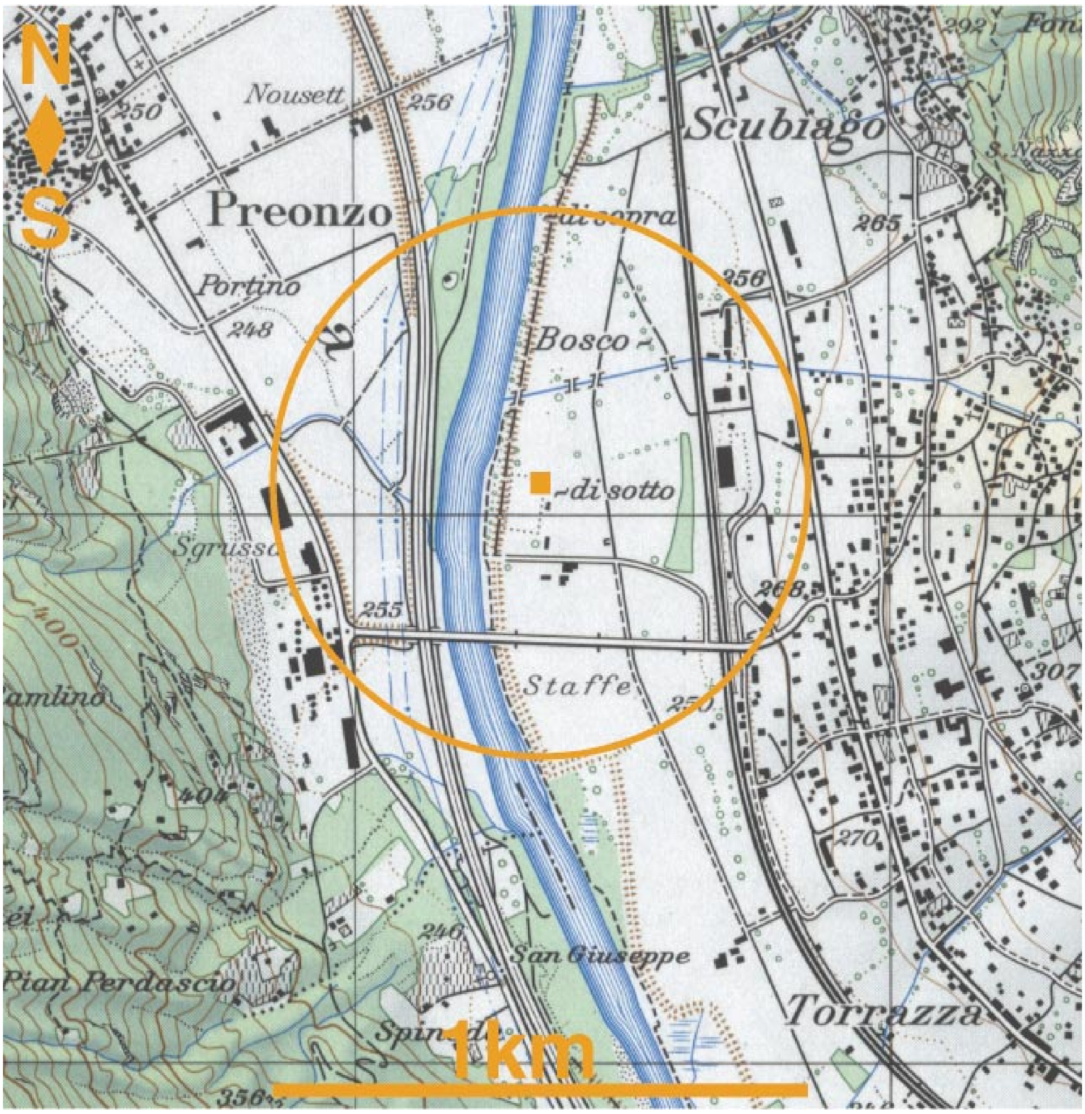

Fig.3.1-3: 1km area around the station Bosco di Sotto (A1). © Bundesamt fuer Landestopographie 2000 (JD002102)

3.1.2 Site A2: San Giuseppe

No permanent observations. For description see 4.1.

3.1.3 Site B: Rored

This site was located on the east facing slope at an height of 760m a.s.l. (Fig. 3.1-4). The terrain has an eastward exposition and an inclination of 25^0-35^0. The 30m tower is a guyed telescopic mast. Eddy-covariance measurements were made at 3 levels with sonic anemometers combined with krypton fast-response hygrometers at the middle level. Net radiation and precipitation at 1 level (Tab 3.1-III). The surrounding forest is dominated by chestnut, and beech trees which offer an homogeneous vegetated fetch in all directions. The trees have a mean height of 15m.

Tab.3.1-III: Micrometeorological measurements and instrumentation at Rored (B).

Variable	Nominal height [m]	Instrument (serial number)	Sampling interval [Hz]	Averaging period	Output signal	Calibration	Person responsible
u, v, w, speed of sound	15.34	Gill R2 (0035)	20.8	raw data, calibrated	[m s^{-1}], [K]	manufac-turer and relative	Andretta
u, v, w, speed of sound	23.78	Gill R2 (0030)	20.8	raw data, calibrated	[m s^{-1}], [K]	manufac-turer and relative	Andretta
u, v, w, speed of sound	29.75	Gill R2 (0036)	20.8	raw data, calibrated	[m s^{-1}], [K]	manufac-turer and relative	Andretta
Water vapor density fluct.	23.78	Krypton KH2O (1370)	20.8]	raw data, calibrated	[g m^{-3}]	manufac-turer and relative	Andretta
Temp./ Humid-ity vent.	23.34	VAISALA AMP45DSP (410011)	0.05	30 [min]	[K], [%]	manufac-turer	Schroff
Precipita-tion	11.80	Raingauge Tognini ()	0.05	30 [min]	[mm]	manufac-turer	Schroff
Net radi-ation	11.50	Swisstech S-1 (8184)	0.05	30 [min], 2 [min]	[W m^{-2}]	manufac-turer	Schroff
PC's		Digital 486					Andretta
Logger		Campbell 21X					Schroff

3.1.4 Site C: Pian Perdasacio

Situated on the lower part of the eastern mountain ridge. A mast of 5m height was mounted in the center of a small and steep vineyard surrounded by forest (Fig. 3.1-5). Eddy-covariance measurements were taken at the top of the mast with a sonic anemometer (no screening by the mast body). Net radiation and precipitation were measured at 1 level (Tab. 3.1-IV).

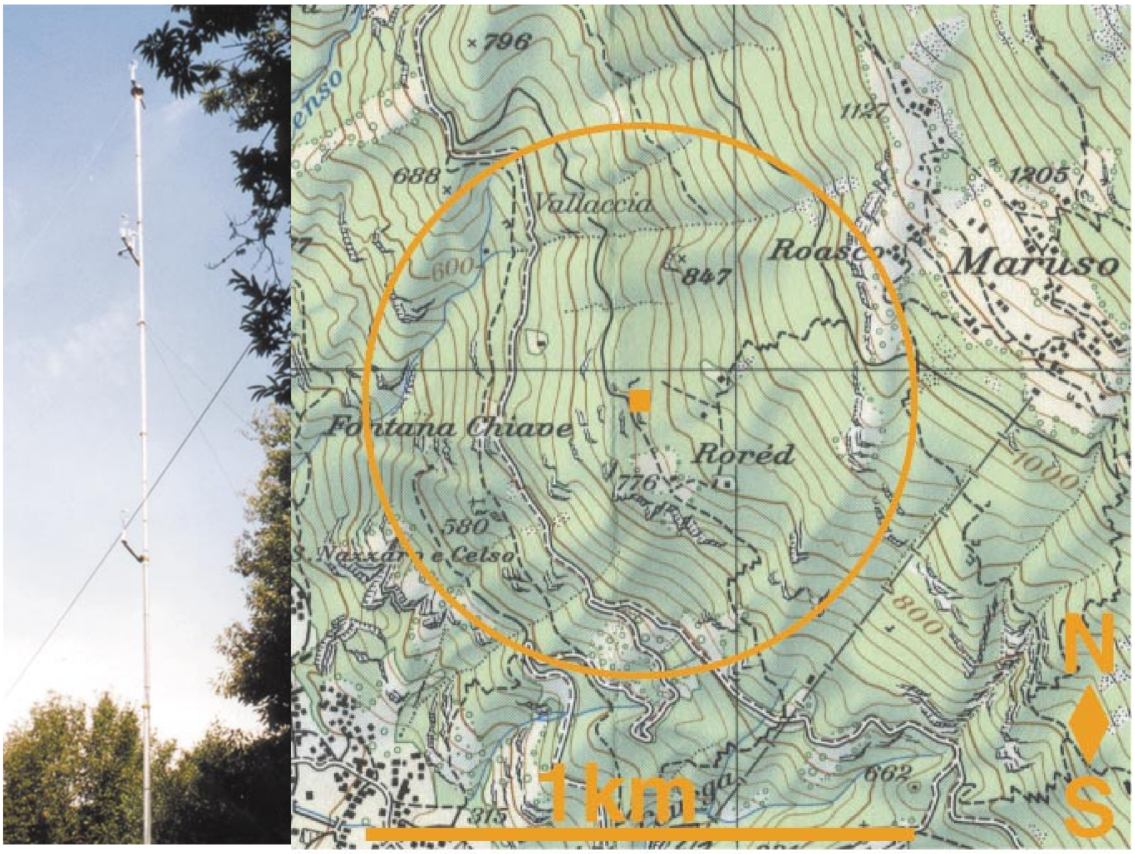

Fig.3.1-4: View 30m Telescopic mast and topography at Rored (B). © Bundesamt fuer Landestopographie 2000 (JD002102)

Fig.3.1-5: Mast view towards the east at the Pian Perdascio site (C).

Tab.3.1-IV: Measured variables and instrumentation at Pian Perdascio (C).

Variable	Nominal height [m]	Instrument (serial number)	Sampling [Hz]	Averaging period	Output signal	Calibration	Person responsible
u, v, w, t	6.33	Gill R2 (0054)	20.8	raw data, calibrated	[m s^{-1}], [K]	manufacturer and relative	Andretta
Precipitation	3.43	Raingauge Tognini (1002)	0.07	30 [min]	[mm]	manufacturer	Schroff
Net radiation	3.13	Swisstech S-1 (8198)	0.07	30 [min], 2 [min]	[W m^{-2}]	manufacturer	Schroff
PC		Digital 486					Andretta
Logger		Campbell 21X					Schroff, Andretta

The micrometeorological data were collected at the center of a small vineyard (Fig. 3.1-6) which offered a homogeneously vegetated fetch of 100m in the eastern and western directions and 50m in the northern and southern directions. The vine-props had a mean height of 2m and the vintage happened the 22nd of September. At the lower end of the vineyard (east) are some sparse one-story buildings surrounded by meadow. The site had a east-northeast exposition and a local inclination of 40^0 -45^0. The mean inclination of the eastern slope is 30^0-35^0. The vineyard is surrounded by forest, mainly composed of 15m high chestnut and beech trees.

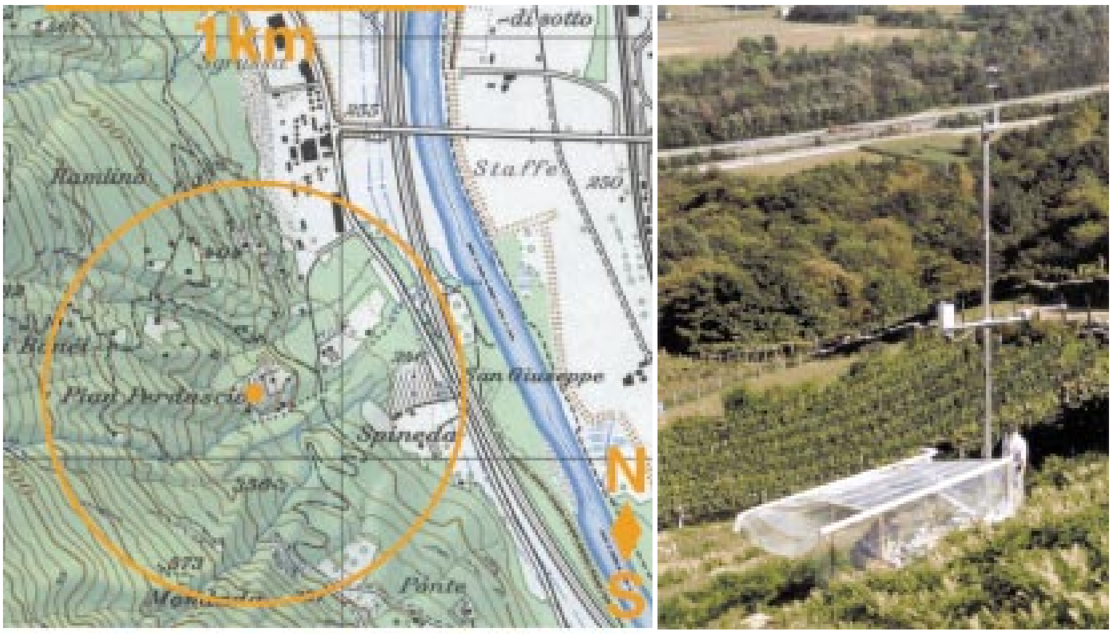

Fig.3.1-6: Topography and view of site C. © Bundesamt fuer Landestopographie 2000 (JD002102)

3.1.5 *Site D: Torrazza*

Located on a small meadow field at the southern border of the town of Claro. Eddy-covariance measurements at the top of a 5m mast (no screening by the mast body) were performed (Fig.3.1-7). The sonic anemometer measured continuously during the period 16.8.-8.10. and calibrated raw data were stored on a PC. After the 20th of September a krypton fast-response hygrometer was added to the original setup.

Fig.3.1-7: Small telescopic mast with sonic and krypton in Torrazza (D).

Tab.3.1-V: Measurements and instrumentation at Torrazza (D).

Variable	Nominal height [m]	Instrument (serial number)	Sampling [Hz]	Averaging period	Output signal	Calibration	Person responsible
u, v, w, speed of sound	5.77	Gill R3A (0103)	10	raw data, calibrated	[ms^{-1}], [speed of sound]	manufac-turer and relative	Cieslik, Andretta
Water vapor density fluct.	5.78	Krypton KH2O (0000)	10	raw data	[$g\ m^{-3}$]	manufac-turer and relative	Cieslik, Andretta
PC		Digital 486					Cieslik, Andretta

The data were collected in the center of a small meadow (Fig.3.1-8), which offered an homogeneously vegetated (grass with heights between 0.1 and 0.6m) fetch of 30-50m in all directions. Eastward the meadow sloped gently down and then raises abruptly towards the railway. On the other side of the railway the land use is the same as for the southern part of the Campagna nuova area (see 3.1.1). Isolated two-story buildings are present in the sector going from southeast to northeast. The town of Claro lies north of this site.

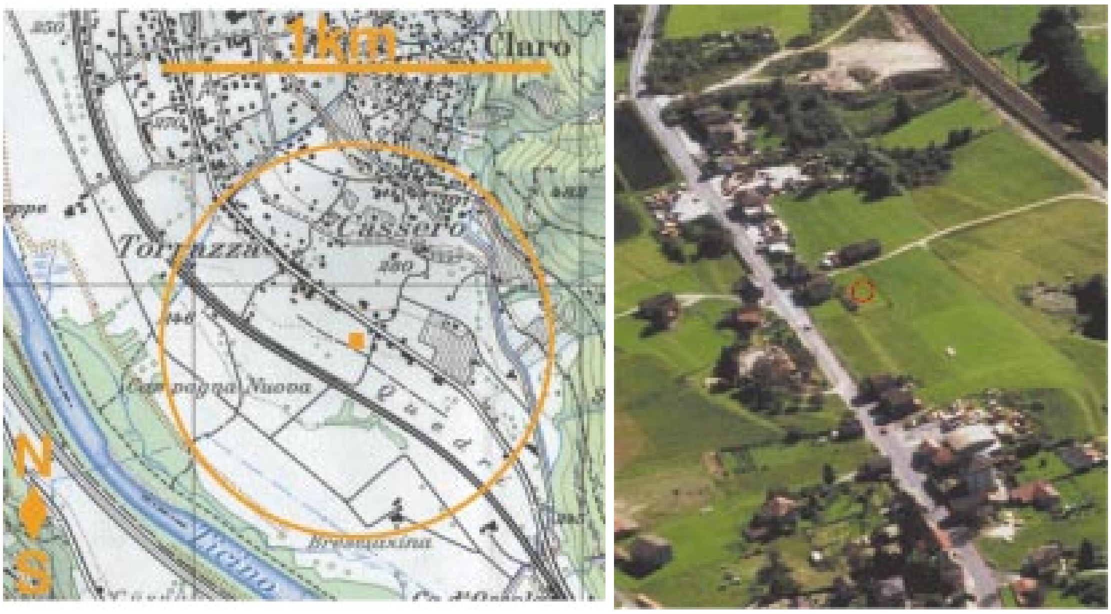

Fig.3.1-8: View of the area surrounding the Torrazza station. © Bundesamt fuer Landestopographie 2000 (JD002102)

A relative field calibration has been performed during the last two days of operation (Oct. 6 to 8 1999). For this purpose the sonic anemometer together with the krypton were installed near the lowest sonic at the site A1.

3.2 Sites E-G: (MCR-Lab, University of Basel)

Micrometeorological measurements were carried out at six sites which were located on the westward slope of the Riviera valley and formed the upper part (between 800 and 2000 m) of the valley transect (see Tab. 3.2-I and Fig. 2.3). The main measurement period was during August and September 1999. An overview on data availability for all stations is given in Fig. 3.2-1.

Tab. 3.2-I: Coordinates and heights of sites E-G (see also map in Fig. 2.3).

Site name		height a.s.l. (m)	coordinates	
Roasco	E1	1060	46°16'00"N	9°02'14"E
Monte Nuovo	E2	1030	46°16'14"N	9°02'11"E
Alpe Domàs	F1	1750	46°16'12"N	9°03'19"E
Alpe di Gagèrn	F2	2110	46°16'22"N	9°03'39"E
Alpe di Motto	F3	1860	46°16'19"N	9°03'11"E
Censo	G	870	46°16'27"N	9°01'54"E

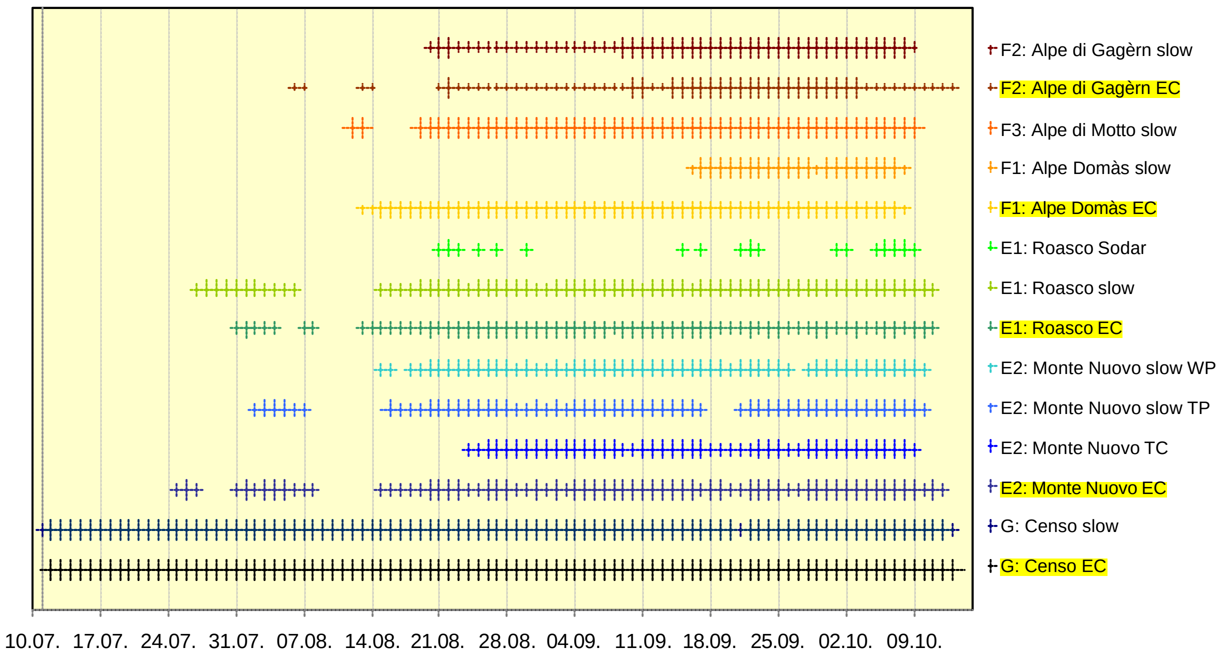

Fig. 3.2-1: Overview on data availability at stations E to G. Large markers: whole day available. Small markers: Only part of the day available. EC = eddy covariance, "slow" means measurement of temperature, humidity, wind speed and components of net radiation. Different set-ups at different stations. WP = wind profile, TP = temperature profile, TC = thermocouple profile. Stations are grouped according to height.

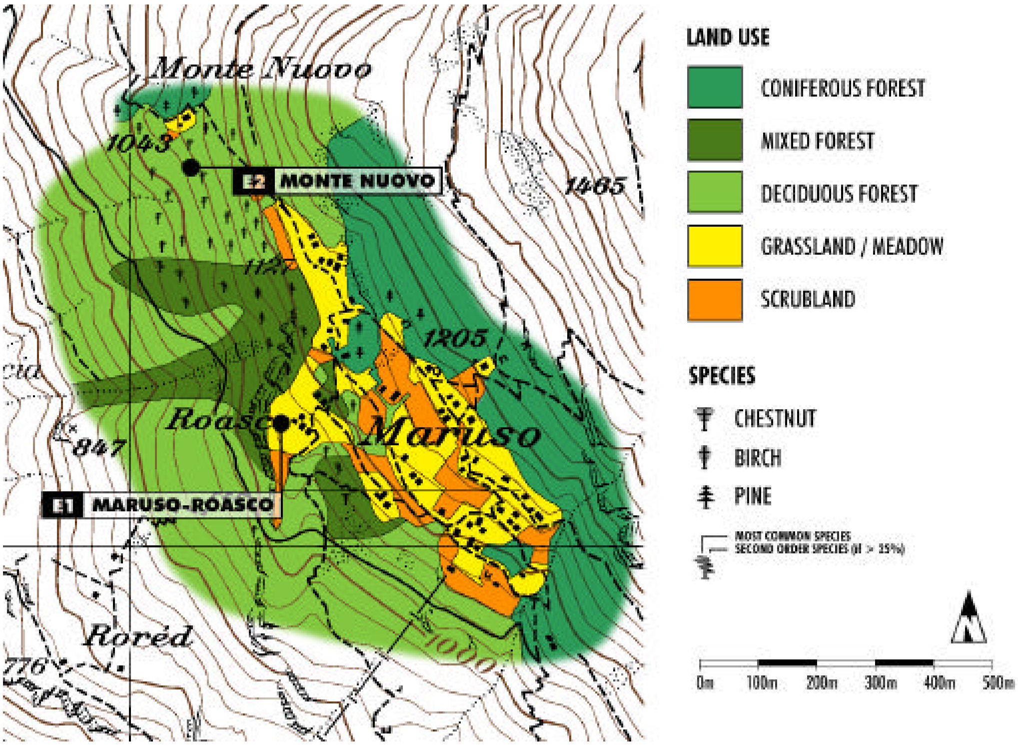

Fig. 3.2-2: Map of surrounding at stations *Monte Nuovo* and *Roasco*. Base Map: Carta Nazionale della Svizzera 1314 1:25'000, 1998, © Bundesamt für Landestopographie 2000 (JD002102).

E1: Maruso-Roasco

Roasco is a little spot SW of the small village *Maruso*, and lies 1060 m above sea level. The village is inhabited during summer months only; and nowadays it is mainly used for recreation.

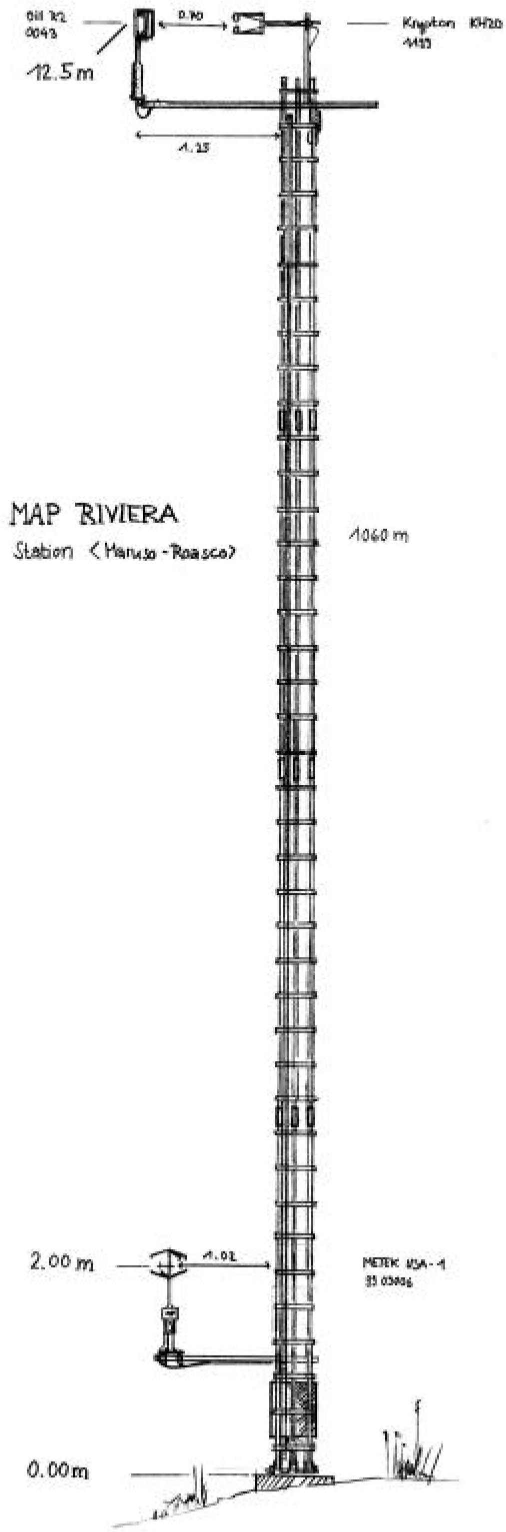

Fig. 3.2-3: Top: view on measuring site and the set-up of the radiation measurements. Bottom right and left: view of the EC mast that was mounted in *Roasco*. Right: Sketch of the tower at *Roasco*.

A 12 m mast was mounted close to an approximately 5m high rock wall on a grass field in the western part of *Roasco*. Two sonic anemometer-thermometers were fixed to the mast. A Metek USA1 was installed 1.5 m above ground at a 1m boom directed southward. On top a Gill R2 was mounted at a 1.2 m boom together with a Krypton hygrometer. Raw data were stored via serial ports on a PC. Details of instrumentation can be found in Tab. 3.2-II and in Fig. 3.2-3. From Fig. 3.2-2 it is obvious, that the mast is in a rather heterogeneous surrounding. Inclination and vegetation varied: westward, downhill, the forest bordered on a rock wall. Eastward, uphill, the slope was only 15° and after about 50 m of grassland the slope (now 35°) was covered with forest again. The radiation measurements were located 30 m ENE from the tower. All components of the radiation balance were measured slope-parallel as well as horizontal. A SODAR was installed 30 m south of the mast in an enclosure of 2 m height (see section 4.6).

Tab 3.2-II: Overview on measurements and instrumentation at site E1, *Maruso-Roasco*.* = Measurements of ETHZ (Hydrology).

variable	height above tow. base (m)	instrument	serial number	sampling interv. (s)	averaging period (s)	output	calibration
u, v, w, t	2.0	Metek USA-1	9903006	0.1	raw data	(m s^{-1}),(K)	wind tunnel
water vapour density fluctuation	12.7	KH2O	1199	0.05	raw data	(g m^{-3})	manufacturer
u, v, w, t	12.7	Gill R2A	43	0.05	raw data	(m s^{-1}),(K)	wind tunnel
precipitation	1.5	Campbell ARG100	n/a	2	60	(mm)	manufacturer
pressure	-	Vaisala PTB100B	n/a	2	60	(hPa)	manufacturer
long-wave radiation (horizontal)	1.59	Eppley PIR	30323f3	2	60	(W m^{-2})	
long-wave radiation (horizontal)	0.95	Kipp & Zonen CG2	970042	2	60	(W m^{-2})	reference instruments
short-wave radiation (horizontal)	1.64	Kipp & Zonen CM21	910004	2	60	(W m^{-2})	
components of radiation balance (slope-parallel)	1.2	Kipp & Zonen CNR1	980080	2	60	(W m^{-2})	reference instruments
short-wave radiation (horizontal)	1.1	Kipp & Zonen CM11	903185	2	60	(W m^{-2})	reference instruments
soil temperature	-0.27 -0.12	Campbell CBT	6 2	2	60	(°C)	manufacturer
soil humidity*	-0.15 to -0.25	TDR	-	3600	3600	(Vol-%)	manufacturer
leaf humidity*	0.1		-	3600	3600	(%)	manufacturer

E2 Monte Nuovo (Birke)

The site of observation was located 100 m South of a little clearing called *Monte Nuovo* on a slope with a westward exposition and an inclination of ≈35°. A 22 m mast was mounted in a roughly 13 m high forest which mainly consisted of birch trees. Other species were chestnut, and few beech trees as well as hazel. The forest floor was covered with sparse understorey vegetation, mainly grass with heights up to 0.3 to 0.4 m.

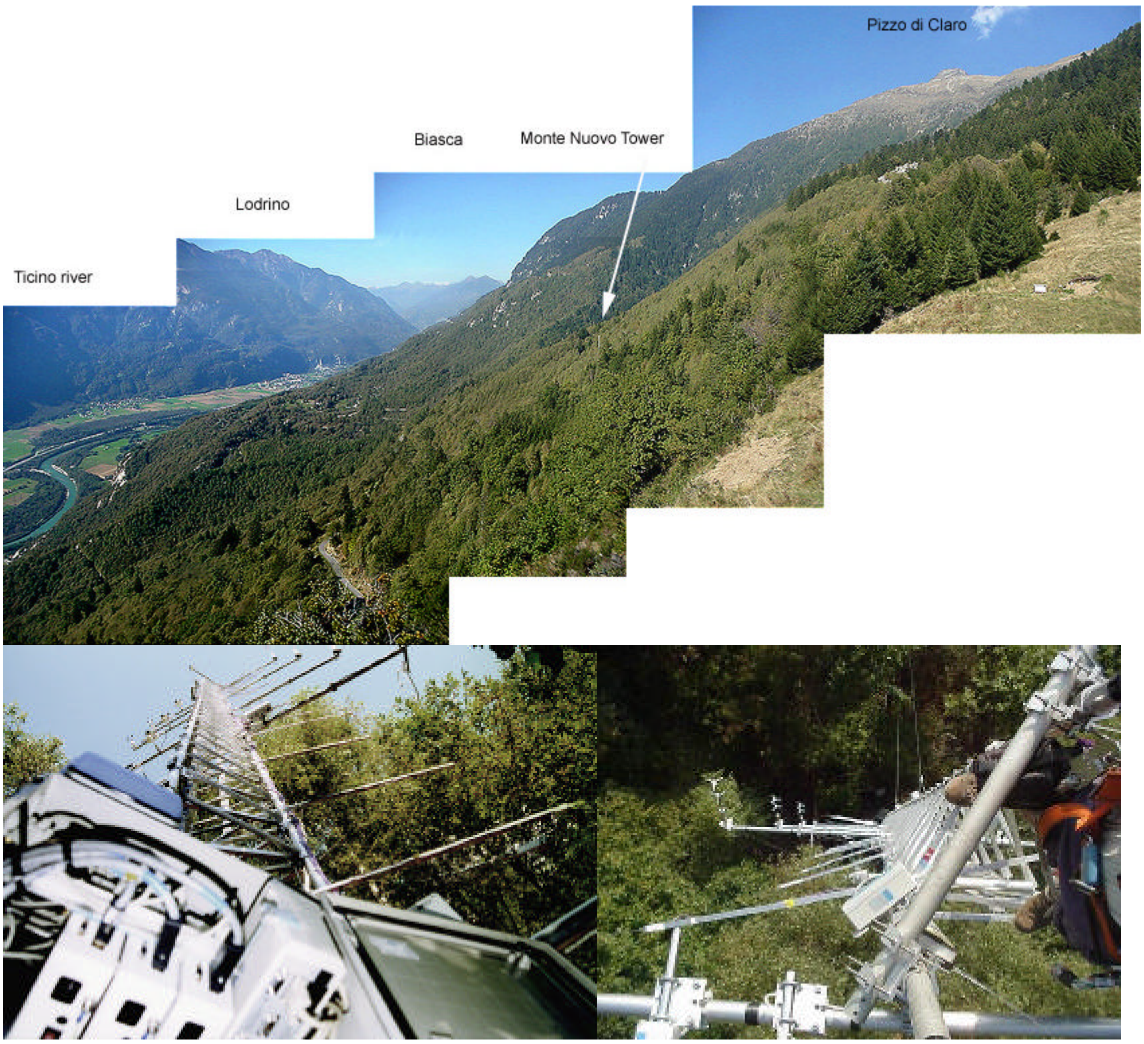

Fig. 3.2-4: Top: view on the slope with *Monte Nuovo* in the centre. Below left and right: bottom up and top down view of the tower at *Monte Nuovo*.

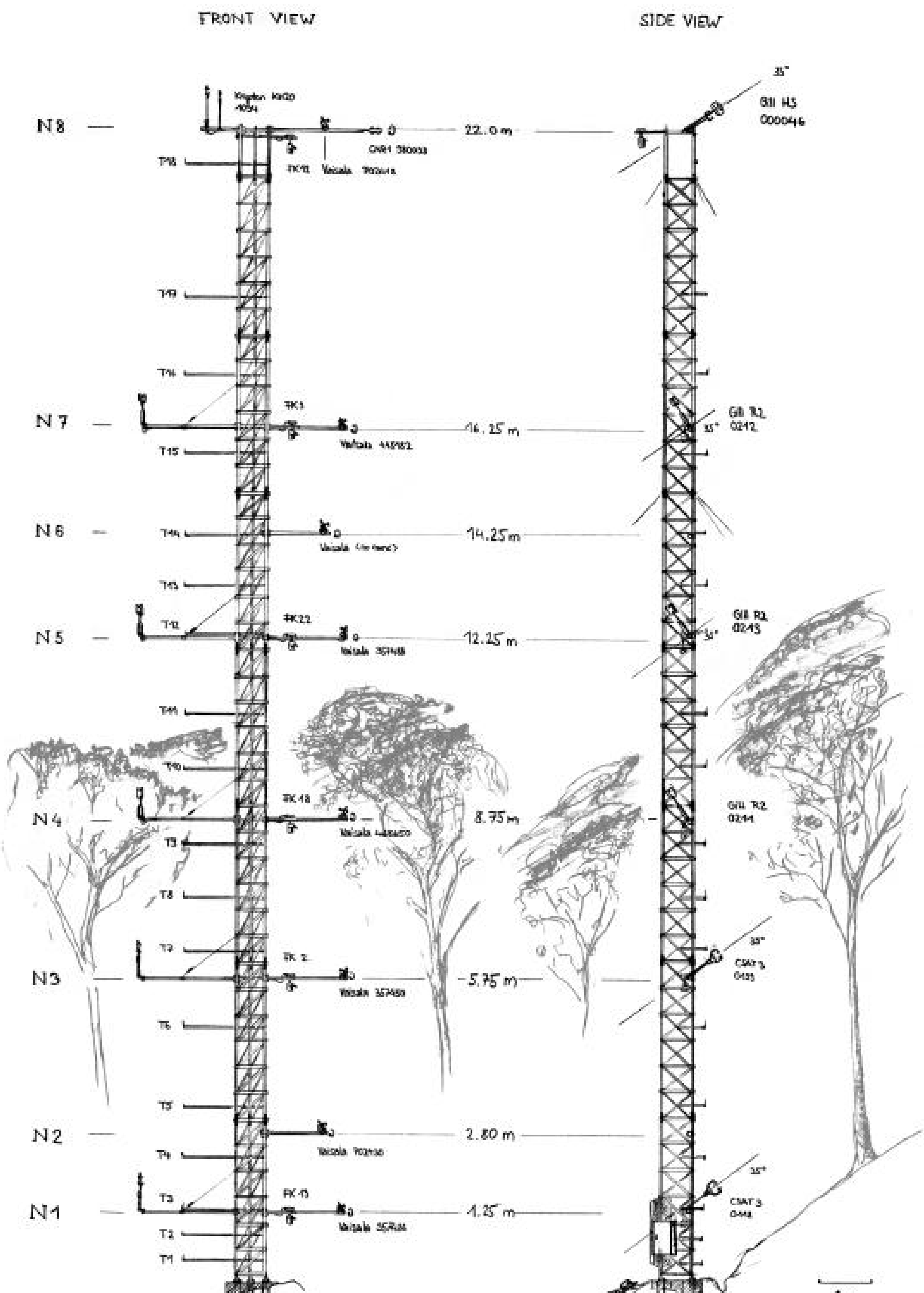

Fig. 3.2-5: Sketch of tower at *Monte Nuovo*. Down valley and side view.

The mast was in the middle of a relatively "homogeneous" part of the slope. Up- and downhill a kind of fetch was around 150 to 200 m. The same type of more or less homogeneous surface conditions, both in terms of tree height and species, were prevailing 100 m slope-parallel to the North and South. Figure 3.2-4 gives an idea of that "homogeneous" part of the slope.

The mast supported a profile of sonics, profile measurements of wind speed, temperature and humidity, and a high resolution profile of thermocouples. On top a net pyrradiometer was installed slope-parallel and measured the long- and short-wave components of net radiation. Details of the equipment are listed in Tab. 3.2-III and can be seen in Fig. 3.2-5.

Tab 3.2-III: Overview on measurements and instrumentation at station E2 *Monte Nuovo*.

variable	height above tow. base (m)	instrument	serial number	sampling interv. (s)	averaging period (s)	output	calibration
water vapor density fluctuation	22.68	Krypton KH_2O	1094	0.05	raw data	(g m^{-3})	manufacturer
u, v, w, t	22.68	Gill HS	000046	0.05	raw data	(m s^{-1}),(K)	wind tunnel
u, v, w, t	16.82	Gill R2	0212	0.05	raw data	(m s^{-1}),(K)	wind tunnel
u, v, w, t	12.82	Gill R2	0213	0.05	raw data	(m s^{-1}),(K)	manufacturer
u, v, w, t	9.32	Gill R2	0211	0.05	raw data	(m s^{-1}),(K)	manufacturer
u, v, w, t	6.34	CSAT	0199-2	0.05	raw data	(m s^{-1}),(K)	wind tunnel
u, v, w, t	1.84	CSAT	0118-2	0.05	raw data	(m s^{-1}),(K)	wind tunnel
components of radiation balance (slope-parallel)	22.00	Kipp & Zonen CNR1	098	4	60	(W m^{-2})	reference instruments
temperature humidity	22.0, 16.25, 12.25, 8.75, 5.75, 1.25	psychro-meter	FK12, FK09, FK22, FK18, FK??, FK13	4	60	(°C) (%)	water bath
wind speed	22.00, 16.25, 14.25, 12.25, 8.75, 5.75, 2.8, 1.25	Vaisala WAA15	P02418 445182 n.a. 357488 468650 357450 P02430 357486	1	60	(m s^{-1})	manufacturer
temperature fluctuations (18 levels)	21.27, 18.77, 17.27, 15.77, 14.27, 13.27, 12.27, 10.77, 9.77, 8.27, 7.27, 6.27, 4.77, 3.27, 2.27, 1.27, 0.77, 0.27	Thermo-couple	-	0.5 to 4	0.5 to 4	(°C)	no

F1 Alpe Domàs

At *Alpe Domàs* a station was put up in a avalanche track at 1750 m a.s.l.. Trees within the track had an average height of 8m and were rather sparse: The slope was exposed towards 216° with an inclination of 27.5°. The width of the track was ≈100 m and it was bordered by spruce forest.

Fig. 3.2-6: View uphill towards *Alpe Domàs*.

On top of the tower a sonic anemometer was mounted. Temperature fluctuations were measured with a thermocouple. One minute averages of first and second moments were stored on a Campbell 21X logger. At three heights wind speed, temperature and humidity were measured. The cup anemometers were fixed in 1 m distance from the mast. Furthermore the net radiation was measured with a pyrradiometer. Two heat flux plates were installed to get the soil heat flux and soil temperature were sampled with four thermistors. A view on the avalanche track is given in Fig. 3.2-6 and details of measurements and set-up can be found in Tab. 3.2-IV and Fig. 3.2-7.

Tab 3.2-IV: Measurements and instrumentation of station F1, *Alpe Domàs*.

variable	height above tow. base (m)	instrument	serial number	sampling interv. (s)	averaging period (s)	output	calibration
u, v, w, t	6.3	Gill Enhanced	009	0.2	60	(m s^{-1}),(K)	manufacturer
net radiation horizontal	2.0	Ph. Schenk Mod. 8111	8477	2	60	(W m^{-2})	reference
soil heat flux	-0.02	HFP	65638 65640	2	60	(W m^{-2})	manufacturer
soil temperature	-0.02, -0.05, -0.1, –0.15	Campbell CBT		2	60	(°C)	manufacturer
temperature humidity	2.0 3.0 5.0	Vaisala HMP35AC	424129 394832 394828	2	60	(°C) (%)	manufacturer
wind velocity	2.0 3.0 5.0	Vaisala WAA15	n/a 445200 357476	2	60	(m s^{-1})	manufacturer

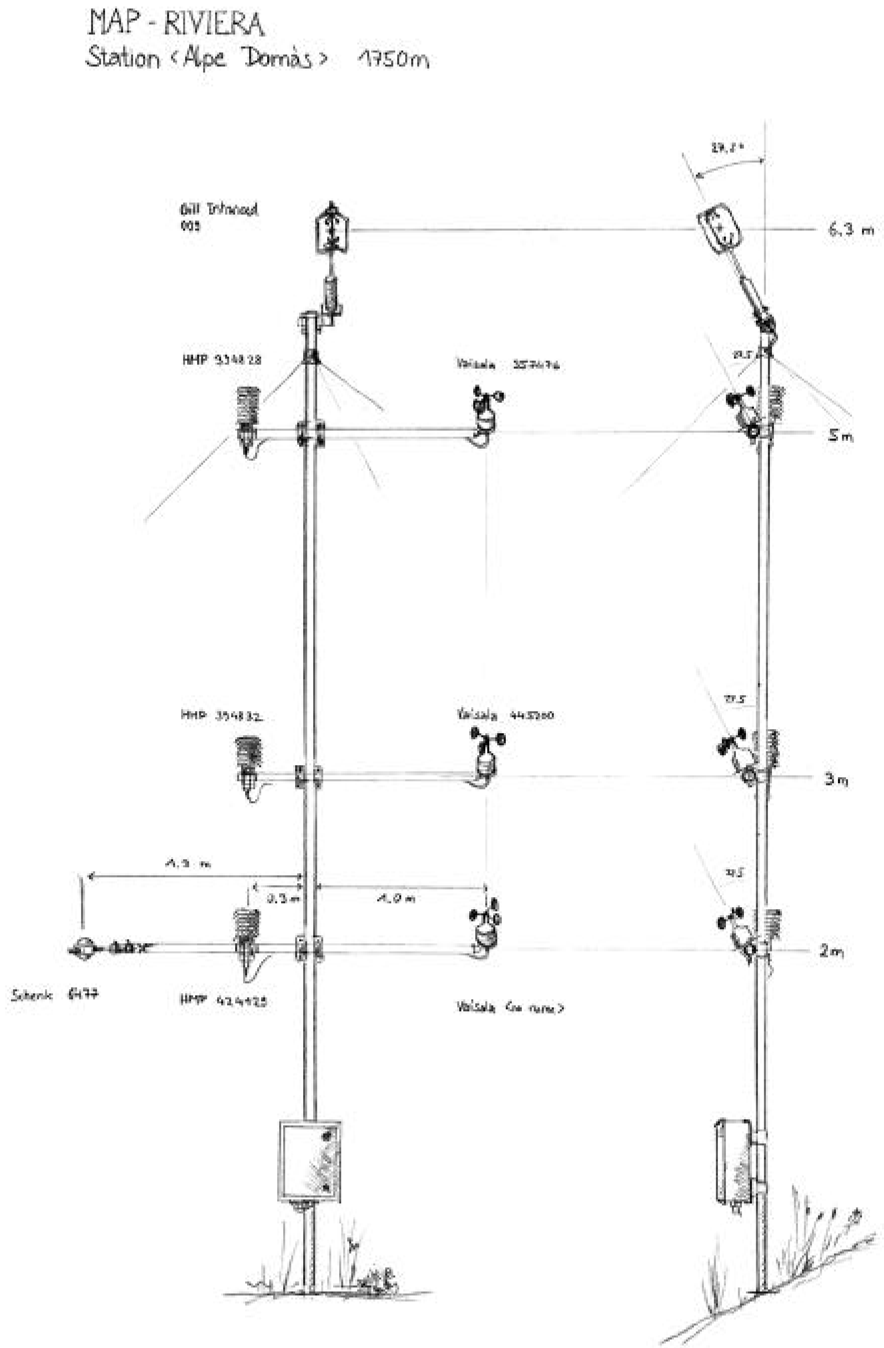

Fig. 3.2-7: Sketch of tower at *Alpe Domàs*. Down valley and side view.

F2 Alpe di Gagèrn (Krete)

The measurement tower was situated South of *Alpe di Gagèrn* 2110 m a.s.l.. This topmost site lay roughly 75 m below the crest on a slightly terraced part of the slope. The latter had an inclination of 40° on average and was exposed towards 240°. The tree line lay 300 m below the measuring site. The alpine vegetation was dominated by scrubs and alpine herbs. The plant cover was interspersed with rocks.

The instruments were mounted on a 11 m high tower. Two ultrasonic anemometer-thermometers measured the components of the wind vector as well as the temperature fluctuations at two heights. The sonics were mounted perpendicular to the slope. The upper sonic was mounted directly onto the mast whereas the lower one was fixed on a 2m boom in westward direction. From August 8, until September 9, raw data (20.83 Hz) were stored synchronously on a PC. From September 9 until October 10, 1 min averages of first and second moments were sampled using a Campbell 21X logger. Net radiation was measured at 2 m height. One set-up measured all components of net radiation parallel to the slope,

Fig. 3.2-8: Top: view South from Pizzo di Claro towards *Alpe di Gagèrn*. Bottom left: view on site F2 *Alpe di Gagèrn*. Bottom right: boom carrying radiation instruments.

another set-up measured horizontally exposed global and reflected global radiation. At three heights temperature and humidity measurements were carried out. Soil heat flux was measured directly with three heat flux plates and the soil temperature was sampled in four different depths. Additionally pressure and precipitation were measured. A view on the site is given in Fig. 3.2-8 and details of measurements and set-up can be found in Tab. 3.2-V and in Fig. 3.2-9.

Tab 3.2-V: Overview on measurements and instrumentation at station F2 *Alpe di Gagèrn*.

variable	height above tow. base (m)	instrument	serial number	sampling interv. (s)	averaging period (s)	output	calibration
u, v, w, t	3.10/1.90	Gill R2	0208	0.05/0.2	0.05/60	(m s^{-1}),(K)	manufacturer
u, v, w, t	-/11.00	Gill R2	0160	0.05/0.2	0.05/60	(m s^{-1}),(K)	wind tunnel
precipitation	1.50/1.50	RIMCO	206185	4	60	(mm)	manufacturer
pressure	1.00/1.00	Vaisala PTP101	T2430015	4	60	(hPa)	manufacturer
shortwave radiation horizontal	2.10/1.90	Kipp & Zonen CM21	950239	4	60	(W m^{-2})	
components of radiation balance (slope-parallel)	2.15/1.90	Kipp & Zonen CNR1	142	4	60	(W m^{-2})	reference
shortwave radiation horizontal	1.93/2.00	Kipp & Zonen CM11	902804	4	60	(W m^{-2})	
soil heat flux	-0.04 -0.04 -0.06	HFP	G0057 HP365628 G0050	4	60	(W m^{-2})	manufacturer
soil temperature	-0.03 -0.05 -0.10		CBT2 CBT8 CBT10	4	60	(°C)	manufacturer
temperature humidity	0.7/ 0.6 2.2/2.0 -/10.6	Vaisala HMP35A	476730 424125 424142	4	60	(°C) (%)	manufacturer

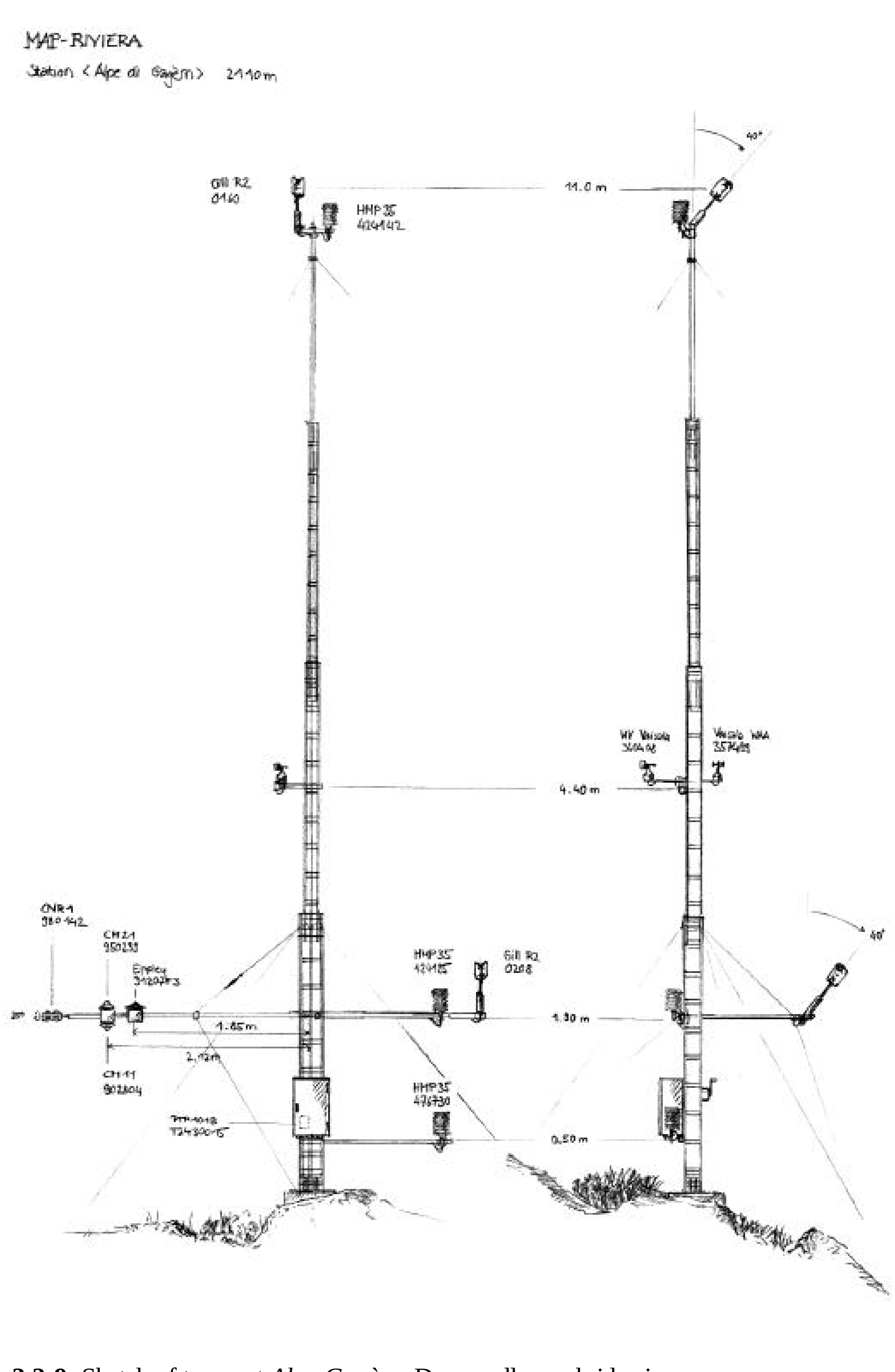

Fig. 3.2-9: Sketch of tower at *Alpe Gagèrn*. Down valley and side view.

3 Alpe di Motto

A small station was set up on *Alpe di Motto* at 1860 m a.s.l. to monitor wind velocity and wind direction wind vane. Net radiation was measured with a pyrradiometer. Details are listed in Tab. 3.2-VI and the set-up can be seen in Fig. 3.2-10.

The station was situated on a SW oriented ridge which lies between *Alpe Domàs* and the station *Alpe di Gagèrn*.

Tab 3.2-VI: Overview on measurements and instrumentation at station F3 *Alpe di Motto*.

variable	height above ground (m)	instrument and serial number	sampling rate/averaging period (s) and output	calibration
wind speed	2.2	Young MCR-035	3/60 (m s^{-1})	manufacturer
wind direction	2.2	Young MCR-035	3/60 (°)	manufacturer
net radiation	1.7	Ph. Schenk Mod. 8111	3/60 (W m^{-2})	reference

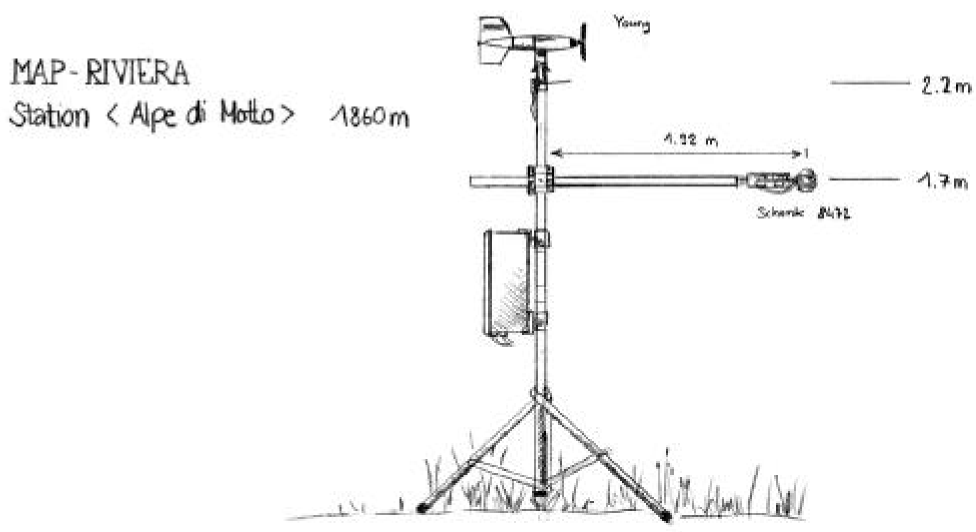

Fig. 3.2-10: Sketch of set-up at *Alpe di Motto*

G Censo (Kerbtal)

The station *Censo* was built on a bridge which crosses a river at a narrow point of the valley. The catchment area is about 4 km^2 and is covered with forest (mainly chestnut and birch). The valley cross-section at the bridge has a depth 12 to 15 m and its width is 15 to 17 m.

The wind vector was monitored with a sonic anemometer which was mounted on top of the mast at a height of 5.25 m above the bridge and ≈18 m above the bottom of the valley. Additionally the temperature fluctuations were measured with a thermocouple (75 µm). First and second moments were stored as 1 min averages. Furthermore temperature, humidity and the scalar wind speed were measured at two heights above and below the bridge (3.05 and 2.10 m). The latter were sampled by a Campbell CR10, and the eddy covariance measurements by a Campbell 21X. Details are listed in Tab. 3.2-VII and the set-up can be seen in Fig. 3.2-11.

Tab 3.2-VII: Overview on measurements and instrumentation at station G, *Censo*.

variable	height above tow. base (m)	instrument	serial number	sampling interval (s)	averaging period (s)	output	calibration
u, v, w	5.25	Gill Enhanced	n/a	0.2	60	(m s^{-1})	manufacturer
t‘	5.25	thermo-couple	-	0.2	60	(K)	-
wind speed	3.05	Vaisala WAA15	357399	1	60	(m s^{-1})	manufacturer
wind speed	-2.1	Vaisala WAA15	436021	1	60	(m s^{-1})	manufacturer
temperature/humidity	3.05	Vaisala HMP35A	476728	1	60	(°C), (%)	manufacturer
temperature/humidity	-2.1	Vaisala HMP35A	476724	1	60	(°C), (%)	manufacturer

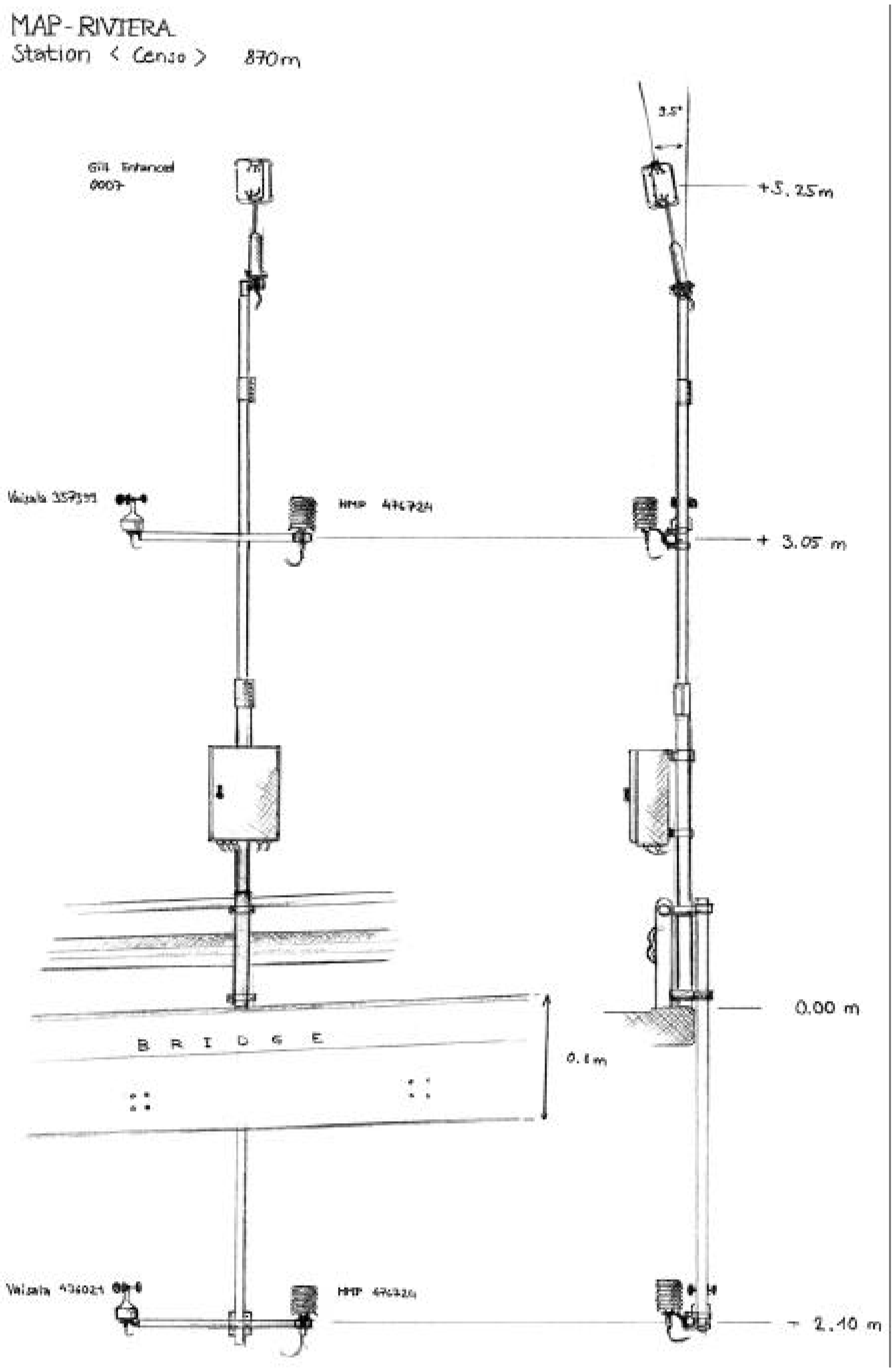

Fig: 3.2-11: Sketch of tower at *Censo*.

3.3 Hydrological Observations

3.3.1 Motivation

The hydrology sub-project is integrated in the EU-MAP-Project RAPHAEL (Runoff and Atmospheric Processes for Flood Hazard Forecasting and Control). The aim of the this subproject is the spatial distributed modelling of the hydrologic processes in the Ticino/Verzasca/Maggia-basins to calculate the spatial differences in runoff generation, evapotranspiration and soil moisture for runoff simulation and for the estimation of surface ground truth to the atmospheric model inputs. The connected hydrologic processes are estimated by the temporal and spatial variations of climate elements, by topography, by vegetation cover, by the soil characteristics and by the soil moisture. The well established parameterisation and validation of hydrologic models need specific investigations and measurements for modelling evapotranspiration and soil moisture at selected sites (Figure 3.3-1) with different microclimatological conditions, with differences in topography altitude and exposure) and with different types of landuse and different soil conditions.

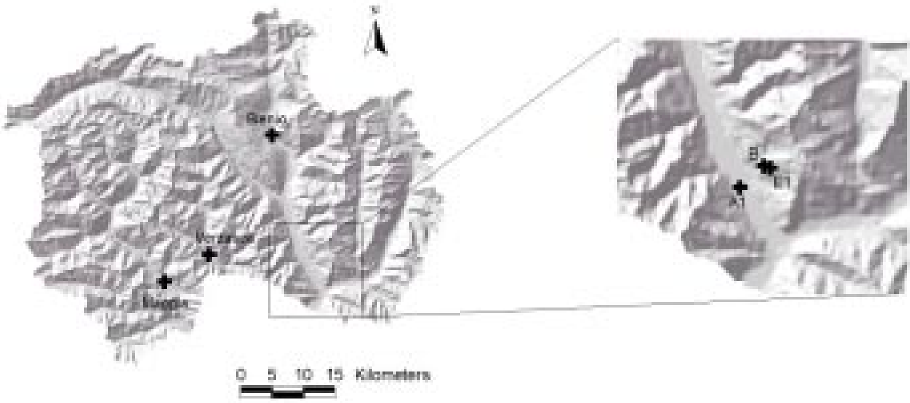

Figure 3.3-1: MAP Riviera. Hydrological observation. Locations of the sites described in the text (Zappa et al. 2000).

The estimation of evaporation will be realised for selected sites taking account of:

- The Bowen ratio method by measurement of different radiation components (global and short-wave reflected radiation, long-wave radiation) for the calculation of net radiation and monitoring of ground heat flux. Estimation of the ratio between sensible heat flux and latent heat flux using the vertical gradients of air temperature and air humidity close to the ground of the boundary layer. At various sites the result from the Bowen ratio can be compared to the direct observations of the latent heat flux using the eddy covariance technique (see sections 3.1 and 3.2 for details).
- Measurements of the soil water fluxes by mean modern soil water measurement techniques (TDR-Time Domain Reflectometry) in different soil depths, of precipitation and of wind speed. The water fluxes in the root zone to the top are equivalent to the extraction of soil water by evapotranspiration.

- Simulation with the Watershed Model PREVAH (Precipitation Runoff Evaporation Hydrotope related Model). The potential and the actual evapotranspiration will be simulated with the Penman-Monteith approach.
- Calculation with other empirical and physical approaches.

3.3.2 Observations at site A1, "Bosco di Sotto"

The main research area for the hydrological observation was in Claro at site A1. The soil water content was measured hourly under a corn field with a Tektronix-TDR-System and stored with a Campbell 21x Datalogger. Six TDR detectors and three temperature detectors have been buried in the soil at different depths to obtain a representative profile (0 until 120 cm depth) of the vertical changes of soil temperature and water content. In the near meadow land ten additional TDR detectors were buried at different depths (0 until 130 cm depth). In this case the measurement of the soil's water content has to be made by hand daily and if possible shortly after intensive rainfall. This should allow to obtain the value of the relative maximum of the water content, to follow the decrease of the soil moisture in the following days and to determinate evapotranspiration and infiltration. Another way to determinate the water content using the TDR method is with the TRIME T3 detector. A 160 cm deep borhole with a plastic tube was drilled into the soil, next to the meadow profile, and another tube was installed in a bush next to site A1. With TRIME FM3 and T3 System it is possible to measure the mean soil's water content in a 20 cm range and to get a vertical profile of the soil moisture. This measurement was made by hand daily. The instrument gives directly the value of the volumetric water content in percent. Two HPC01SC Hukseflux thermal detectors measured every hour the soil heat flux at 5 cm depth under corn and under meadow. Other collected data includes precipitation with a Tognini gauge and leaf humidity. See section 3.1 for the description of the meteorological observations at site A1.

Remarks: the meadow was mowed once the 9^{th} of September, the corn was harvested the 27 September 1999.

Table 3.3-I Summary of the hydrological observations at the site A1.

variable	Land use	Nominal height (or depth).	Instrument (incl. serial number)	Sampling Interval	Averaging Period / Sampling frequency	Output signal (or reference to conversion formula)
Precipitation	-	3 m	Tognini	60 min	60 min	[mm]
Soil heat flux	Corn	-5 cm	Hukseflux HPC01SC - 57	Instant.	60 min	66.4 $\mu V/(Wm^{-2})$
Soil heat flux	Meadow	-5 cm	Hukseflux HPC01SC - 58	Instant.	60 min	66.5 $\mu V/(Wm^{-2})$
Leaf humidity	Meadow	10 cm	BNHM # 4	Instant.	60 min	Table 3.3-V
Soil moisture, TDR	Corn	-5 cm	Tektronix Be_21	Instant.	60 min	Menzel (1995)
Soil moisture, TDR	Corn	-15 cm	Tektronix Be_5	Instant.	60 min	Menzel (1995)
Soil moisture, TDR	Corn	-35 cm	Tektronix Be_4	Instant.	60 min	Menzel (1995)
Soil moisture, TDR	Corn	-50 cm	Tektronix Be_3	Instant.	60 min	Menzel (1995)
Soil moisture, TDR	Corn	-80 cm	Tektronix Be_2	Instant.	60 min	Menzel (1995)
Soil moisture, TDR	Corn	-105 cm	Tektronix Be_1	Instant.	60 min	Menzel (1995)
Soil temperature	Corn	-5 cm	T107	Instant.	60 min	[°C]
Soil temperature	Corn	-20 cm	T107	Instant.	60 min	[°C]
Soil temperature	Corn	-50 cm	T107	Instant.	60 min	[°C]
Soil moisture, TDR	Meadow	5 cm	Tektronix 201	Instant.	1 day	[Vol%]
Soil moisture, TDR	Meadow	-15 cm	Tektronix 202	Instant.	1 day	[Vol%]
Soil moisture, TDR	Meadow	-30 cm	Tektronix 203	Instant.	1 day	[Vol%]
Soil moisture, TDR	Meadow	-40 cm	Tektronix 204	Instant.	1 day	[Vol%]
Soil moisture, TDR	Meadow	-60 cm	Tektronix 205	Instant.	1 day	[Vol%]
Soil moisture, TDR	Meadow	-80 cm	Tektronix 206	Instant.	1 day	[Vol%]
Soil moisture, TDR	Meadow	-100 cm	Tektronix 207	Instant.	1 day	[Vol%]
Soil moisture, TDR	Meadow	-100/-130 cm	Tektronix 208	Instant.	1 day	[Vol%]
Soil moisture, TDR	Meadow	0/-30 cm	Tektronix 209	Instant.	1 day	[Vol%]
Soil moisture, TDR	Meadow	-40/-70 cm	Tektronix 210	Instant.	1 day	[Vol%]
Soil moisture, Tube	Meadow	0/-170 cm	TRIME-FM3 TRIME-T3	Instant.	1-2 day	[Vol%]
Soil moisture, Tube	Bush	0/-80 cm	TRIME-FM3 TRIME-T3	Instant.	1-3 day	[Vol%]
Logger			Campbell 21X			
Multiplex			Campbell			

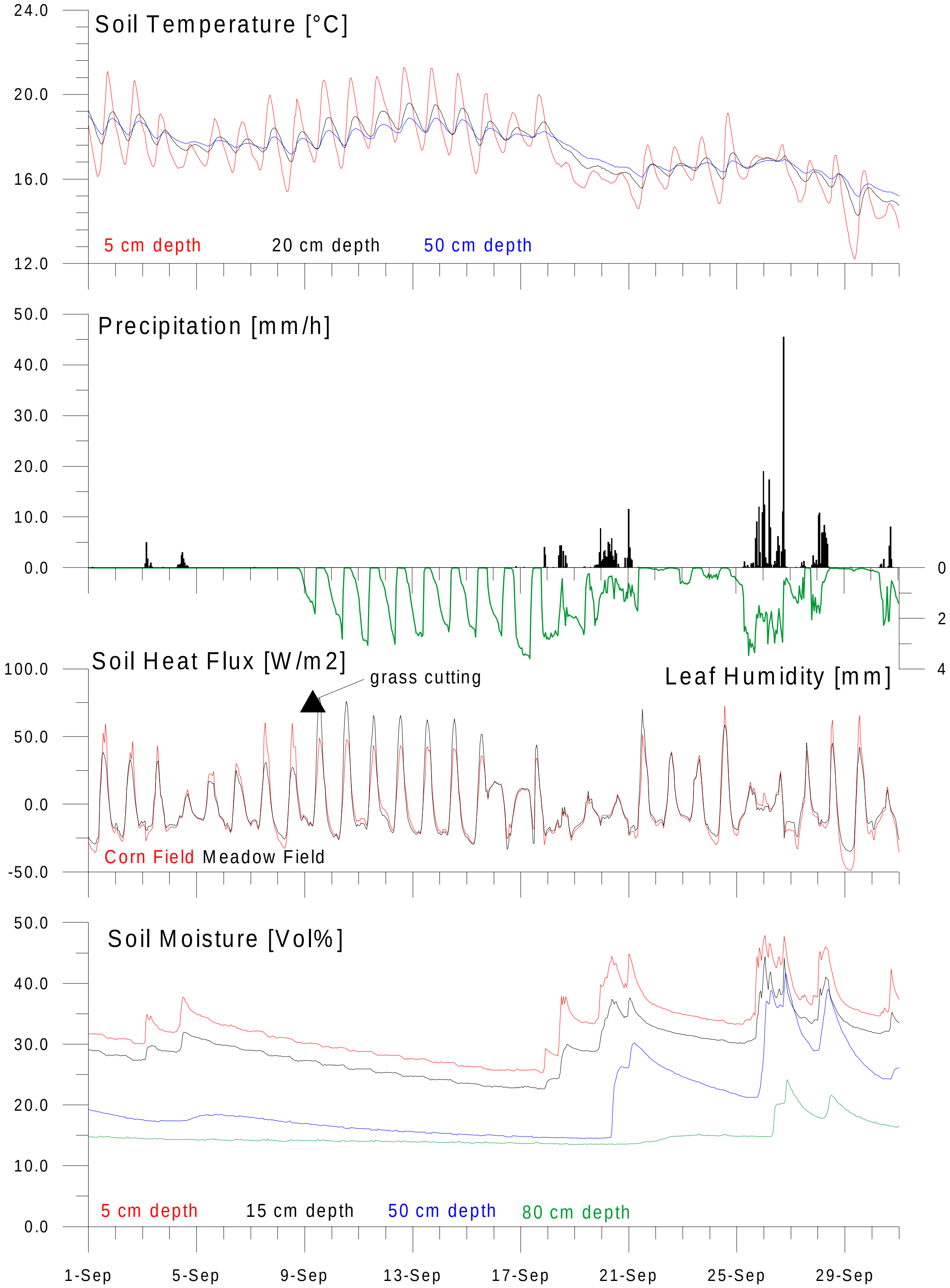

Figure 3.3-2: MAP Riviera. September 1999. Not yet quality checked plot of selected hydrological variables measured at the site A1 (Zappa et al. 2000).

Table 3.3-II Availability of hydrological observations at the site A1.
Key: black: complete - grey: not complete - white: missing.

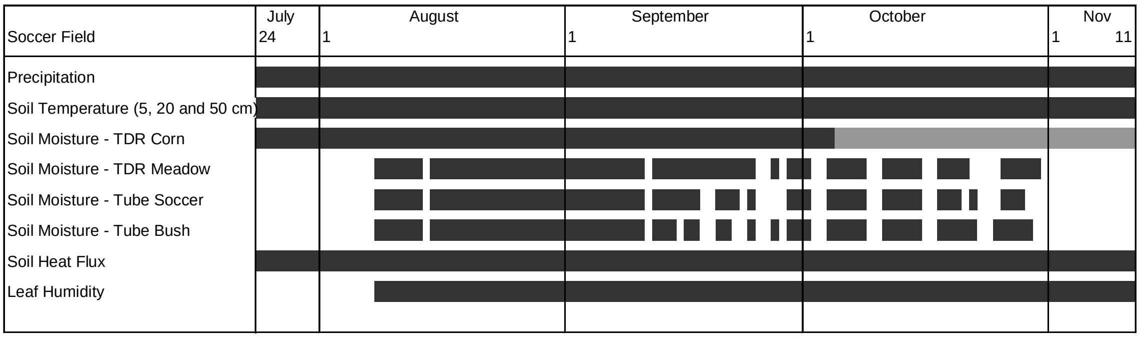

Table 3.3-III Site A1, Corn Profile. Calibration of the Tektronix equipment and description of the soil structure.

Instrument	Depth	L_W	Nominal cable length	Calibrated cable length	Porosity	Soil structure
Be_21	5	1.84	3.42	8.44	0.51	Humus
Be_5	15	1.84	5.06	10.9	0.488	Humus, with many roots
Be_4	35	1.84	4.72	10.4	0.547	Humus, with less roots
Be_3	50	1.88	5.15	11.0	0.503	Sand, dry with roots
Be_2	80	1.84	5.56	11.66	0.528	Sand, wet
Be_1	90-120	1.94	5.78	12	0.515	Sand, very wet

L_W = Propagation time of the TDR signal in pure water at 20.0°C

Table 3.3-IV Site A1, Meadow Profile. Calibration of the Tektronix equipment and description of the soil structure.

Instrument	Depth	L_W	Calibrated cable length	Porosity	Soil structure
201	5	1.82	2.14	0.497	Humus,
202	15	1.84	2.22	0.506	Humus, with many roots
203	30	1.80	2.22	0.52	Transition zone, with less roots
204	40	1.80	2.30	0.508	Sand, dry, with roots
205	60	1.82	2.30	0.504	Sand, dry
206	80	1.80	2.20	0.513	Sand, dry
207	100	1.80	2.34	0.551	Sand, dry
208	100-130	1.80	2.34	0.551	Sand, wet
209	0-30	1.80	2.30	0.51	Humus, root zone
210	40-70	1.80	2.22	0.505	Sand, dry

L_W = Propagation time of the TDR signal in pure water at 20.0°C

Table 3.3-V Sites A1, B, E1. Calibration equation of the leaf humidity detectors.

Instrument	Location	Calibrated function: LU=f(V)
BNHM # 4	A1	LU = exp(0.0506788*V)* 0.00627294
BNHM # 3	B	LU = exp(0.0626393*V)* 0.00175272
BNHM # 5	B	LU = exp(0.0505443*V)* 0.002375
BNHM # 2	E1	LU = exp(0.054706*V)* 0.00636802

3.3.3 Observations at site B, "Rored"

At site B another automatic station to retrieve hourly data of the soil moisture had been installed. The soil's water content was measured hourly under chestnut forest with a TRIME-EZ-System and stored with a Campbell 21x Datalogger. Five TDR detectors and two temperature detectors had been buried between 20 cm and 90 cm depth. Three rain gauges measured the throughfall and a fourth gauge measured the free land precipitation. A HPC01SC Hukseflux thermal detector measured every hour the soil heat flux at 5 cm depth under chestnut trees. Other collected data include net radiation, leaf humidity (once next the surface and once an a tree branch) and a soil moisture profile between 10 and 70 cm (TRIME FM3 and T3 System).

Table 3.3-VI Summary of the hydrological observations at the site B.

variable	Land use	Nominal height (or depth).	Instrument (incl. serial number)	Sampling Interval	Averaging Period / Sampling frequency	Output signal (or reference to conversion formula)
Free land Precipitation	-	7.5 m	Tognini	30 min	30 min	[mm]
Canopy Precipitation	Chestnut	1 m	3 x Tognini	30 min	30 min	[mm]
Soil heat flux	Chestnut	-5 cm	Hukseflux HPC01SC - 34	Instant.	30 min	66.4 µV/(Wm-2)
Net radiation	-	7.5 m	S-1 , # 8184	30 min 2 min	30 min 2 min	sw 37.57 µV/(Wm-2) lw 37.80 µV/(Wm-2)
Leaf humidity	Chestnut	10 cm	BNHM # 3	Instant.	30 min	Table 3.3-V
Leaf humidity	Chestnut	150 cm	BNHM # 5	Instant.	30 min	Table 3.3-V
Soil moisture, TDR	Chestnut	-15 cm	TRIME-EZ-8243	Instant.	60 min	[Vol%]
Soil moisture, TDR	Chestnut	-30 cm	TRIME-EZ-8244	Instant.	60 min	[Vol%]
Soil moisture, TDR	Chestnut	-50 cm	TRIME-EZ-8245	Instant.	60 min	[Vol%]
Soil moisture, TDR	Chestnut	-70 cm	TRIME-EZ-8246	Instant.	60 min	[Vol%]
Soil moisture, TDR	Chestnut	-85 cm	TRIME-EZ-8247	Instant.	60 min	[Vol%]
Soil temperature	Chestnut	-20 cm	T107	Instant.	30 min	[°C]
Soil temperature	Chestnut	-50 cm	T107	Instant.	30 min	[°C]
Soil moisture, Tube	Chestnut	0/-70 cm	TRIME-FM3 TRIME-T3	Instant.	1-3 day	[Vol%]
Logger			Campbell 21X			

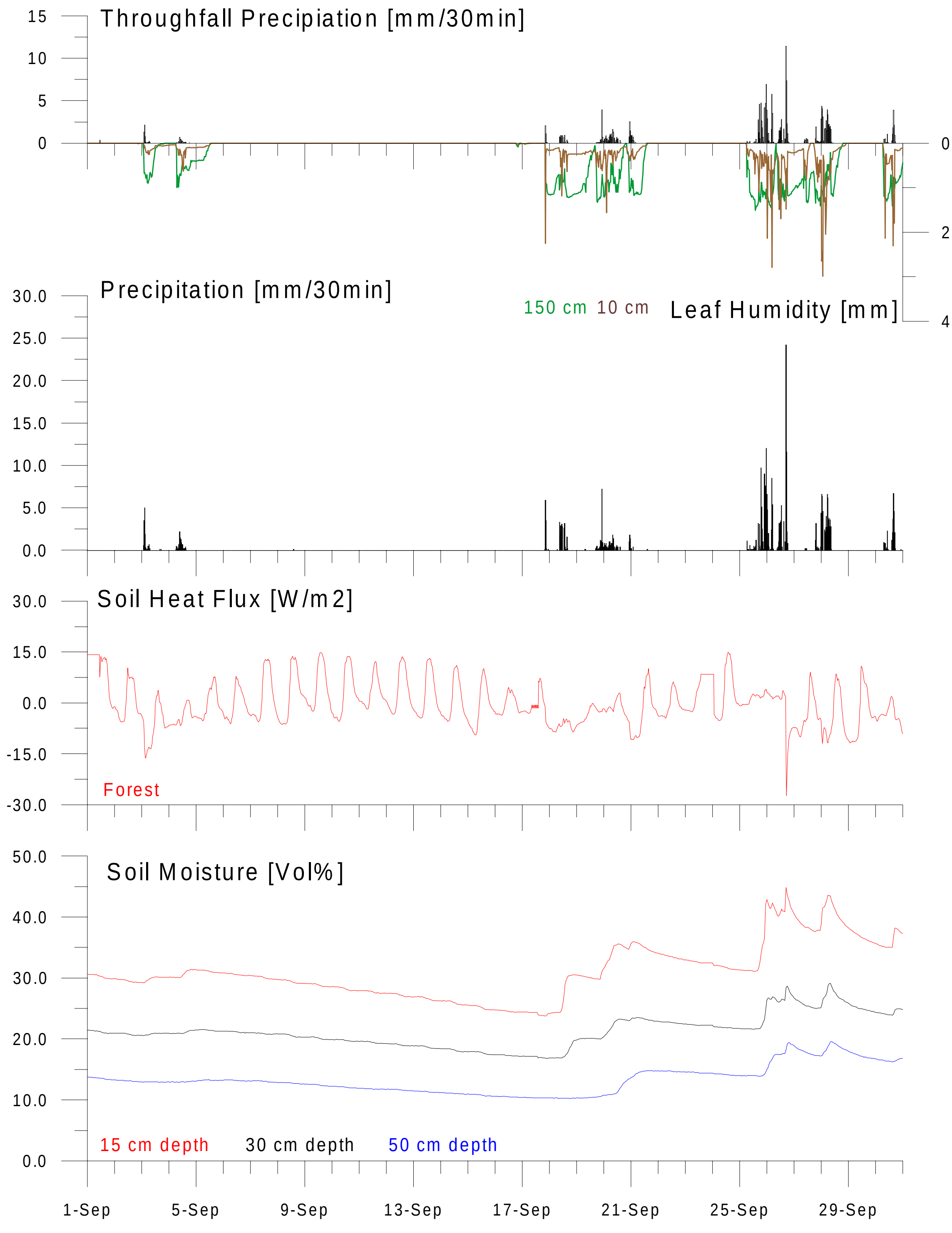

Figure 3.3-3: MAP Riviera. September 1999. Not yet quality checked plot of selected hydrological variables measured at the site B (Zappa et al. 2000).

Table 3.3-VII Availability of hydrological observations at the site B.
Key: black: complete - white: missing.

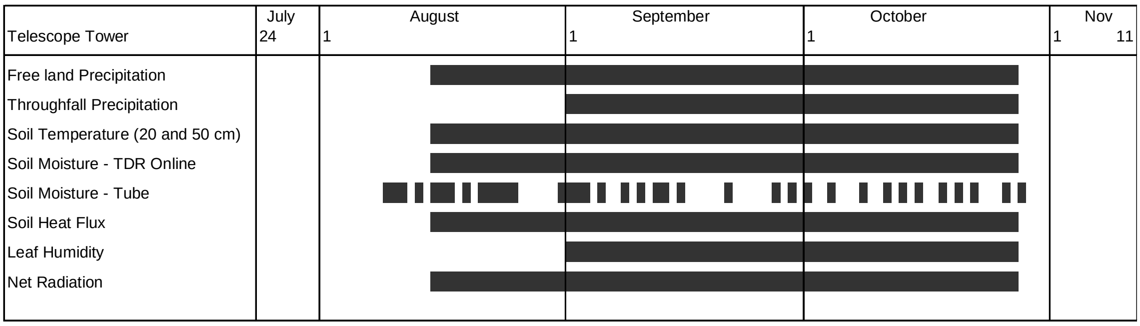

3.3.4 Observations at site E1, "Maruso-Roasco"

In Maruso-Roasco the soil moisture under meadow was collected hourly at 20 cm depth with a TRIME-EZ-System. Other collected data included leaf humidity, soil temperature and a soil moisture profile between 10 and 50 cm (operationally measured by hand using TRIME FM3 and T3 System). . See section 3.2 for the description of the meteorological observations at site E1.

Table 3.3-VIII Availability of hydrological observations at the site E1.

variable	Land use	Nominal height (or depth).	Instrument (incl. serial number)	Sampling Interval	Averaging Period / Sampling frequency	Output signal (or reference to conversion formula)
Leaf humidity	Meadow	10 cm	BNHM # 2	Instant.	60 min	Table 3.3-V
Soil moisture, TDR	Meadow	15 cm	TRIME-EZ-8248	Instant.	60 min	[Vol%]
Soil moisture, Tube	Meadow	0-50 cm	TRIME-FM3 TRIME-T3	Instant.	1-3 day	[Vol%]

Table 3.3-IX Availability of hydrological observations at the site E1.
Key: black: complete - white: missing.

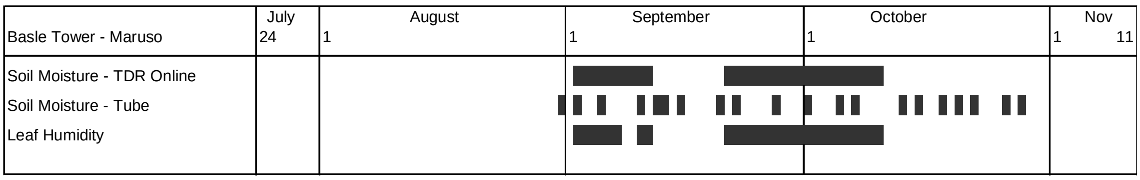

3.3.5 Additional hydrological observations

Precipitation was observed at the site C "*Pian Perdascio*" (see section 3.1 for details). Three tubes were installed additionally for episodical (weekly) soil moisture measurements in the Blenio valley near Dongio, in the Verzasca valley near Lavertezzo and in the Maggia valley near Ronchini (TRIME FM3 and T3 System, see Table 3.3-I for specifications). The aim of these measurements was to get more information about the soil moisture distribution for the hydrological modelling within these catchments. The measured soil moisture values were transmitted during the MAP-SOP to the MAP centre in Innsbruck and in the MAP-Hydrology data bank for using in the coupled meteorological and hydrological forecast.

Table 3.3-X Time series hydrological observations in the Valleys.
Key: black: complete - white: missing.

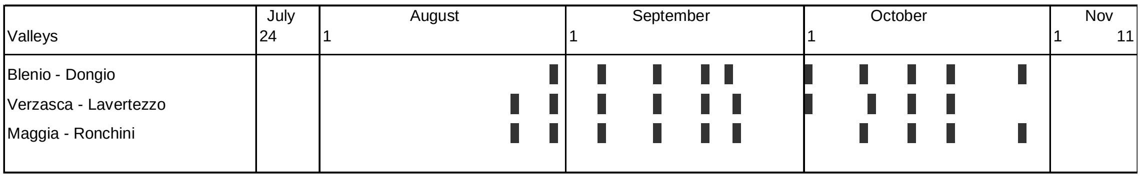

4 Acknowledgements

Karl Schroff is acknowledged for his precious technical work on the field instrumentation. We are thankful to Alessia Bassi, Shari Carlaw, Mélanie Raymond, Martin Dippon, Nicolas Matzinger and Simone Regazzi for their precious help during different phases of the hydrology sub-project.

References:

Menzel, L. (1995): Bodenfeuchtemessung mittles Time Domain Relectometry (TDR), Berichte und Skripte - Funktion und Anwendung, GIETHZ, 1995

Zappa M., Matzinger N., Gurtz J. (2000). Hydrological and Meteorological Measurements at Claro (CH)- Lago Maggiore Target Area in the MAP-SOP 1999 RIVIERA experiment including first evaluation, in: Hydrological aspects in the Mesoscale Alpine Programme-SOP experiment, edited by B. Bacchi and R. Ranzi, Technical Report of the Dept. of Civil Engineering-Univ. of Brescia, 10(2), in press.

Contact

Joachim Gurtz
Tel. ++41 1 635 52 28
E-mail gurtz@geo.umnw.ethz.ch

Massimiliano Zappa
Tel. ++41 1 635 52 27
E-mail zappa@geo.umnw.ethz.ch

4.1 scintillometry

4.1.1 Sites and instrumentation: scintillometry

Two displaced beam scintillometers SLS20 (SCINTEC) were set up during the two R-IOPs in the Riviera valley. Figure 4.1-1shows one of the laser beam emitters, fixed on a theodolite, for easy alignment.
Meteorological output variables of the standard SLS20 algorithm are:

- sensible heat flux H
- momentum flux M
- Obukhov length L
- structure function of refractive index C_n^2
- structure function of temperature C_T^2
- the inner scale of turbulence l_o
- dissipation rate of turbulent kinetic energy ε

The turbulent fluxes of sensible heat and momentum and the Obukhov length are calculated for the assumption of stable and unstable conditions, which one is appropriate has to be decided from other measurements. Beside the above mentioned meteorological parameters, additional information is also stored in the output files, such as the percentage of error free diagnosis data periods within the main data period, measurement high z and length R of the propagation path. The sampling period for all scintillometer measurements was 6 seconds and the data are stored as one minute mean. Time is always given in Central European Time (CET), e.g. local time -1 hour. Further information about the periods, data were collecting, is given in info Tables 4.1-I and 4.1-II.

Figure 4.1-1.: Transmitter of one of the SLS20 scintillometer, fixed on a theodolite.

Two different sites were chosen for the scintillometer measurements in the bottom of the Riviera valley, near the village Claro: site *San Giuseppe* (A2-a, A2-b) and site *Torraza* (D). For an overview of the locations see Figure 4.1-2.

.

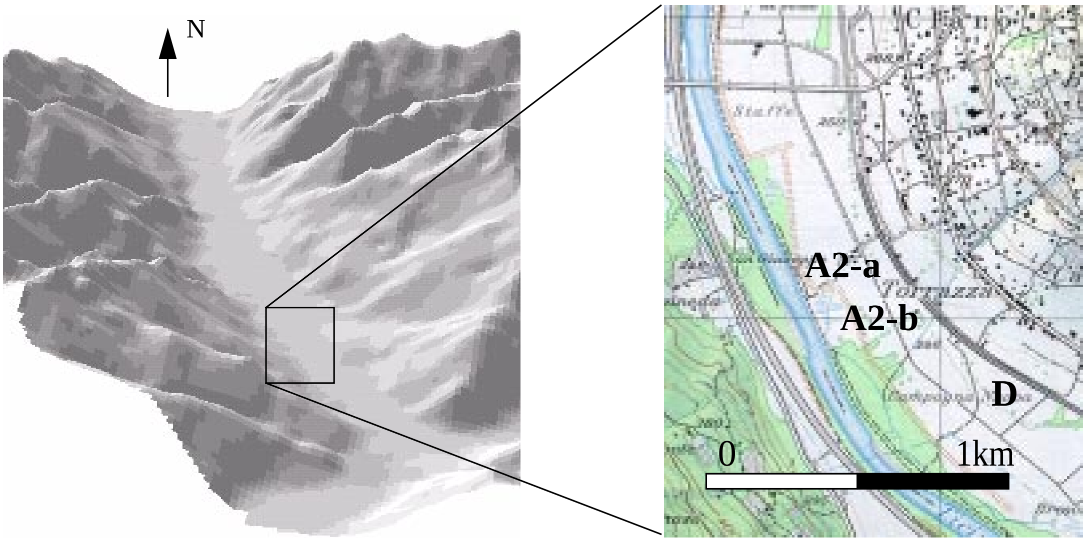

Fig. 4.1-2: Overview of the Riviera valley (DHM25 ©1998 Bundesamt fuer Landestopographie) and the scintillometer measurements sites A2-a, A2-b and D near the village Claro (© Bundesamt fuer Landestopographie 2000 , JD002102)

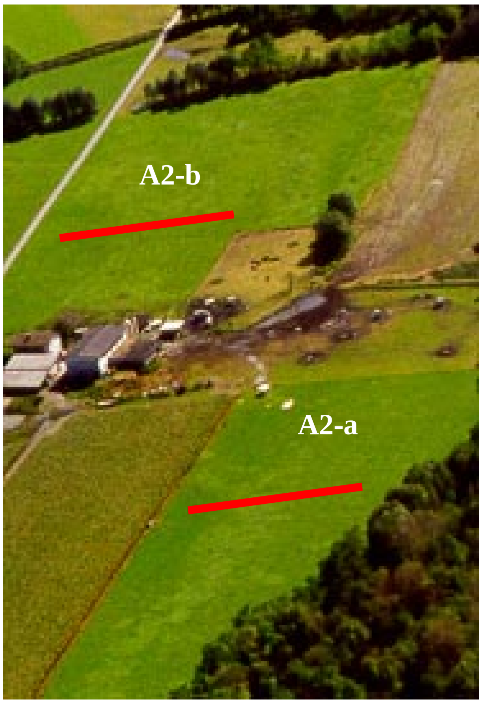

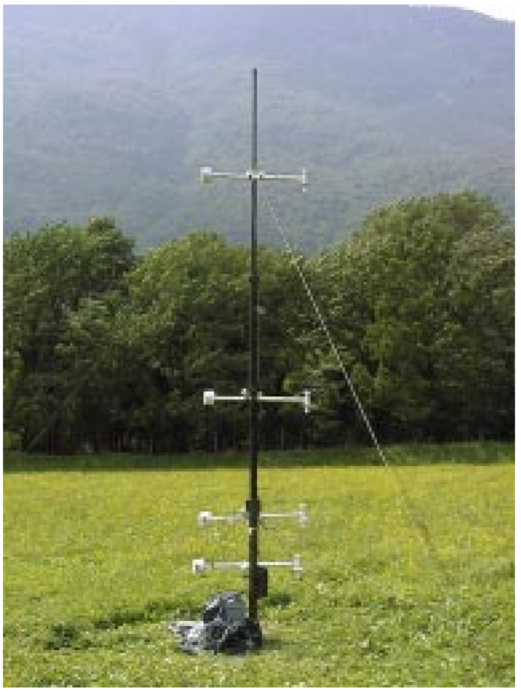

Fig. 4.1-3: Picture of measurement sites *San Giuseppe* A2-a and A2-b (left side) and small instrumental tower for temperature measurements in the middle of the scintillometer propagation path on site *San Giuseppe* (right side).

One scintillometer (A) was set up on flat grass land at the valley bottom on one of two meadows near a farm house (site *San Giuseppe*, A2-a and A2-b), see Figure 4.1-3 left side.

Together with scintillometer A, a small instrumental tower was set up for additional temperature measurements. Four PT-1000 temperature sensors (Joung) were installed at levels of 0.8 m, 1.25 m, 2.43 m and 4.8 m, respectively, see Figure 4.1-3 right side.

The second scintillometer (B) was set up in the valley bottom on grass land with a slight slope (site *Torraza*, D) together with a small eddy-correlation tower in the propagation path of the scintillometer, see Figure 4.1-5. The tower was equipped with a sonic-anemometer (Solent R3, Gill) at a level of 5 m during R-IOP1. During R-IOP2 the eddy-correlation tower was additionally equipped with a Krypton hygrometer on the level of the sonic anemometer, see Figure 4.1-6. During two days, scintillometer B was set up at the *San Giuseppe* site A2-a, parallel to scintillometer A. For further details see info Tables 4.1-I and 4.1_II.

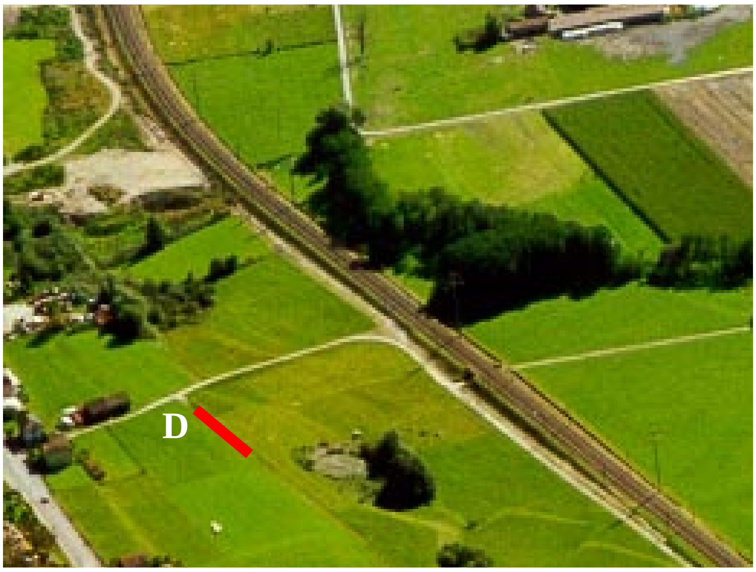

Fig. 4.1-4: Picture of measurement site *Torraza* D, with scintillometer propagation path (red line).

Fig. 4.1-5: Set up of Scintillometer B on site *Torraza* D.

Fig. 4.1-6: Eddy-correlation tower at R-IOP2, equipped with a sonic-anemometer and a Krypton hygrometer at a height of 5 m. This tower was set up at site D in the scintillometer propagation path. During R-IOP1 the tower was equipped only with the sonic-anemometer.

4.1.2 Calibration of the instruments

Relative calibration of the two scintillometers was made during the instrument intercomparison at the airport in San Vittore in July, before the R-IOPs (see Section 7.2). The four temperature sensors on the small instrumental tower were relatively calibrated in a laboratory under different temperatures, so that the data could be depending on the temperature corrected.

4.1.3 Info Tables special observations, scintillometry

The info Tables give an overview of the days and the measuring period (Δt) during these days, on which the two scintillometers and the small instrumental tower were collecting data. Info Table 4.1-I presents R-IOP1 and Table 4.1-II R-IOP2. Time is given in CET. Moreover, the sites, the measurement height *z*, the length of the propagation path *R* of scintillometers are given and additional remarks for the particular day are presented. The remark '*flight day*' means, that on this day additional research flights were made, see Sections 4 and 5 for more details. The remark '*rain*' give the information, that the scintillometer data contains gaps during these periods, because rain was interrupting the laser beam.

Further information about the eddy-correlation tower of site D can been found in Section on the permanent observations 3.1.

Table 4.1-I: Measuring days during R-IOP1, scintillometry

	scintillometer A	scintillometer B	small temp. tower	additional remarks
17.08.1999	z: 1.1m, R: 76m Δt: 12:47-17:38 site: A2-a	---	---	
18.08.1999	z: 1.1m, R: 76m Δt: 09:24-15:34 site: A2-a	---	---	
19.08.1999	z: 1.1m, R: 76m Δt: 08:19-15:32 site: A2-a	---	Δt: 08:19-15:32	
21.08.1999	z: 1.1m, R: 76m Δt: 07:35-17:42 site: A2-a	z: 2.6m, R: 62m Δt: 08:29-24:00 site: D	Δt: 06:57-18:38	* flight day 1
22.08.1999	z: 1.1m, R: 76m Δt: 07:55-17:42 site: A2-a	z: 2.6m, R: 62m Δt: 00:01-24:00 site: D	Δt: 08:03-17:11	* flight day 2
23.08.1999	z: 1.1m, R: 76m Δt: 09:07-13:35 site: A2-a	z: 2.6m, R: 62m Δt: 00:01-24:00 site: D	Δt: 09:48-12:32	
24.08.1999	---	z: 2.6m, R: 62m Δt: 00:01-24:00 site: D	---	
25.08.1999	z: 1.1m, R: 76m Δt: 07:41-17:06 site: A2-b	z: 2.6m, R: 62m Δt: 00:01-24:00 site: D	Δt: 07:42-16:31	* flight day 3

Table 4.1-II: Measuring days during R-IOP2, scintillometry

	scintillometer A	scintillometer B	small temp. tower	additional remarks
21.09.1999	z: 1.1m, R: 77m Δt: 08:23-18:09 site: A2-a	z: 2.6m, R: 63m Δt: 16:41-24:00 site: D	Δt: 08:23-24:00	* flight day 4 * tethered balloon measurements on site A2-a
22.09.1999	z: 1.1m, R: 77m Δt: 09:24-24:00 site: A2-a	z: 2.6m, R: 63m Δt: 00:01-24:00 site: D	Δt: 09:24-24:00	* flight day 5 * tethered balloon and radio sounding measurements on site A2-a
23.09.1999	z: 1.1m, R: 77m Δt: 00:01-15:52 site: A2-a	z: 2.6m, R: 63m Δt: 00:01-16:17 site: D	Δt: 00:01-24:00	
24.09.1999	z: 1.1m, R: 77m Δt: 00:01-15:52 site: A2-a	z: 2.6m, R: 63m Δt: 00:01-16:17 site: D	Δt: 00:01-15:39	
28.09.1999	z: 1.1m, R: 77m Δt: 11:29-16:33 site: A2-a	z: 2.6m, R: 63m Δt: 00:01-24:00 site: D	Δt: 11:29-16:33	* flight day 6 * tethered balloon and radio sounding measurements on site A2a * rain: ~0:00-12:00
29.09.1999	z: 1.1m, R: 77m Δt: 06:52-16:37 site: A2-a	z: 2.6m, R: 63m Δt: 00:01-24:00 site: D	Δt: 06:52-16:37	* flight day 7
30.09.1999	---	z: 2.6m, R: 63m Δt: 00:01-24:00 site: D	---	* rain: ~0:00-12:00 and~15:00-20:00
01.10.1999	z: 1.1m, R: 77m Δt: 07:01-24:00 site: A2-a	z: 2.6m, R: 63m Δt: 00:01-24:00 site: D	Δt: 07:1-16:57	* flight day 8 * tethered balloon measurements on site A2-a
02.10.1999	z: 1.1m, R: 77m Δt: 00:01-16:41 site: A2-a	z: 2.6m, R: 63m Δt: 00:01-24:00 site: D	Δt: 07:13-16:41	* comparison of temperature sensors tethered balloon and temperature sensor 2 of small tower *rain: ~21:00-24:00

4.2 Meteorological Temperature Profiler MTP-5

4.2.1 Introduction

The MTP-5 is a passive microwave sensor, which allows the determination of the air temperature profile from ground up to 600m, at a vertical resolution of 50m and at a time resolution of 5 minutes. It has originally been developped by ATTEX, a Russian company specialised in radiation instrumentation and it is presently being distributed through Kipp&Zonen. It was Kipp&Zonen, through an intervention of Meteodata GmbH and markasub AG that kindly made available an instrument for the MAP-Riviera field campaign, which was used during the two R-IOPs.

As part of the Riviera program, temperature profile observations were made using radio soundings (section 4.3). To investigate the performance of the MTP-5, 28 comparisons were made with the corresponding temperature profiles from the radio soundings at site A1 (Fig. 2.3). These comparisons took place from the 18.8.99 to the 22.8.99 (R-IOP1) and from the 21.9.99 to the 27.9.99 (during R-IOP2) and are reported in section 7.3. Later, the MTP-5 was moved to site D (Fig. 2.3), i.e. closer to the west-facing slope of the valley. Together with the radio soundings (site A1) and the tethered balloon observations (site A2, section 4.4) this allows the investigation of the spatial structure of the temperature filed in the valley.

Fig. 4.2-1 Photograph of the MTP-5 during operation in the Riviera valley, site A1.

4.2.2 The Instrument

The MTP-5 essentially measures the thermal radiation of the atmosphere at the centre of the molecular oxygen absorption band (close to 60 GHz) at different angles. The cover is made of a rotating and an immobile part and was mounted on 3m high mast (Fig. 4.2-1). The thermal radiation of the atmosphere is observed at different elevation angles and reflected to the input of the receiver though a mirror that is located within the rotating part. The scanning of the mirror is carried out from 0° up to 90° in 11 steps under computer control. The amplitude of the observed frequency yields the brightness temperature. From the brightness temperature an inversion procedure (Kadygrov and Pick 1998; Weber 2000) can be applied to obtain the temperature profile. As input, a 'ground temperature' is required, the sensor for which may be seen under the mounting platform in Fig. 4.2-1. Some of the characteristics and specifications of the instrument are listed in Table 4.2-I. The MTP-5 is operating under all weather conditions.

Instrument	MTP-5 ATTEX
altitude range	600 m
Vertical resolution	50m
number of angles measured	11
duration of measurement at every angle	10s
Frequency of observation for an entire profile	Every 5min[1]
nominal height of instrument	3m
accuracy	0.2-0.5°C
Output signal	T/m
Responsible person	Rotach, (ATTEX for technical information)

Table 4.2-I Specifications of the MTP-5 meteorological temperature profiler.

References:

Kadygrov, E.N and Pick, D.R.: 1998, 'The potential for temperature retrieval from an angular-scanning single channel microwave radiometer and some comparisons with in-situ observations', *Meteorol. Appl.*, **5**, 393-404.

Weber, H.: 2000, 'Untersuchung der thermischen Verhältnisse in der Planetaren Grenzschicht im Gebirge mit Hilfe des MTP-5'. Diploma thesis, Institute for Climate Research ETH, 56 pp.

Contact:

Mathias Rotach, Institute for Climate Research ETH (see contact information)

[1] A somewhat higher frequency (up to 2min) is possible, but 5min.was used throughout the MAP-Riviera programmme.

4.3 Radiosoundings

Soundings of the troposphere and lower stratosphere were carried out with Vaisala's RS80 radiosondes and the MW11 receiving system. Sondes were launched from site A1, Bosco di Sotto, starting August 18 (beginning of R-IOP1) through October 1 (end of R-IOP2). Additional soundings from the same site were carried out in the post R-IOP2 phase of MAP.

The analog radiosondes of the series RS80 are equipped with standard PTU sensors and a 8-channel digital GPS receiver (Tab. 4.3-I).

Table 4.3-I: Technical specifications RS80 radiosonde (raw data).

parameter	sensor/receiver	range	resolution	accuracy	sampling frequency	lag
pressure	BAROCAP capacitive aneroid	1060 / 3 hPa	0.1 hPa	0.5 hPa	$1\ s^{-1}$	
temperature	THERMOCAP capacitive bead	-90 / +60 ^oC	0.1 ^oC	0.2 / 0.4 ^oC	$1\ s^{-1}$	3 s
humidity	HUMICAP film capacitator	0 / 100 %	1 %	3 %	$1\ s^{-1}$	1 s
position/wind	GPS			$0.5\ m\ s^{-1}$	$2\ s^{-1}$	

Raw data were automatically edited by the receiving system (quality control, filtering) and stored on PC at 1 s^{-1} frequency (though the wind is sampled at only 0.5 s^{-1}).

From August 18 to October 1, 1999, a total of 69 soundings were carried out (Tab. 4.3-II). During the first three days of operation, difficulties in decoding the GPS information prevented the computation of the wind components (see column GPS in Tab. 4.3-II). Full operability of the wind finding system was recovered on August 24, 1999, following an update of the MW11-hardware and software.

In slightly more than 50% of the soundings, the radio signal was lost before the sonde could reach the tropopause. The reason for the problem is not known.

Table 4.3-II: List of soundings. Column GPS indicates availability of wind data.

sounding number	date (day.month)	start (hr.min, UTC)	stop (altitude, m)	GPS
111	18.08	09.00	7095	NO
112	20.08	12.06	8781	NO
114	20.08	21.19	11038	NO
116	21.08	00.04	12007	NO
117	21.08	06.09	12563	NO
118	21.08	09.02	12388	NO
119	21.08	12.07	14523	NO
120	21.08	15.00	10756	NO
121	21.08	18.08	14857	NO
122	21.08	21.12	6102	NO
123	22.08	00.03	9751	NO
124	22.08	05.58	16537	NO
125	22.08	09.20	11758	NO
126	22.08	12.09	15766	NO
127	22.08	15.00	11886	NO
128	22.08	17.55	14248	NO
129	22.08	21.04	10589	NO
130	24.08	12.06	24580	
131	24.08	17.55	21904	
132	25.08	00.01	11166	
133	25.08	06.00	10407	NO
134	25.08	07.39	8310	
135	25.08	09.15	20995	
136	25.08	12.08	21918	
137	25.08	15.08	7977	
138	25.08	18.00	18720	
139	25.08	21.18	19359	
200	19.09	11.02	6892	
201	19.09	17.14	8737	
202	19.09	23.07	5941	
203	20.09	05.01	3125	
204	20.09	06.08	8158	
205	20.09	11.04	3610	
206	20.09	16.56	10578	
207	20.09	23.14	7890	
208	21.09	05.03	9798	
209	21.09	08.09	15420	
210	21.09	11.03	9030	
211	21.09	13.58	10311	
212	21.09	16.51	6919	

sounding number	date (day.month)	start (hr.min, UTC)	stop (altitude, m)	GPS
213	21.09	22.55	5880	
214	22.09	05.01	9027	
215	22.09	07.58	7010	
216	22.09	10.59	6867	
217	22.09	14.01	7812	
218	22.09	16.58	8992	
219	27.09	11.09	8300	
220	27.09	16.55	6702	
221	27.09	23.03	3164	
222	28.09	05.09	2557	NO
223	28.09	10.55	12389	
224	28.09	14.01	12592	
225	28.09	16.55	9808	
226	28.09	19.55	11232	
227	28.09	22.56	9312	
228	29.09	04.58	9056	
229	29.09	07.58	8215	
230	29.09	10.57	8593	
231	29.09	13.56	9529	
232	29.09	16.58	8305	
233	29.09	22.56	6264	
234	30.09	05.00	4491	
235	30.09	11.08	5356	NO
236	30.09	16.58	6626	
237	30.09	22.58	15496	
238	01.10	04.59	22158	
239	01.10	10.55	17154	
240	01.10	13.55	15452	
241	01.10	16.56	10397	

4.4 Tethered balloon

Tethered balloon profiles were obtained at a gras field near the Ticino River in Claro on September 21, 22, 28, 29, and October 1, all in R-IOP2. The location of the tethered balloon site is given in Figure 4.4-1. Note that the same gras field was also used for scintillometer measurements (see also section 4.1).

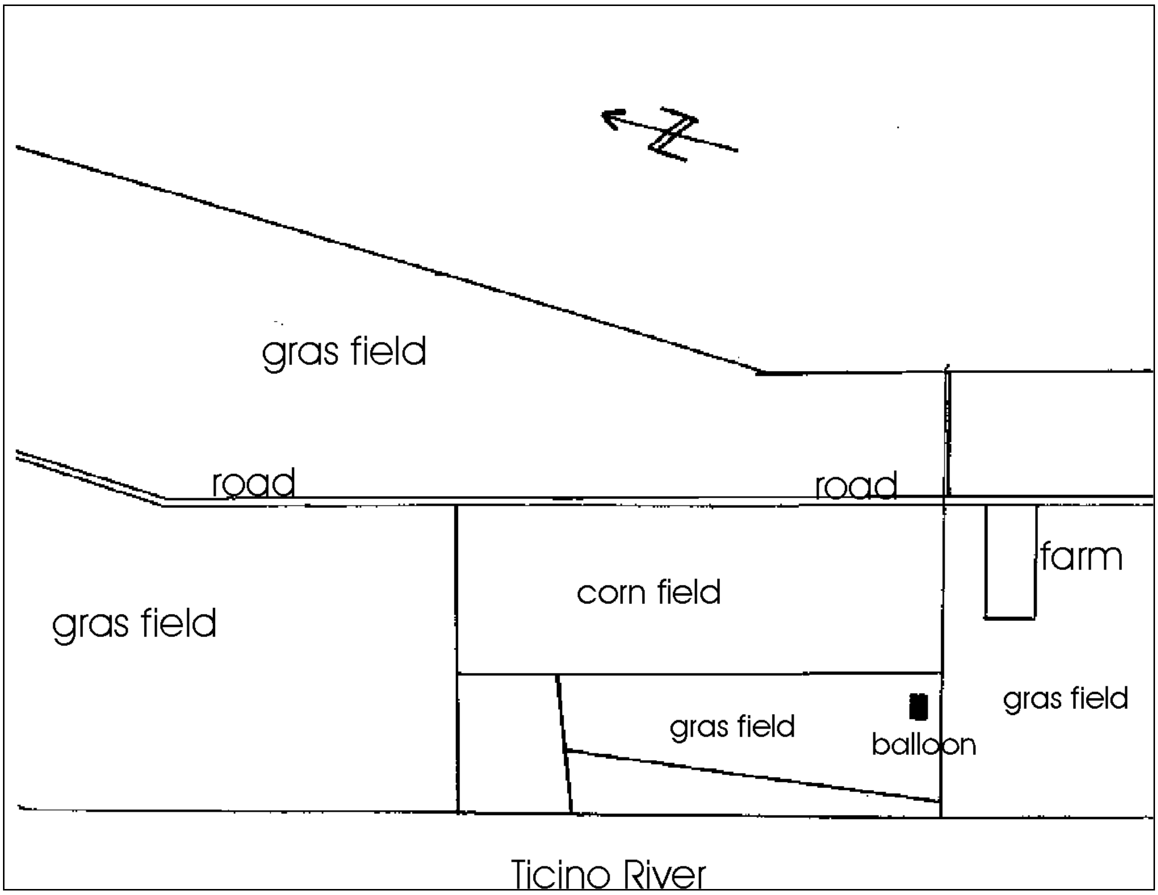

Figure 4.4-1: Location of the tethered balloon site ('balloon').

Soundings consisted of deployment of an Atmospheric Instrumentation Research Inc. (AIR) tethersonde (TS-3A-SPH) beneath a $5m^3$ helium-filled balloon. Ascent and descent were controlled by an electric winch with a typical sounding reaching 800 m. One balloon flight took roughly 30 minutes, 15 minutes for the ascent, 15 minutes for the descent. It was attempted to keep the ascent and descent rate constant but this was not always possible, e.g., when radio transmission errors were present.

The name of the data files has the following convention:

DDMM_XX.DATX

Where:

DD= day of the month

MM= month of the year
XX= flight number

The datafiles contain 9 columns:

Column 1: Decimal Time (UTC)
Column 2: Wind Direction (Deg.)
Column 3: Wind Speed (m/s)
Column 4: Dry Bulb Temperature (°C)
Column 5: Internal Temperature (°C)
Column 6: Pressure (mbar)
Column 7: not used
Column 8: Relative Humidity (%)
Column 9: Height (m)

One datafile contains data of a total flight, i.e., of an ascent as well as a descent. Column 6 and 9 were modified from the original datafiles to account for a drift in the pressure during the time of flight. The data were corrected in a linear fashion. Consequently, the height and the pressure of the first and last data point are exactly the same.

Two tethersondes, numbered 1 and 4 were used. Sonde 1 in particular had some problems with the temperature sensors and temperatures are off by 1-2 °C (as revealed from comparisons with radiosonde data and temperature sensors at the surface, see section 7.4) and the data may not be very reliable. Occasionally, problems with the humidity sensors occurred for both sensors. The details of the problems are not yet understood at this point. Testing of the tethersonde was also performed in a windtunnel and it appeared that wind speeds as measured by the sondes are about 10% too high. Details can be obtained from the contact person.

In table 4.4-I information is given about the start an end time of a flight (in UTC) and the sonde that was used in a particular flight.

Table 4.4-I

9/21/99 flight no,	Start (UTC)	End (UTC)	Sonde no.
1	8:59	9:45	4
2	9:49	10:18	4
3	10:22	10:47	4
4	10:50	11:22	4
5	11:27	11:58	4
6	12:02	12:28	4
7	12:32	12:59	4
8	13:01	13:30	4
9	13:47	14:18	4
10	14:20	14:47	4
11	14:50	15:15	4

12	15:17	15:43	4
9/22/99			
1	7:53	Flight terminated	4
2	8:29	9:02	4
3	9:05	9:34	4
4	9:41	10:11	4
5	10:55	11:25	1
6	12:02	12:35	1
7	13:00	13:28	1
8	13:44	14:21	1
9	15:00	15:23	1
9/28/99			
1	10:50	11:20	1
2	11:26	11:56	1
3	12:05	12:37	1
4	12:51	13:28	1
5	13:43	14:16	1
6	14:26	14:55	1
7	15:21	15:50	1
9/29/99			
1	6:14	6:54	4
2	6:59	7:27	4
3	7:31	8:05	4
4	8:18	8:47	4
5	8:55	9:31	4
6	9:36	10:07	4
7	10:15	10:45	4
8	10:59	11:26	4
9	11:37	12:10	4
10	12:17	12:46	4
11	13:10	13:39	4
12	13:59	14:24	4
13	14:29	15:00	4
14	15:08	15:35	4
10/1/99			
1	6:14	6:43	4
2	6:46	7:13	4

3	7:16	7:47	4
4	7:50	8:19	4
5	8:24	8:54	4
6	9:08	9:37	4
7	9:44	10:25	4
8	10:28	10:54	4
9	10:59	11:27	4
10	11:30	11:56	4
11	12:00	12:30	4
12	12:35	12:59	4
13	13:03	13:29	4
14	13:33	13:58	4
15	14:02	14:30	4
16	14:34	14:58	4
17	15:00	15:27	4
18	15:29	15:51	4

Contact person:

Stephan de Wekker
Atmospheric Science Programme
Dept. of Earth and Ocean Sciences (& Dept. of Geography)
University of British Columbia
#217 - 1984 West Mall
Vancouver, B.C., V6T 1Z2
Canada

e-mail: dewekker@geog.ubc.ca
tel: (604) 822-6407
fax: (604) 822-6150

4.6 SODAR site E1

A SODAR was operated by MCR Lab mainly during the IOPs of the MAP Riviera measuring period. Details can be found in Tab. 4.6.1. The SODAR was placed in *Maruso-Roasco* and a detailed description of the site is given in chapter 3.2.

Fig. 4.6.1: Left: The Flat Array SODAR inside the enclosure. Right: View on enclosure and SODAR at *Maruso-Roasco*.

The SODAR was a monostatic Flat Array Sodar (Scintec FAS64). Its antenna consists of 64 piezoelectric and it was put in a octagonal enclosure (Fig. 4.6.1 right). The SODAR configured with a height dependent resolution, i.e. the highest vertical resolution (10 m) was close to ground and diminished with increasing altitude. Up to ten different frequencies where chosen for one pulse sequence and the number of layers varied between 10 and 13 (Table 6.4.1). The averaging period was 30 min with the exception of 27.8. and 30.8.99 where 20 min averages were sampled.

Tab. 4.6.1: Overview of the settings of SODAR measurements at *Maruso-Roasco*.

Date	Lowest height (m)	resolution (m)	Number of layers	vertical frequency (Hz)	cycle sequence
21.08. 08:00 - 23.08. 19:00 25.08. 06:30 - 19:00 01.10. 07:00 - 02.10. 17:00 07.10. 09:30 - 09.10. 04:00	20 40 80 110 150 200 280 400	10 20 30 40 50 80 120 150	2 2 1 1 1 1 1 4	2022.0 2141.9 2261.9 2381.8 2501.8 2621.7 2741.7 1902.0 1782.1 1662.1 always same sequence for tilted beams (-22°/29°)	**orientation** v N E v S W **number of pulses*:** 1 **frequency:** 1747.8 (Hz) **direction:**29°
21.09. 08:00 - 23.09. 07:00					**orientation** v S E
06.10. 07:30 - 07.10. 09:00					**orientation** v S W
05.10. 08:30 - 06.10. 07:00	20 50 70 100 150 230 350 550	10 20 30 50 80 120 200 150	3 1 1 1 1 1 1 3		**orientation** v S W
27.08. 16:20-17:20 30.08. 11:00-18:20	20 60 100 160	10 20 60 120	4 2 1 3	2022.0 2141.9 2261.9 2381.8 2501.8 2621.7 2741.7 1902.0	**orientation** v N E v S W **number of pulses*:** 1 **frequency:** 1747.8 (Hz) **direction:** 29° * not vertical

5 Research Flights

On a total of eight 'flight days' (see section 8), research flights were performed with an instrumented light aircraft of MetAir GmbH (Fig. 5-1). Type and characteristics of the aircraft are compiled in Table 5-I. The observed parameters and their specifications are given in Table 5-II.

Fig. 5-1 The ECO-Dimona HB-2335 on the airfield Locarno-Magadino. The pots under the wings contain most of the scientific instrumentation.

Table 5-I Specifications of the research aircraft of MetAir

Aircraft	ECO-Dimona HB-2335
Maximum mass (incl. 2 persons, fuel, and up to 130 kg of instrumentation, 2 x 50 kg in pods, and 30 kg in fuselage)	930 kg
Min- / Max- / and normal cruising speed	120 / 260 / 150..180 km/h
Maximum altitude (normally / with oxigen for crew)	4000 mMSL / 8000 mMSL
Climb rate with full weight	3 m/s
Endurance with full equipment or full fuel	4 h / 5 h (depending also on speed, climbs, etc.)

Table 5-II Mesured and recorded parameters on board of MetAir's aircraft "ECO-Dimona HB-2335" (marked yellow: active during MAP-RIVIERA); grey background: planned for 2000)

parameter	**instrument/ method**	**range from..to**	**resolution parameter / time**	**precision / accuracy**	**calibration or checks**
position (x,y,z)	GPS TANS Vector	global	1m / 1s	5..100m[a]	fix points
ground speed (vx, vy)	GPS TANS Vector	global	0.1 ms^{-1} / 1 Hz	0.1..0.5 ms^{-1} [a]	zero and wind
attitude (azi, pitch, roll)	GPS TANS Vector	0..360° / 60°	0.1° / 10Hz	0.1 / 0.5°	fix and wind
acceleration (vert.+long.)	Kistler/DLR	-20..+30 ms^{-2}	0.01ms^{-2} / 10 Hz		
air temperature	Meteolabor thermocouple	-50..50°C	0.1°C / 10Hz	0.1 / 0.5°C[b]	ice-water / mercury
dewpoint	Meteolabor dewopoint mirror	-50..50°C	0.1°C / 1Hz	0.1 / 0.5°C	Psychro-meter
5 pressures (1 absolute, 4 diff.) for ...	Keller capacitve sensors	300-1300; 0..50hPa	0.02hPa / 10Hz	0.1 / 0.5hPa	factory calibrated
...flow angles	differences of pairs (left/right, top/bottom)	-20..20°	0.1° / 0.1s	0.1°/0.5°	wind residuals
...true airspeed,	calculated (p,T,u)	10..70 ms^{-1}	0.1 ms^{-1}/ 10Hz	0.2 / 0.5 ms^{-1}	wind residuals
...and pressure altitude	integrated (p,T,u)	0..7000 mMSL	1m / 4s	3 / 10m	Mountain tops
height above ground	radar altimeter TERRA	15..800m	1m / 1s	1 / 5m	against press. alt.
3-d-wind (x,y,z)	post flight processing from above parameters	0.5..30 ms^{-1}	0.5ms^{-1}/ 10Hz	0.5 / 1.0 ms^{-1}	wind during maneuvers
aerosols (0.3 and 0.5 µm)	MetOne LASER particle counter	0..150 cm^{-3}	1cm^{-3} / 1s	1 / 10cm^{-3}	factory calibration
aerosols (>10 nm)	TSI condensation particle counter	0..1e[4] cm^{-3}	1cm^{-3} / 1 s	1 / 10cm^{-3}	fact.cal. + zero

[a] *depending on the setting by the US military; highest precision available with dGPS within Switzerland, or with other differential references elsewhere.*

[b] *Specification for a sampling rate of 1 Hz. Enhanced noise 10Hz.*

Table 5-2 continued

parameter	**instrument/method**	**range from..to**	**resolution parameter / time**	**precision / accuracy**	**calibration or checks**
O_3 (slow, accurate)	PSI / UV absorption	2ppb .. 1 ppm	1ppb / 4s	1 / 2ppb	cal. gas
O_3 (fast, but, drifting) [c]	Scintrex LOZ-3 (Eosin-Y chemilum.)	1 ppb..1 ppm	0.1ppb / 10Hz	10ppb	against UV-photometer
speciated hydrocarbons (C_4..C_{10})	Gaschromatograph Airmotec HC-1010	10ppt .. 10ppb	10ppt / 10s	10ppt / 50ppt or 20%	cal.gas
NO_2, NO_x, NO_y, HNO_3, PAN, O_x [b]	MetAir-NOxTOy: 6-channel Luminol-detector with CrO_3- and Mo-converters	0.5..500 ppb	0.1 ppb / 1..5 s [d]	0.1 /0.5ppb	NO2 calibration gas
SO_2	FIAMS, Adelaide (Luminol with H_2O_2)	0.5..500 ppb	0.1ppb / 1Hz	0.1 / 1.0ppb	cal. gas
Peroxides (H_2O_2 and organic)	Aerolaser (enzymatic fluorometry)	0.1..20 ppb	50ppt / 10s	0.1 / 0.5ppb	H_2O_2 in water
Formaldehyde (HCHO)	similar as for H_2O_2 (above)				HCHO in water
CO_2	NOAA-IRGA (open path IR-absorption)	200..500 ppm (adj.)	0.1ppm/ 20Hz	0.5 / 1ppm	cal. gas / profiles
H_2O	NOAA-IRGA	0.5..30 gkg^{-1} (adj.)	0.01gkg^{-1} / 20 Hz	0.01 / 0.1gkg^{-1}	against dew point

[c] *The signals of the two monitors are combined to get both fast and stable ozone measurements, overlapping in the range between about 30, and 600 seconds. Instead of O_3 from LOZ-3 we now mostly use O_x-NO_2 from NOxTOy as fast ozone signal.*

[d] *both the resolution, and the accuracy are depending of the channel. The direct channels NO_2 and NO_x are both fast and precise, the channels for NO_y, PAN, and O_x are slower due to higher volumes in the converters, and the differences (PAN = [NO_x+PAN]-NO_x, HNO_3 = NO_y-[NO_y-HNO_3], O_3 = O_x-NO_2) have reduced accuracy of about 1 ppb.*

Table 5-2 continued

parameter	**instrument/method**	**range from..to**	**resolution parameter / time**	**precision / accuracy**	**calibration or checks**
CO_2 and H_2O	LICOR-IRGA	same as IRGA	1 Hz	better than IRGA	same as IRGA
CO	Aerolaser		10 Hz	in evaluation	cal. gas
automatic sampling units for VOC's, biog. VOC's, SF_6, etc.	MetAir / FZJ				
IR-scanner	AGEMA / Univ. Basle				

5.1 Flight patterns

A ‘flight day’ either consisted of a ‘morning flight’, an ‘afternoon flight’ or both. Generally, a flight started and/or ended with a ‘temp’, i.e. a profile flown up to about 4000m or to the ceciling height (PATTERN T). Afterwards, a sucession of two different flight patterns was flown:

- Valley traverses at different heights (Fig. 5-2a) yielding a quasi-stationary valley cross-section of mean flow and turbulence characteristics: PATTERN A.
- Along-valley flight legs close to each of the slopes and in the center of the valley at different heights yielding a three-dimensional picture of the valley turbulence structure (Fig. 5-2b): PATTERN B.

A typical flight then consisted of a succesion of flight patterns such as T-A-B-A-B(-T). Depending on the weather conditions and other considerations, longer and shorter successions were flown during the 8 ‘flight days’. A time-space representation of one one of the flights is given in Fig. 5-3.

The raw data were processed by MetAir to yield time series of the physical variables like wind speed, temperature, etc. Later analysis is presently being undertaken by the Institute for Climate Research ETH.

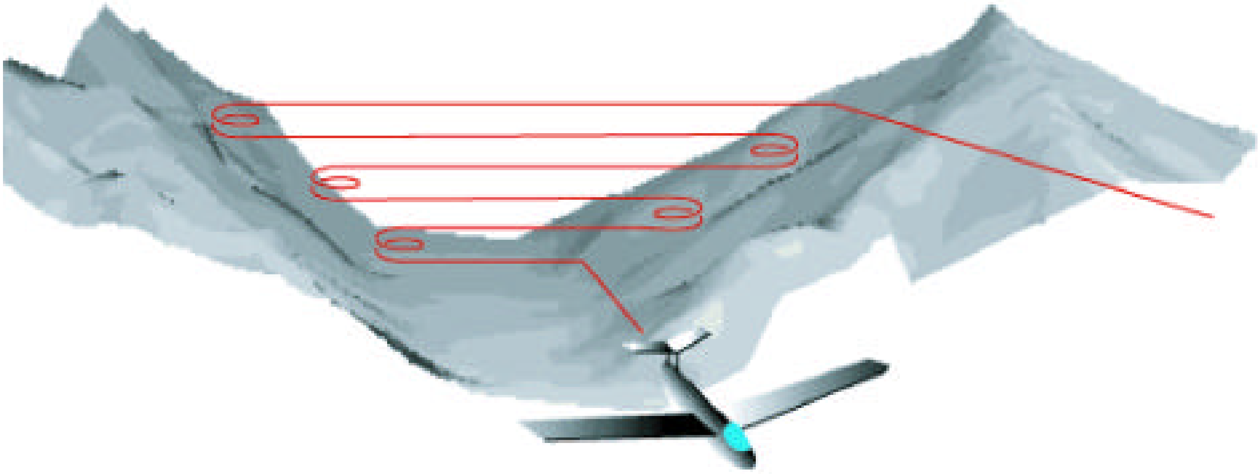

Fig. 5-2a Flight patterns of the research flight during the MAP-Riviera field campaign.
a) cross-valley flight legs (pattern A).

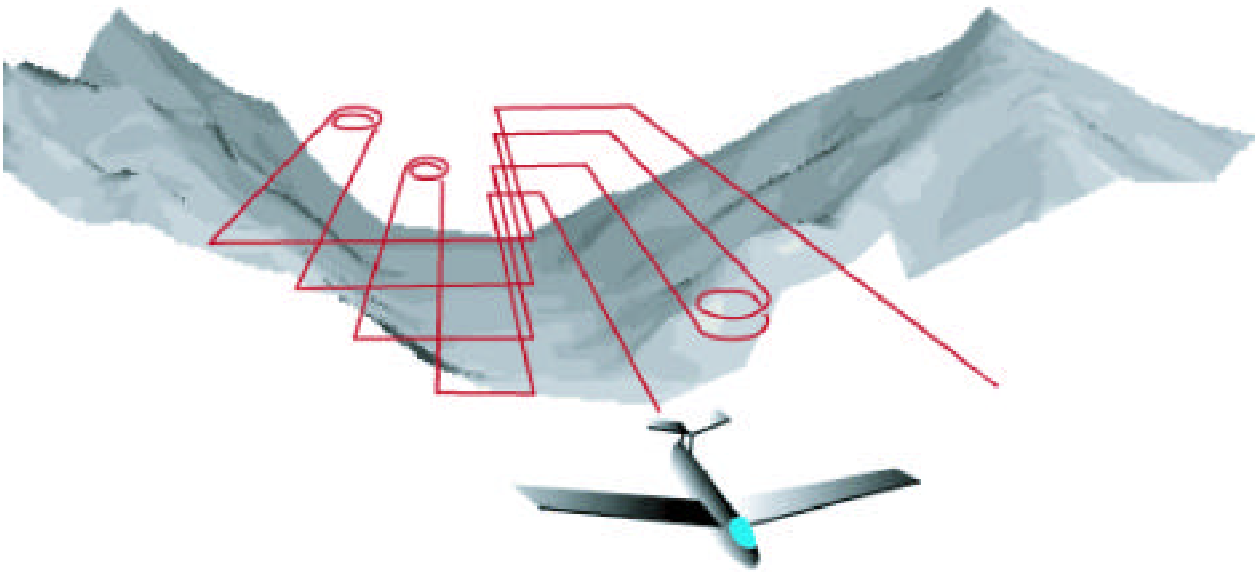

Fig. 5-2b Flight patterns of the research flight during the MAP-Riviera field campaign.
b) along –valley flight legs (pattern B).

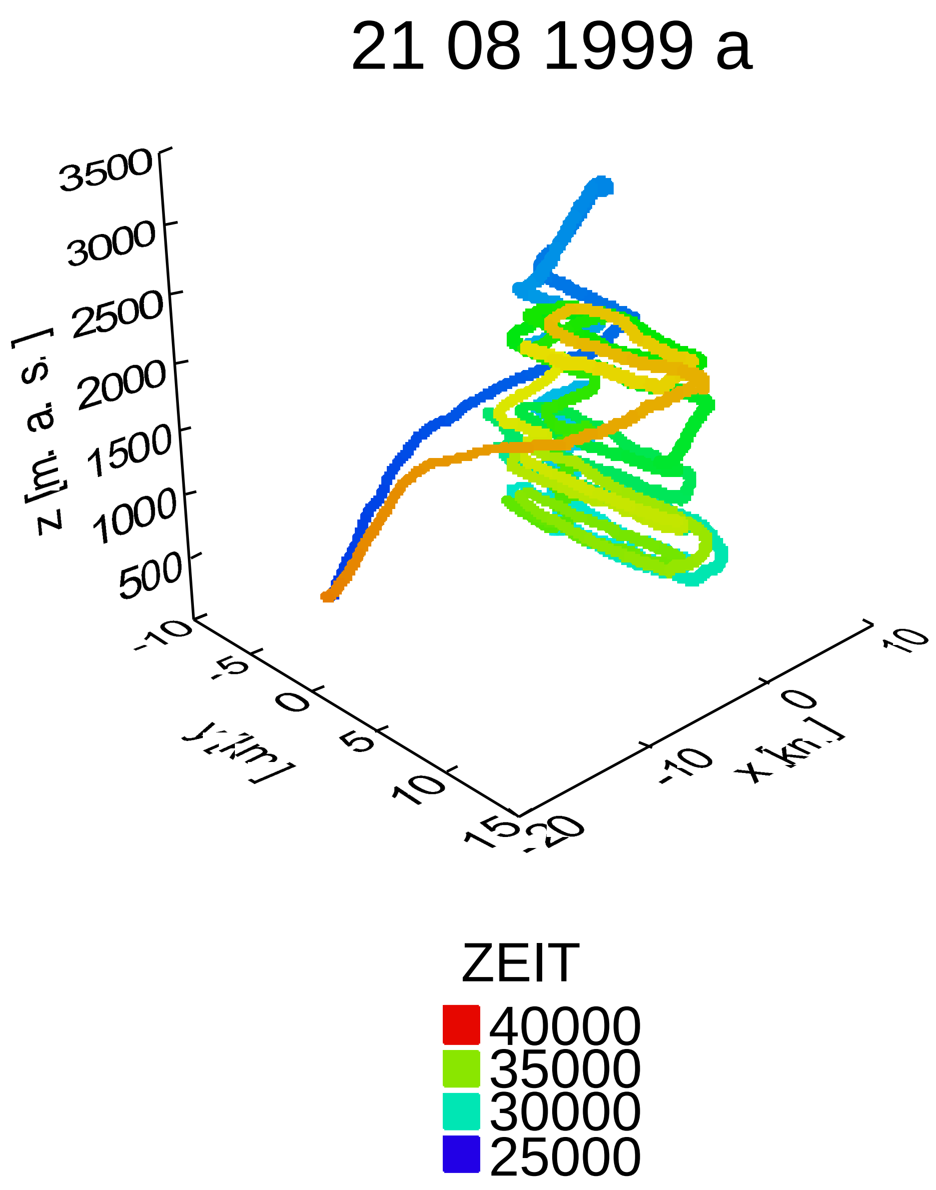

Fig. 5-3 Time-space representation for the morning flight of 21 August 1999. Time is given according to the indicated coloring. This flight corresponds to a succession T-B-A-B.

6 Tracer release experiments

6.1 Overview

The atmospheric tracer technique consists in releasing in the air a substance which is normally absent from air, being neither a natural gas nor a pollutant. The tracer must satisfy certain conditions: it must be non-flammable, non-toxic, non-depositing, chemically inert and not too dense. After being released through a stack, it passively follows air motions. A network of samplers is located around the release point, according to a given geographic distribution. Each of these samplers consists of a series of adsorbing tubes or bags, whose content is analysed afterwards by gas chromatography. In a single sampler, the tubes (or bags) are filled sequentially by air, such that the time evolution of the concentration can be followed at the corresponding point. After completion of the analyses, it is possible to obtain a description of the way the tracer cloud expanded.

The goal was here to observe the fine structure of air motion in the Riviera valley during a thermal circulation episode (valley breeze), following the tracer at a very short distance (< 10 km), both along the axis of the valley and on the slope exposed to the sun.

Table 6-I Position of the samplers on the valley slope (1st and 2nd release). Co-ordinates are given in UTM, which translate into the Swiss co-ordinate system by adding 220 km (X) and by subtracting 5000 km (Y).

Site	X (km)	Y (km)	Elevation a.s.l. (m)
Release	502.3	5122.7	245
Site 01	502.5	5123.0	300
Site 02	502.6	5123.4	310
Site 03	502.7	5123.8	320
Site 04	502.7	5124.5	550
Site 05	502.9	5124.5	620
Site 06	502.4	5125.4	690
Site 07	502.7	5125.9	810
Site 08	503.0	5125.5	970
Site 09	503.2	5125.2	1020
Site 10	503.6	5125.3	1200

Two releases were carried out, on September 29 and October 6, respectively, from a point located near the village of Claro (Swiss co-ordinates X=722.3; Y=122.7). The release took place at 2 p.m. (UTC+2) for both cases, at a height of 5 m above ground, lasted for 25 minutes and was made at a constant rate of 2g/s. For the two releases the maps (Figs. 6-1 and 6-2) show the locations of the samplers that are also reported on the Tables 6-1 through 6-3. Ten samplers equipped with tubes were located on the slope. Each sampler contains 12 tubes programmed to sequentially sample with duration of 20 minutes each. Six samplers equipped with eight bags were placed along the valley; here the sampling time was 30 minutes.

Table 6-II: Position of the samplers along the valley (1st release). See Table 6-I for the definition of the co-ordinates

Site	X (km)	Y (km)	Elevation a.s.l. (m)
Site 01S	502.5	5123.7	300
Site 02S	501.3	5124.0	250
Site 03S	501.1	5123.8	255
Site 04S	498.2	5131.8	275
Site 05S	497.6	5132.6	280
Site 06S	498.7	5132.9	285

Table 6-III Position of the samplers along the valley (2nd release). See Table 6-I for the definition of the co-ordinates

Site	X (km)	Y (km)	Elevation a.s.l. (m)
Site 01S	502.5	5123.7	300
Site 02S	501.3	5124.0	250
Site 03S	501.6	5125.3	260
Site 04S	500.2	5127.7	260
Site 05S	499.2	5130.0	270
Site 06S	498.6	5132.2	280

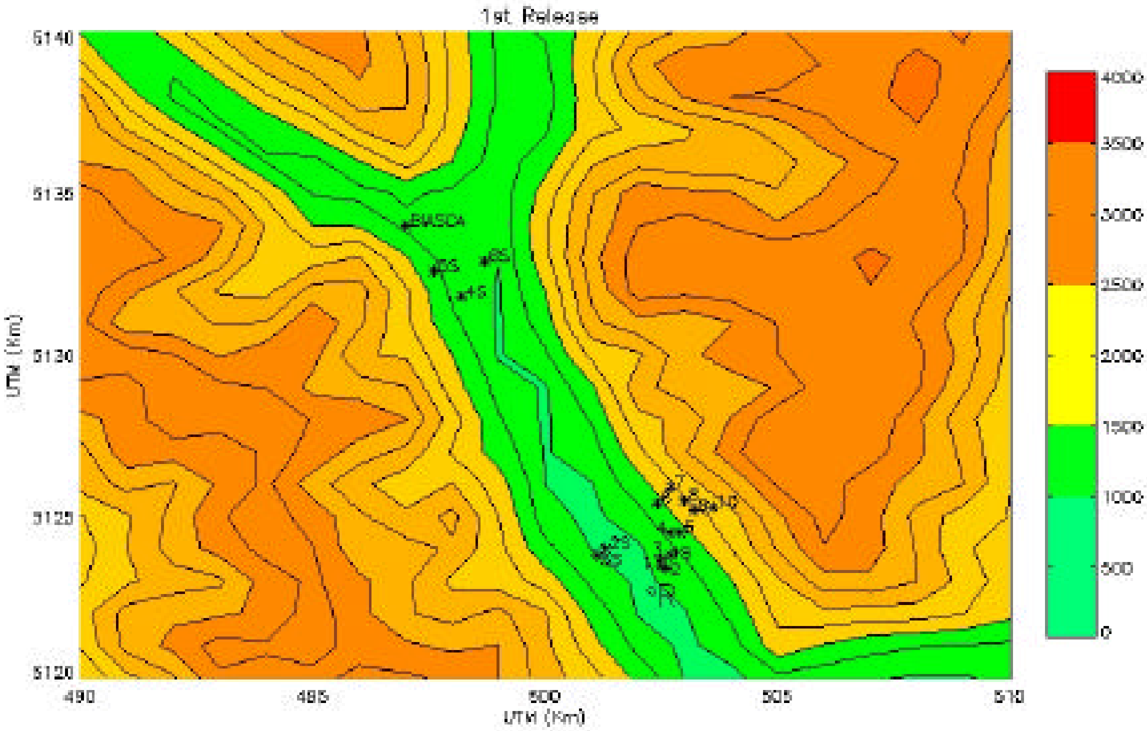

Fig. 6-1 Tracer release point ('R') and the sampler locations for the release of 29 September 1999

6.2 The tracer

The employed tracer belongs to the family of cyclic per-fluoro-carbons (PFCs). The substances are environmentally safe, very stable, non-toxic, insensitive for washing out by rain and detectable by chemical analysis in extremely low concentrations (10-16 v/v, i.e. 1.5 pg/m3). They are colourless and odourless liquids with a high density (1.6-1.8 kg/l) and a relatively low boiling point. They are non-flammable and compatible with almost all materials of construction. PFCs are insoluble in water. They are completely miscible with hexane that is used as a cleaning and rinsing agent for the equipment. The tracer available at the JRC Ispra for use in the MAP-Riviera project, is the Perfluoro-dymethil-cyclohexane (PP3) with the characteristics as described in Table 6-IV.

Table 6-IV Physical properties of tracer liquid

Property	PP3
Molecular weight(g/mol)	400
Density (kg/l)	1.828
Boiling point (°C)	102
Freezing point (°C)	-70
Dynamic viscosity (mPas)	1.919
Surface tension (mNm)	16.6
Vapour pressure (hPa)	48
Heat of vaporisation at boiling point (kJ/kg)	82.9
Specific heat (kJ/kg°C)	0.963
Critical temperature(°C)	241.5
Critical pressure(bar)	18.81
Thermal conductivity (mW/m°C)	60.4
Refractive index ND20	1.2895

6.3 Release equipment

Atmospheric tracers are released as homogeneous air stream containing a few percents of PFC tracer. The release operation consists of the evaporation of the liquid tracer, the mixing of its vapours with a constant stream of air and the injection of the gas mixture into the atmosphere. To this end, liquid PFC is pumped at a controlled flow rate (between 0 and 20 g/s) to an atomiser nozzle, where a spray of fine particles (<70 µm) is formed. This spray is injected into a constant flow of preheated air. The airflow-rate is usually between 40 and 70 Nm^3/h and the temperature is 160-190°C. The flow rate is controlled by the flow rate controller and the control valve. The liquid particles are completely evaporated in this hot air stream and a homogeneous tracer/air mixture is produced, containing between 3 and 10% volume of tracer. The gas stream is passed through a small chimney where the gas is released at the top. The linear velocity of the release is between 30 and 50 m/s and the temperature is 60-80°C. The process of dilution occurs according to a free turbulent jet behaviour, which, leaving an outlet, transfers its momentum to the surrounding fluid. This causes entrainment of surrounding fluid, expansion of the jet and a decrease of the jet velocity. It follows that not higher than 5 meters above the chimney, the tracer injection has lost all its momentum and behaves as still air. From that moment on, it will follow the air movements in the boundary layer.

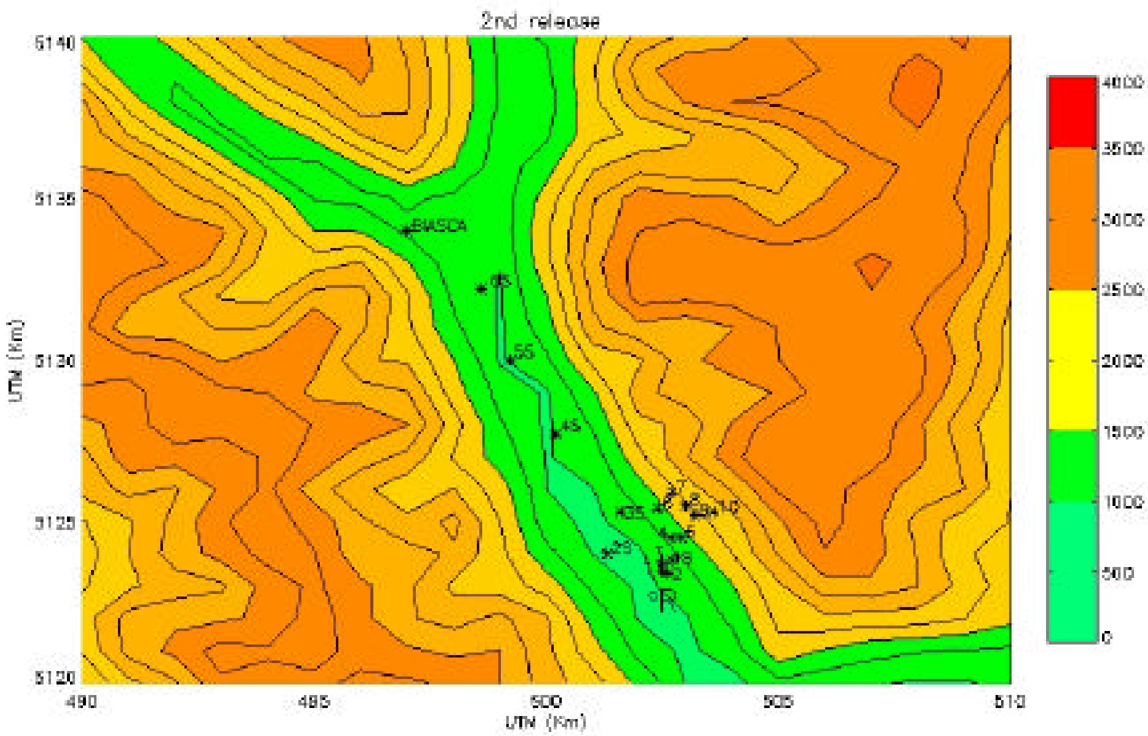

Fig. 6-2 Tracer release point ('R') and the sampler locations for the release of 6 October 1999

Contact (see section 10 for details):

Richard Conolly/ Stefano Galmarini/ Giovanni Graziani (all JRC, Ispra)

7 Instrument intercomparison

7.1 Intercomparison at San Vittore

Ultrasonic anemometers (sonics) are the instruments of choice when the eddy covariance method is applied to measure fluxes. There are different types of sonics available and their design has been improved in the last years. It is, however, still difficult to quantify the uncertainty of sonic measurements e.g. due to flow distortion caused by the probe. There is no standard to compare to and intercomparison studies in real atmospheric flow with different types of sonics are rare. Especially in a study like MAP-Riviera, where the measurements are taken in complex situations (at steep slopes, spatially distributed) it is important to know how the sonics compare to each other. It is of interest, what can be attributed to instrumental effects (e.g. flow distortion, effects due to different sensor design) and what are real properties of the flow. Therefore part of the sonics used in MAP-Riviera were first tested in a wind tunnel and afterwards all were intercompared in a field experiment. Also included in the field tests were the radiations instruments and the cup anemometers from MCR Lab.

The intercomparison took place from July 13 to 16 at the San Vittore airfield.

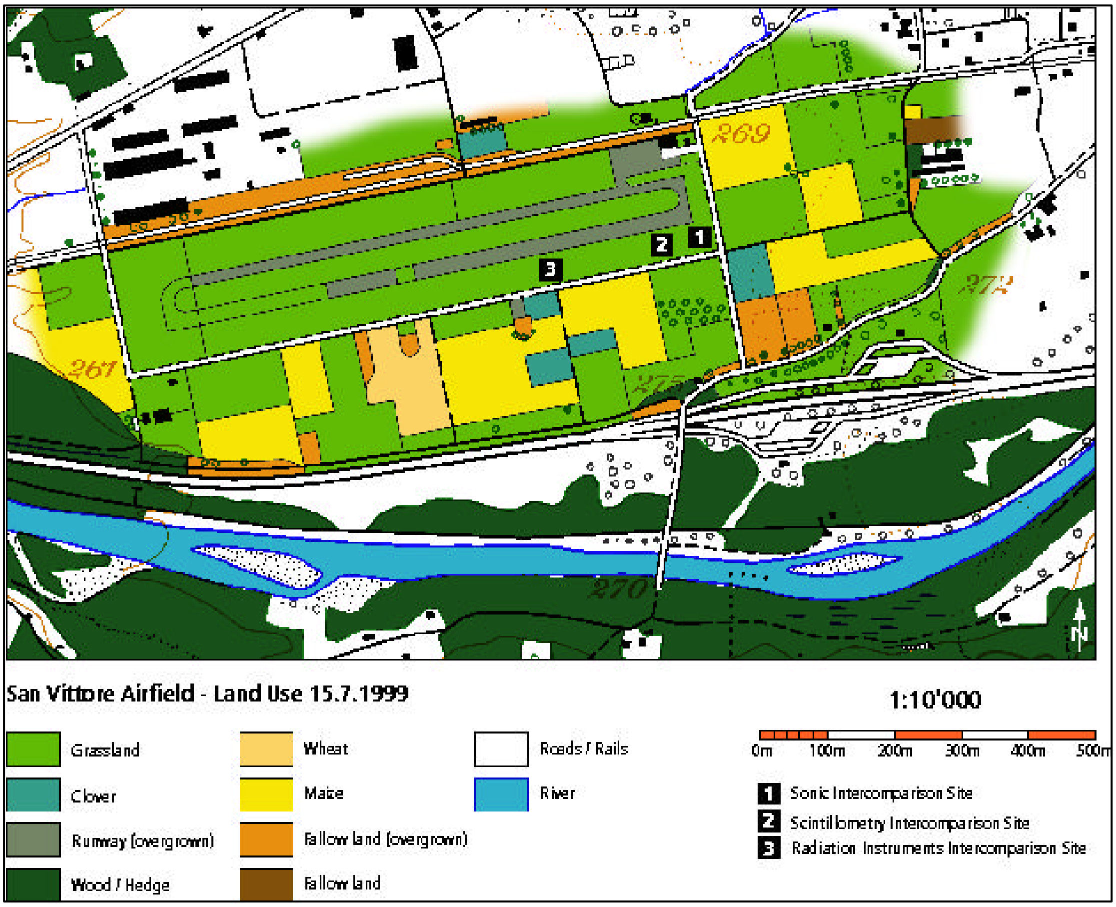

Fig. 7.1-1: Map of the land use around the San Vittore airfield. Base Map: Carta Nazionale della Svizzera 1314 1:25'000, 1998, © Bundesamt für Landestopographie 2000 (JD002102).

The airfield is located 8 km away from the Riviera valley in the Mesolcina valley which is oriented from WSW to ENE. The instruments were placed at the eastern side of the airfield (270 m a.s.l., 46°14'24.6" N, 9°06'0.6"E). An overview on the land-use of the surrounding is given in Fig. 7.1-1 and the roughness features are mapped in Fig. 7.1-2.

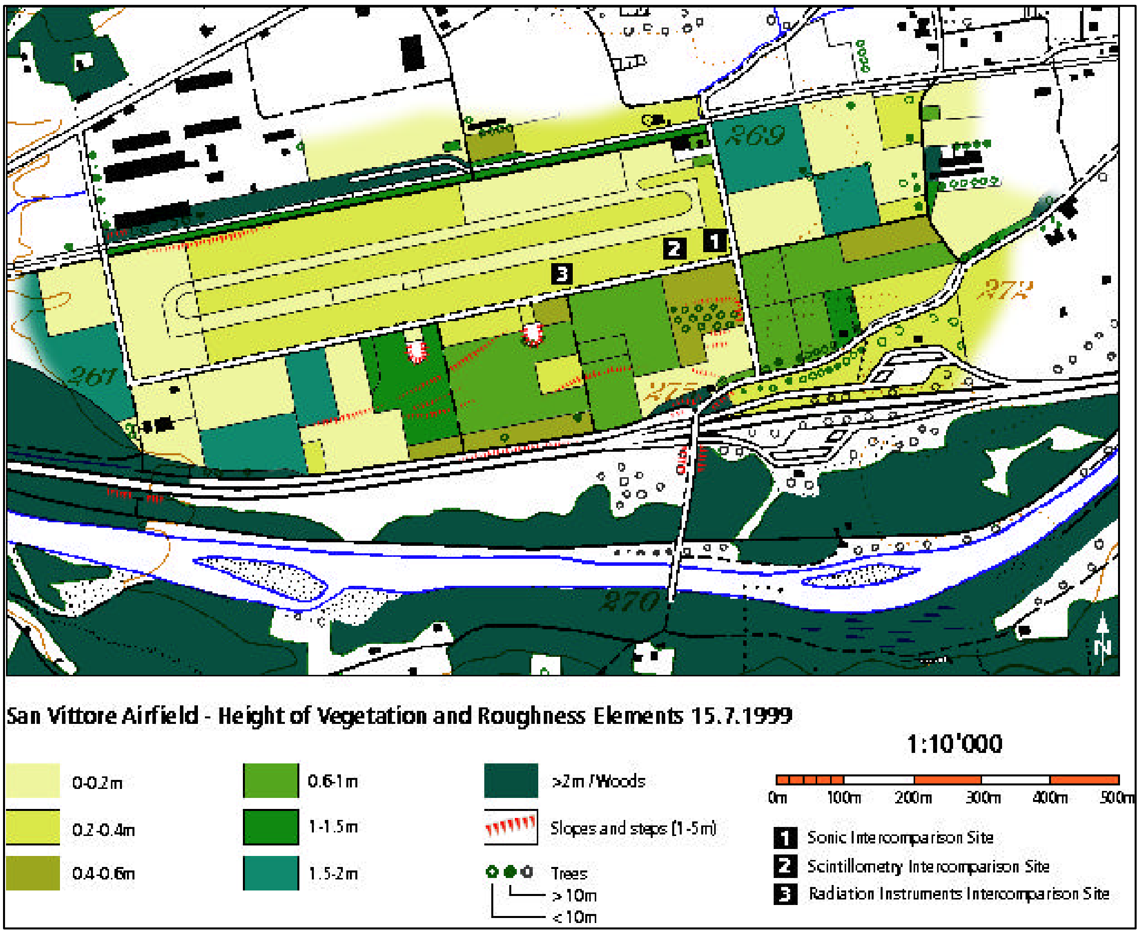

Fig. 7.1-2: Map of the distribution of roughness elements around the San Vittore airfield. Base Map: Carta Nazionale della Svizzera 1314 1:25’000, 1998, © Bundesamt für Landestopographie 2000 (JD002102).

The weather conditions during the intercomparison were generally fine, which can be seen in Fig. 7.1-3.

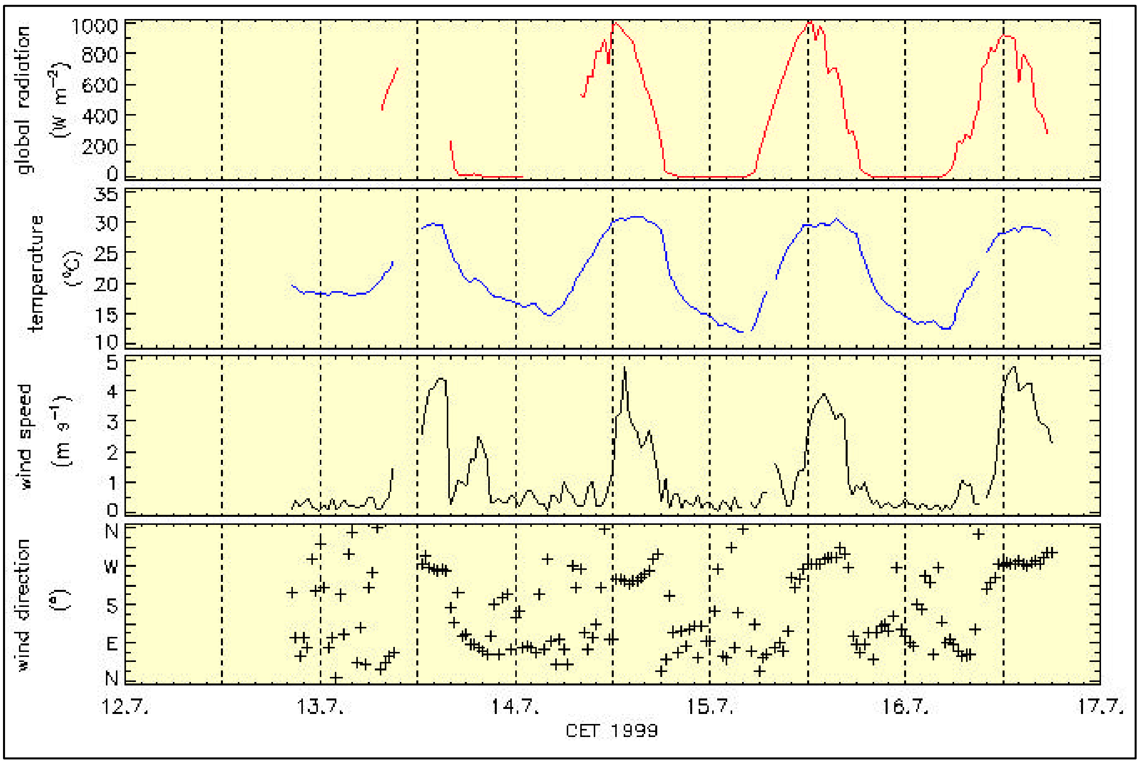

Fig. 7.1-3: Weather conditions during the intercomparison.

7.1.1 Wind tunnel tests

Ten sonics of 7 different designs were characterized in a wind tunnel experiment: 2 Gill R2, 1 Gill R2A, 2 Campbell CSAT3, 3 Metek USA1 (2 different sensor types), 1 Gill HS, 1 Gill R3. The sonics relevant to MAP Riviera are listed in Tab. 7.1-I. All sonics were exposed to 4 wind tunnel speeds (2, 4, 6, 8 ms^{-1}) by rotating them continuously around their vertical axis at eleven different tilt positions: ±25°, ±15°, ±10°, ±5°, ±2.5° and 0°. See Fig 7.1-4 for a view on the experimental set-up in the wind tunnel. Negative tilt means negative vertical component (*w*). The flow distortion effects can easily be visualized and correction matrices are calculated with an azimuth resolution of 4 degrees. This works fine for the tunnel flow but can not be transferred one-to-one to real atmospheric flow.

Tab. 7.1-I: Sketch of sonic types involved in MAP Riviera. All sonics were treated in a way, that an instrument North was defined. The coordinates were transformed so that a wind from North and East gave a positive u- and v-component, respectively.

Campbell CSAT-3, right-handed, instrument North defined towards -u	Gill HS, right-handed, instrument North defined towards +u+.
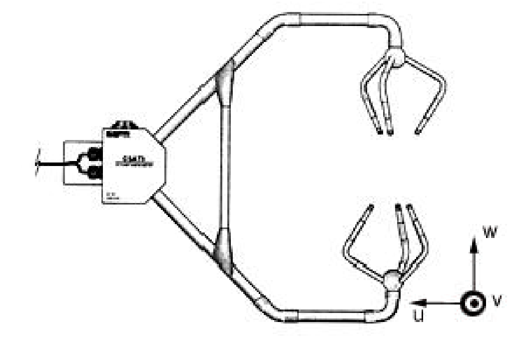	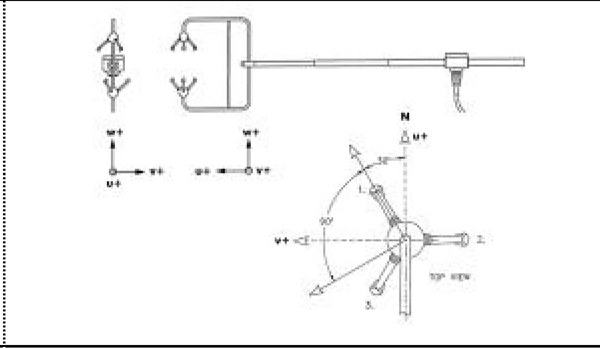
Gill R2, left-handed, -30° offset between instrument North and orientation of u-axis	Metek USA1, left-handed, arrow directs to instrument North.
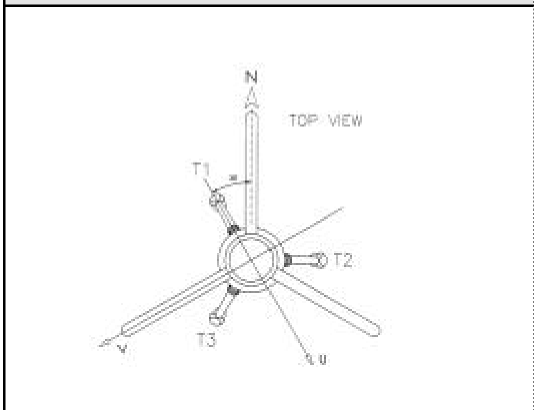	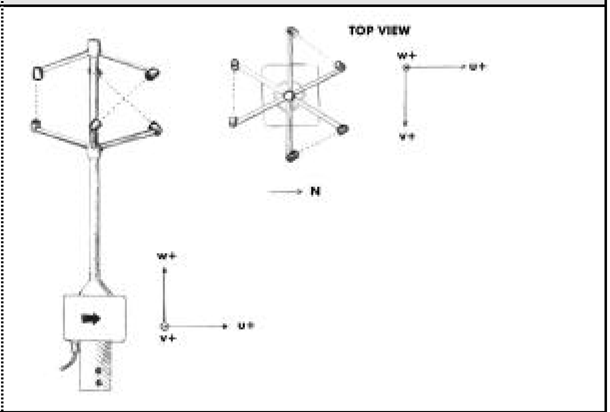

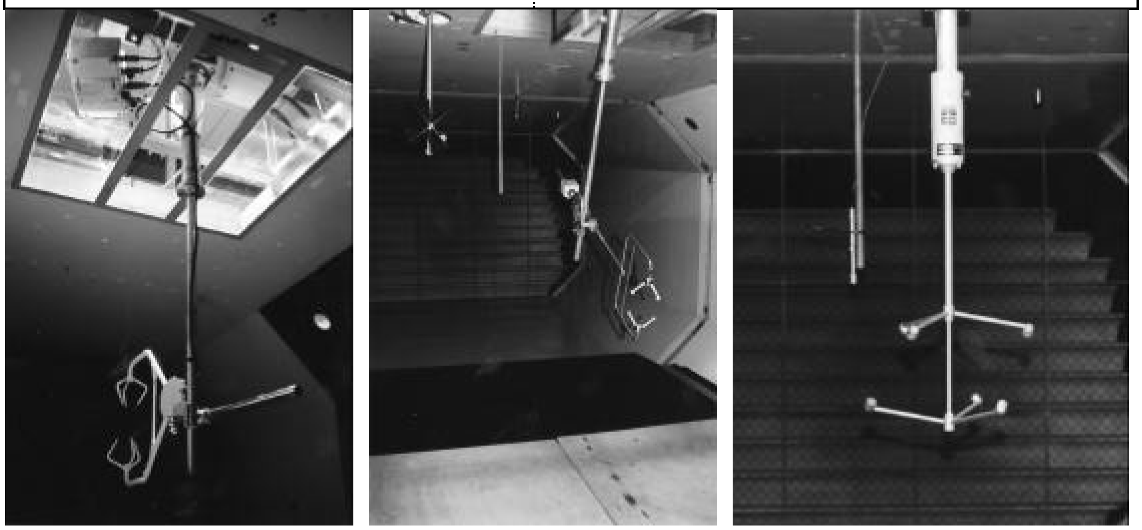

Fig. 7.1-4: Left: Bottom-up view on the rotation tilting device with the Campbell CSAT3. Middle: Gill HS. Right: Metek USA1 mounted upside down. In the same way the Gill R2 and the Gill R3 were mounted.

7.1.2 Sonics

All sonics involved in MAP Riviera were intercompared at the San Vittore airfield. All in all, 18 instruments were operated side by side and raw data were stored for subsequent analysis. In Fig. 7.1-5 an overview on the data availability of the sonics during the intercomparison is given. Figure 7.1-6 gives a view on the instruments and in Fig. 7.1-7 a sketch gives detailed information on position and orientation of the instruments. Three fast UV-hygrometers were also included in the experiment (Tab. 7.1-II). Table 7.1-III lists the details of all sonics, which were compared at the San Vittore airfield.

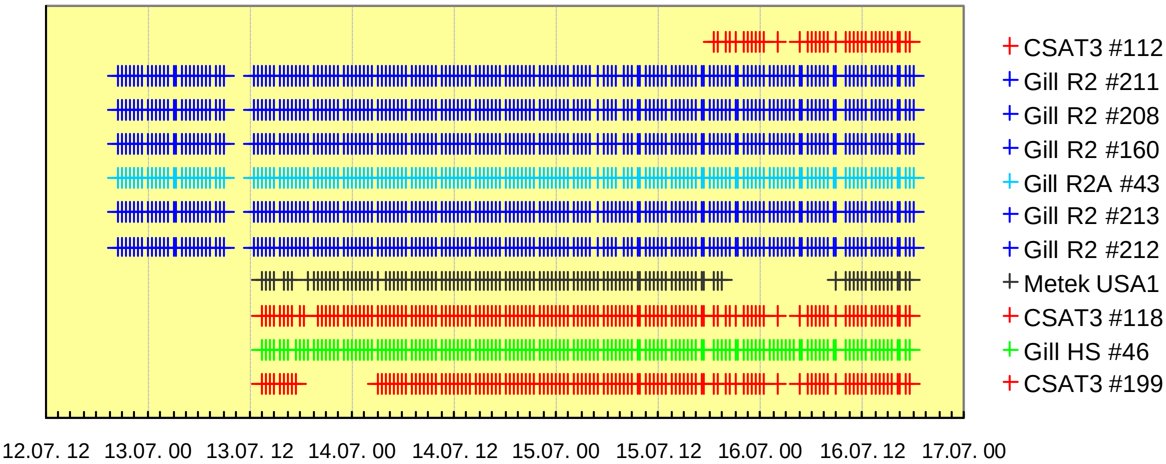

Fig. 7.1-5: Overview on data availability during the intercomparison at the San Vittore airfield (July 1999).

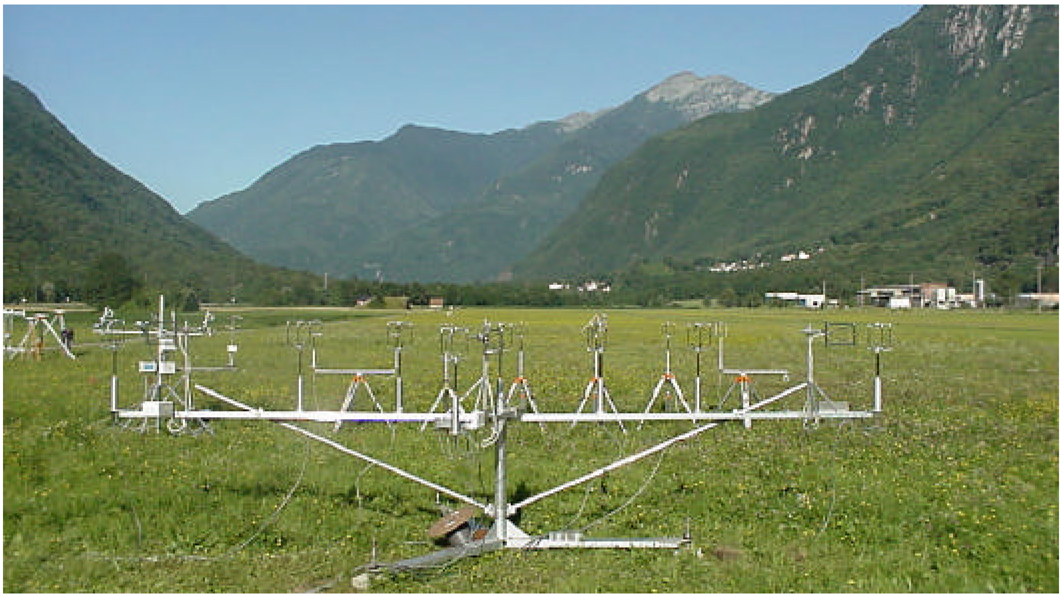

Fig. 7.1-6: View on sonic set-up towards WSW.

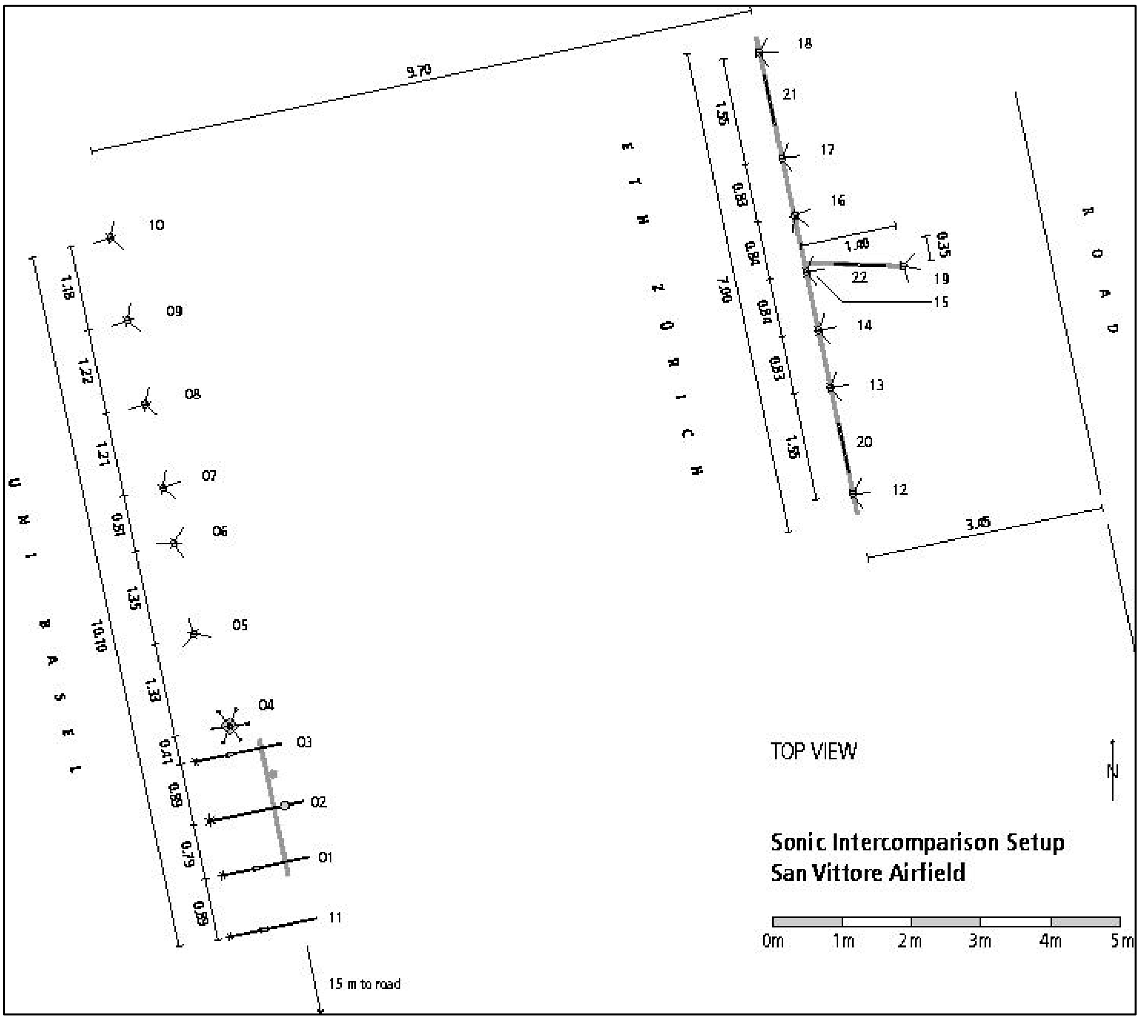

Fig. 7.1-7: Plan of sonic set-up during the intercomparison.

Tab. 7.1-II: Overview on fast hygrometers involved in the intercomparison.

hygrometer type	serial No.	Sampling rate (Hz)	participant	height (m)	position (see map)	distance to sonic (m)
Campbell KH2O Krypton	1300	10	ETHZ	1.80	20	0.4
Campbell KH2O Krypton	1370	10	ETHZ	1.80	21	0.4
Campbell KH2O Krypton	1299	10	ETHZ	1.80	22	0.4

Tab. 7.1-III: Overview on sonics involved in the intercomparison experiment. Columns “position” and “azimuth” refer to periods, where position and/or exposition were changed. (12.-15.7., 15.-16.7., 16.7.).

Sonic type	data mode	serial No.	participant	Sampling rate (Hz)	height (m)	position (see Fig. 7.1.4)	exposition towards (°)
Gill R2A	uvw calibrated	0030	ETHZ	168 / 20.8	1.80	12/12/14	265/260/260
Gill R2A	uvw calibrated	0036	ETHZ	168 / 20.8	1.80	13/13/19	260/78/276
Gill R2A	uvw calibrated	0054	ETHZ£	168 / 20.8	1.80	14/14/12	258/258/260
Gill R2A	uvw calibrated	0055	ETHZ£	168 / 20.8	1.80	15/15/-	260/260/-
Gill R2A	uvw calibrated	0069	ETHZ$	168 / 20.8	1.80	16/16/18	305/305/250
Gill R2A	uvw calibrated	0068	ETHZ$	168 / 20.8	1.80	17/17/17	260/80/260
Gill R2A	uvw calibrated	0047	ETHZ	168 / 20.8	1.80	18/18/16	260/260/260
Gill R2A	uvw calibrated	0035	ETHZ	168 / 20.8	1.80	19/19/13	280/95/260
Gill R2	transit counts	0212	MCR*	168 / 20.8	1.80	05	100
Gill R2	transit counts	0213	MCR *	168 / 20.8	1.80	06	270
Gill R2A	transit counts	0043	MCR	168 / 20.8	1.80	07	250
Gill R2	transit counts	0160	MCR *	168 / 20.8	1.80	08	252
Gill R2	transit counts	0208	MCR *	168 / 20.8	1.80	09	250
Gill R2	transit counts	0211	MCR *	168 / 20.8	1.80	10	252
Gill HS	uvw uncalibrated	000046	MCR	100 / 20	1.82	02	258
Metek USA-1	uvw	9903006	MCR	10 / 10	1.86	04	320
Campbell CSAT3	uvw	0199	MCR	60 / 20	1.86	01	260
Campbell CSAT 3	uvw	0118	MCR	60 / 20	1.84	03	258
Campbell CSAT 3	uvw	0112	UPadova	60 / 20	1.89	-/11/11	-/260/260

*= borrowed from Forschungszentrum Karlsruhe, Institut für Meteorologie und Klimaforschung. £=owned by Paul-Scherrer Institut, $=owned by University of British Columbia.

7.1.3 Cup anemometers

From July 15 13 h to July 16 18 h cup anemometers were intercompared on the airfield. The set-up of the anemometers can be seen in Fig. 7.1.10 and in the sketch in Fig. 7.1.9. As it was planned to carry out measurements on steep slopes the anemometer response in dependence of tilt was tested. For this reason two of the anemometers where tilted by 30 degrees into westward and eastward direction, respectively. After the field phase of MAP Riviera, the dependence on tilt was tested in the wind tunnel of the Forschungszentrum Karlsruhe (Fig. 7.1.8). The results of this experiment are summarized in Fig. 7.1-11.

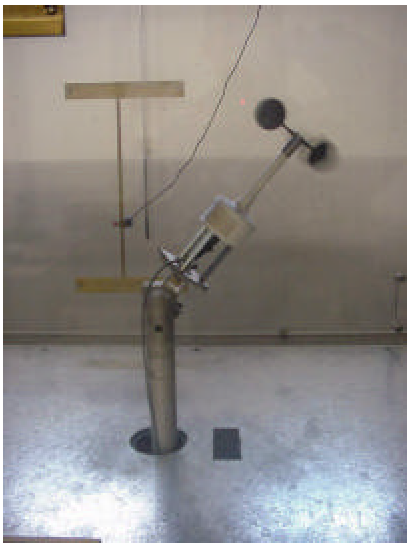

Fig. 7.1-8: Tilted cup anemometer in the wind tunnel.

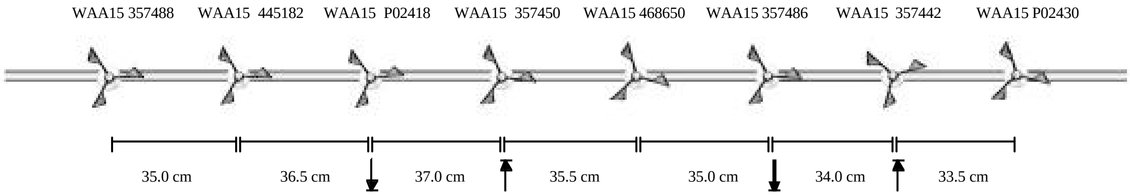

Fig. 7.1-9: View on the set-up of the cup anemometer intercomparison. Arrows indicate inclined anemometers where upwards stands for westward direction.

Fig. 7.1-10: Cup anemometer intercomparison.

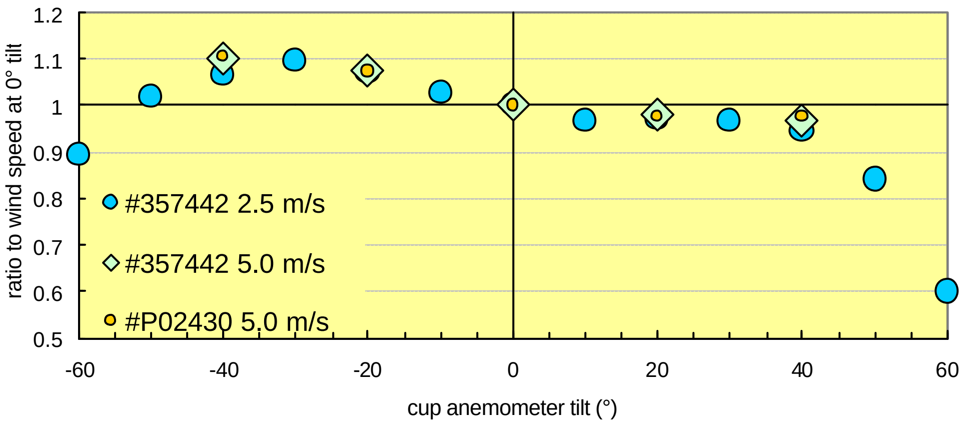

Fig. 7.1-11: Effect of tilt-angle on measured wind speed from cup anemometers. Negative angle means tilt towards the wind.

7.1.4 Radiometers

All radiometers which were used at sites E to G were operated side by side during the intercomparison at San Vittore. A view on the experimental set-up is given in Fig. 7.1-12 and a sketch on details of positions in Fig. 7.1-13. In Tab. 7.1-IV all radiometers are listed and the data availability is depicted in Fig. 7.1-14.

Reference for the long-wave range were two pyrgeometers (Eppley PIR) and for the short-wave range two pyranometers (Kipp & Zonen CM21). These instruments were calibrated at the World Radiation Centre in Davos. The net radiometers of type CNR1 combines two pyranometers and two pyrgeometers on one block. Each component of the radiation balance can be measured separately.

Fig. 7.1-12: View on radiometers during the intercomparison.

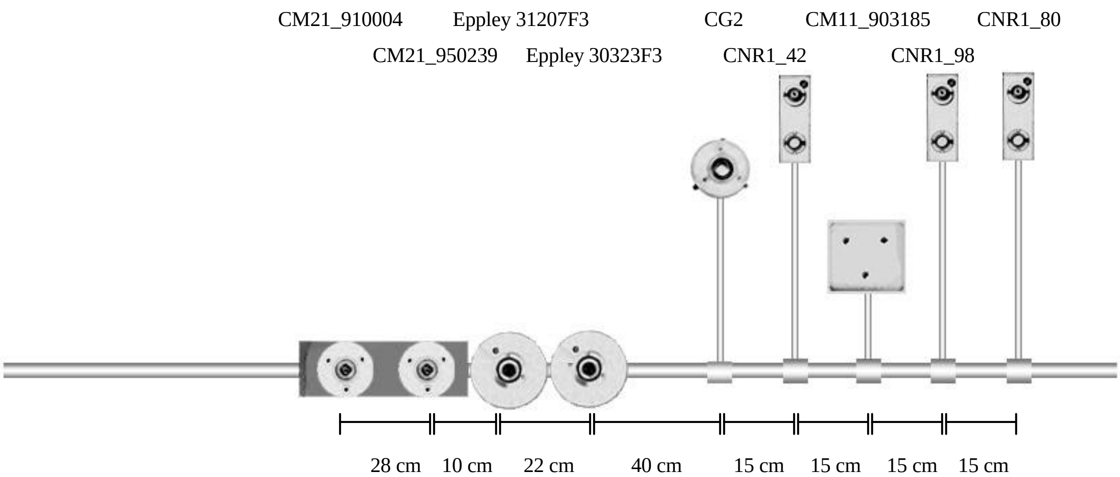

Fig. 7.1-13: Top view of the set-up of radiometer intercomparison.

Tab. 7.1-IV: Overview on radiometers involved in the intercomparison.

instument	manufacturer/type	serial number
pyrgeometer	Eppley PIR	#30332F3, #31207F3
net pyrgeometer	Kipp & Zonen CG2	#970042
net radiometer	Kipp & Zonen CNR1	#42,#80, #98
pyranometer	Kipp & Zonen CM21	#910004, #950239
pyranometer	Kipp & Zonen CM11	#903185

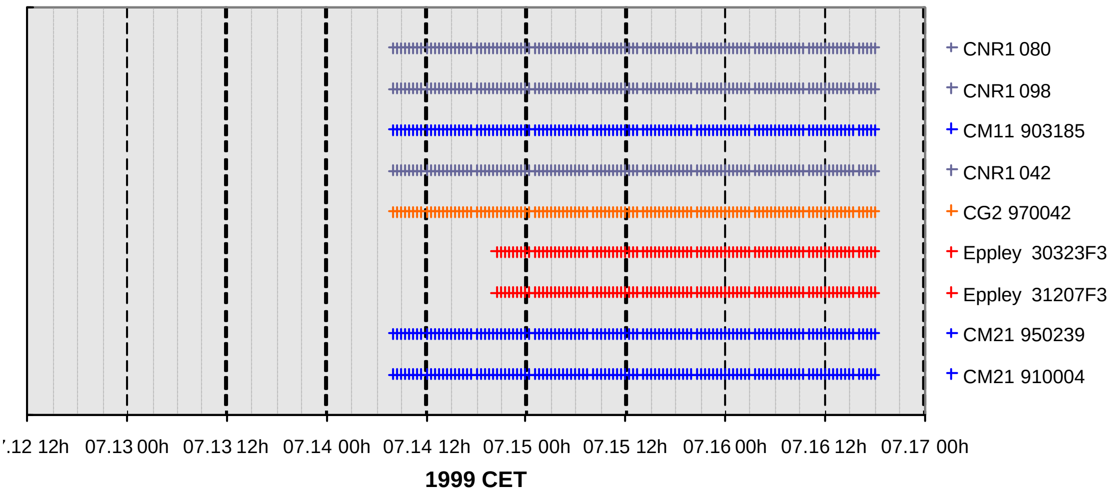

Fig. 7.1-14: Overview on the data availability of the radiometer intercomparison.

7.2 Scintillometers

Three displaced beam scintillometers were compared on the airport of San Vittore, see Figure 7.2-1. Due to technical problems, only two were set up during the Riviera Project and the following results of the instrument intercomparison are of these two scintillometers (A and B).

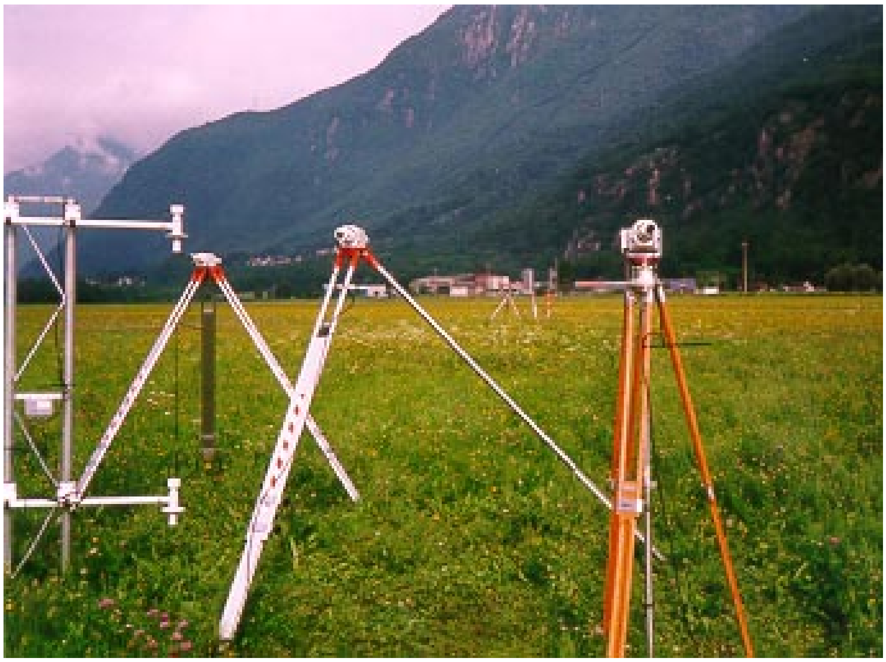

Fig. 7.2-1: Set up of displaced beam scitillometers during the instrument intercomparison, with small instrumental tower. Length of the propagation path *R*= 60m.

7.2.1 Results intercomparison scintillometer:

During two days (13.07.1999 and 14.07.1999) Scintillometer A and B were set up with parallel propagation path of length R = 60 m in San Vittore. Measurement high of scintillometer A was 1.75 m, and of scintillometer B 1.80 m. The set up of the sonic-anemometer intercomparison was about 30 meter displaced from the scintillometers.
Fig. 7.2-2 shows a comparison of the derived sensible heat flux H and momentum flux M of scintillometer A versus scintillometer B. All data, with more than 30% error free diagnosis data are presented. Averaging time is 30 minutes. The correlation coefficient for the comparison of H is 0.997, for the comparison of M is 0.849.

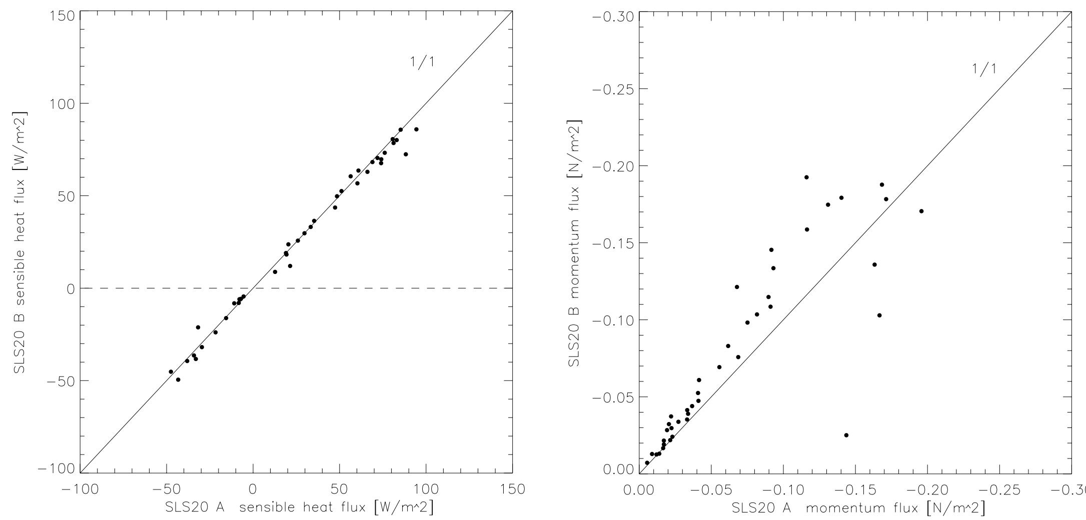

Fig 7.2-2: Comparison of sensible heat and momentum flux derived from scintillometer A versus B, measured on the 13.07.1999 and 14.07.1999 in San Vittore. Only data with more than 30% error free diagnosis data are presented, averaging time is 30 min.

7.2.2 Results intercomparison scintillometer versus sonic-anemometer

The derived turbulent fluxes of scintillometer A and B were primarily compared with the sonic-anemometers A-J. Figure 7.2-3 shows the comparison of the sensible heat flux derived from the two scintillometers versus sonic-anemometer A-J. The Figure shows the comparison for different atmospheric stabilities: unstable (z/L<-0.05), near neutral (-0.05<z/L<0.05) and stable (z/L>0.05), respectively. Figure 7.2-4 presents the same comparison for the derived momentum fluxes.

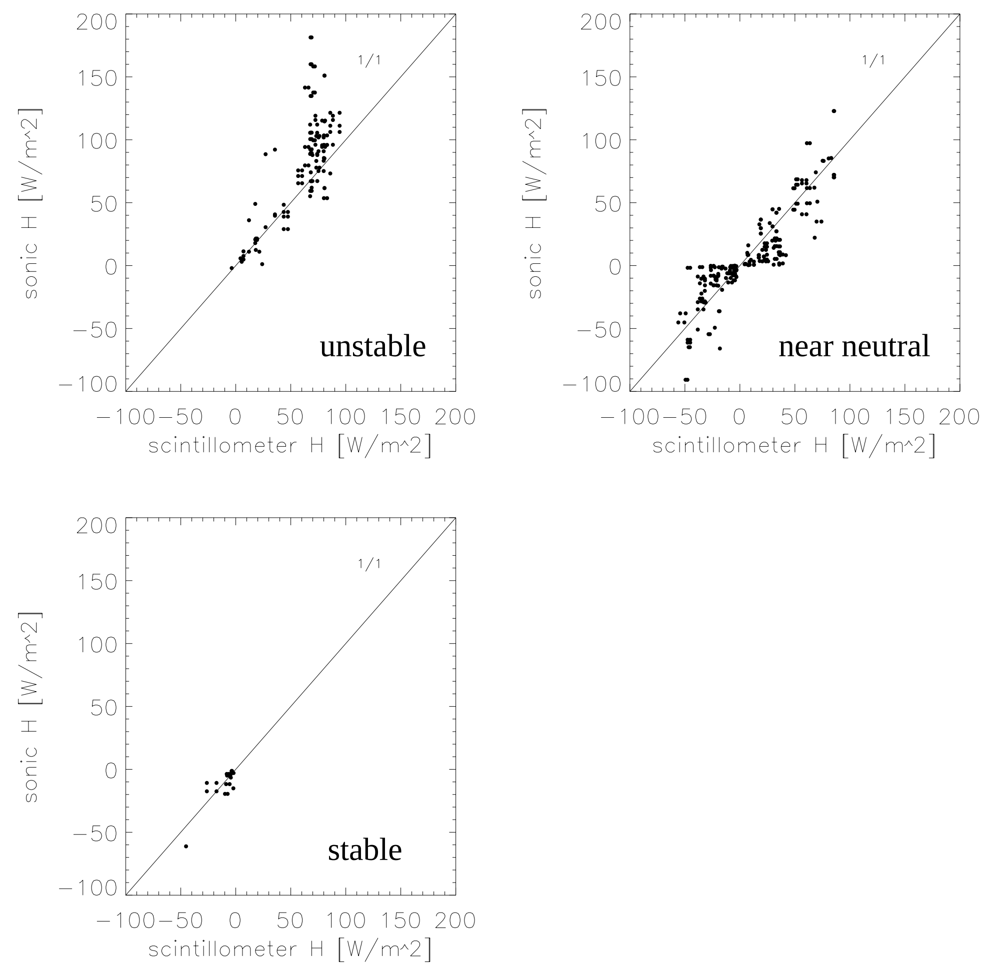

Fig 7.2-3: Comparison of sensible heat flux scintillometer (A and B) versus sonic-anemometer (A-J) for different atmospheric stabilities (unstable, near neutral, stable).

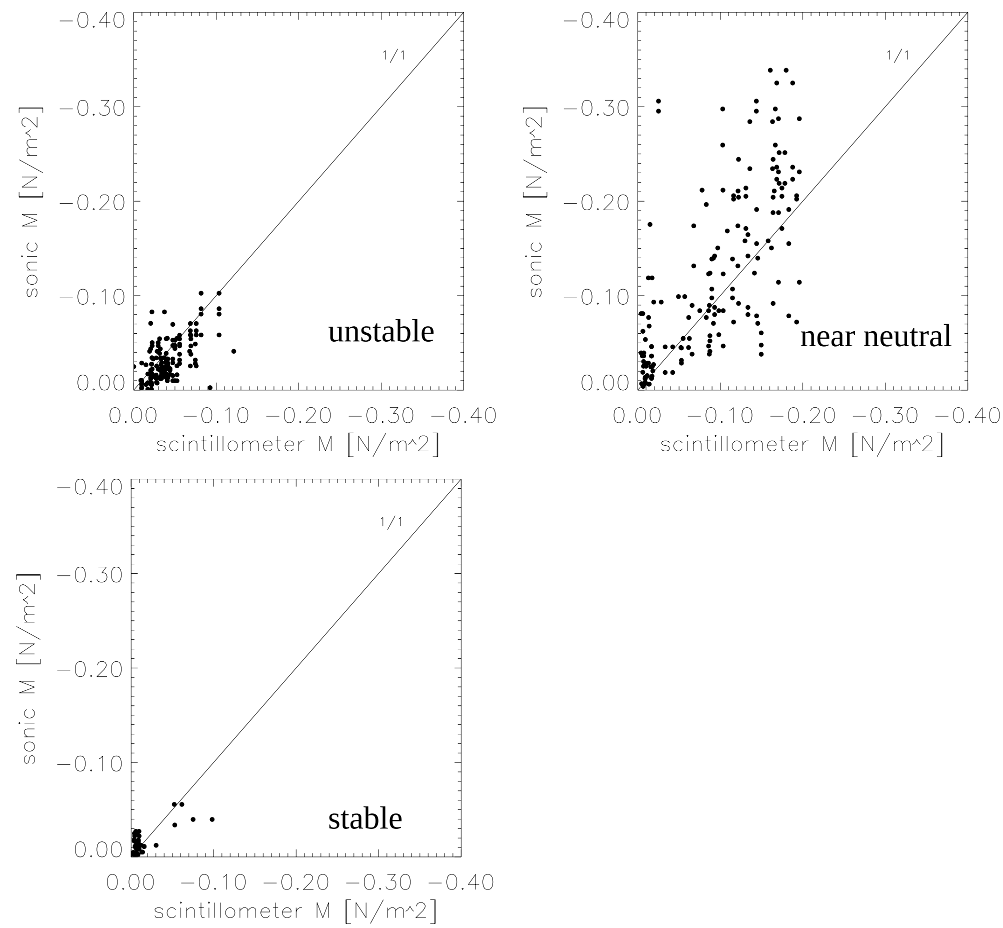

Fig. 7.2-4: Comparison of momentum flux scintillometer (A and B) versus sonic- anemometer (A-J) for different atmospherics stabilities (unstable, near neutral, stable).

THE THERMAL STRUCTURE OF THE ATMOSPHERIC BOUNDARY LAYER IN AN ALPINE VALLEY: RESULTS OF CONTINUOUS REMOTE SENSING MEASUREMENTS AND COMPARISON WITH RADIO SONDE DATA

Evgeny Kadygrov, Vladislav Kadygrov, Evgeny Miller (Central Aerological Observatory, 3 Pervomayskaya Str., Dolgoprudny, Moscow region, 141700 Russia, E-mail: attex@gin.global-one.ru)

Heidi Weber, Mathias W. Rotach (Swiss Federal Institute of Technology, Institute for Climate Research, Winterthurerstrasse 190, CH-8057 Zurich, Switzerland, E-mail: rotach@geo.umnw.ethz.ch)

ABSTRACT

During the field phase of the Mesoscale Alpine Program (MAP) in fall of 1999, the microwave remote sensing temperature profiler (MTP-5) was used for continuous measurement of temperature profiles at an altitude range 0÷600 m. More than 7000 temperature profiles were obtained during the observational period, which gave very useful information for the investigation of the atmospheric boundary layer (ABL) in mountainous regions. A comparison with 52 ascents of radio sondes shows that the rms difference between the two systems was always better than 1K. Examples of time-height cross sections taken during the period of substantial change in ABL temperature structure within the valley atmosphere are presented. These include the characteristics of the (nocturnal) temperature inversion and the temperature regime during the evolution of a typical wind system.

1. INTRODUCTION

MAP has been organised and designed to advance the boundaries of our knowledge and the forecasting capability in mesoscale mountain meteorology. One of the scientific objectives of MAP is to investigate the structure and evolution of the planetary boundary layer (PBL) in complex terrain and its effect on alpine weather systems.

Recognising that thermal radiation fluxes are a major component of atmospheric models, a mobile radiometric system MTP-5 for continuous measurement of atmospheric boundary layer temperature profiles was in August-October 1999 in connection with the MAP-Riviera project (Fig.1).

Fig.1 MTP-5 at the MAP-Riviera project (village Claro, Switzerland, August – October, 1999)

2.INSTRUMENT DISCRIPTION

The instrument used was an angular-scanning single-channel microwave radiometer MTP-5 – commercially produced by the Russian firm ATTEX. This radiometer operates at a central frequency of 59,6 GHz. The sensitivity of the instrument is 0,04K for an integration time of 1 second and a cycle time of 300 seconds for one full profile observation. The vertical resolution is 50 m and the accuracy is specified at 0,5K rms up to 600 m (vertical range) [1, 2].

During the field phase the MTP-5 was installed in the valley near by the 28-m meteorological tower and the radio sonde release station. The period of observation was were obtained from the MTP-5, including 2441 with a temperature inversion. Some statistics of the MTP-5 data quality are shown in Table 1.

Table 1.Statistic of MTP-5 operation in Claro

	Profiles	%
Measured	7231	100
With inversion > 1°C	2441	33
Failure	21	0.3

3. RESULT OF COMPARISON

Previous comparisons of MTP-5 data with those from radio sonde, tethered balloons, meteorological towers, lidar and RASS are described in [3,4].

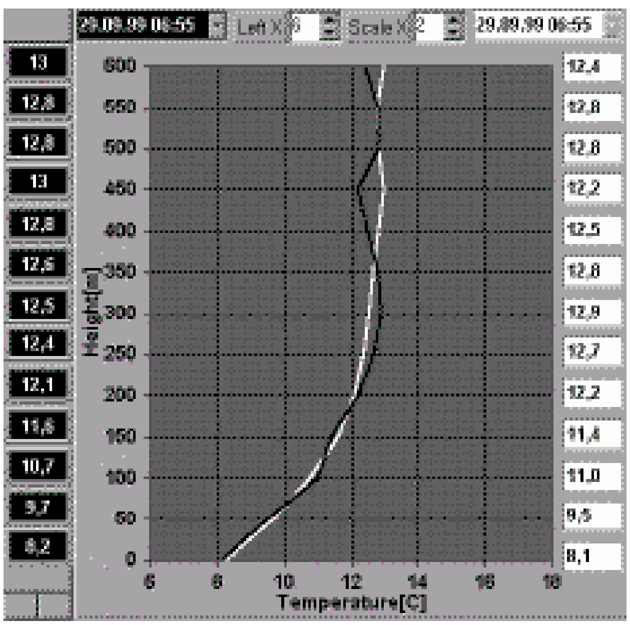

Fig. 2 Example of the comparison of MTP-5 temperature profile data (white) and radio sonde data (black)

In a first step of the MAP–Riviera project, the remote sensing data from MTP-5, which is a relatively new instrument, were compared with simultaneous radio sonde data from the same site. The total number of released radio sondes was 52, and in Fig. 2 an example for such a comparison (temperature profile with inversion) is shown. Some statistical results of the comparison (with 12 radio sonde profiles) are shown in Fig. 3.

The rms difference between the two systems is found to always be better than 1 K. Having yield continuous observations between the radio soundings, which are necessarily discrete in time.

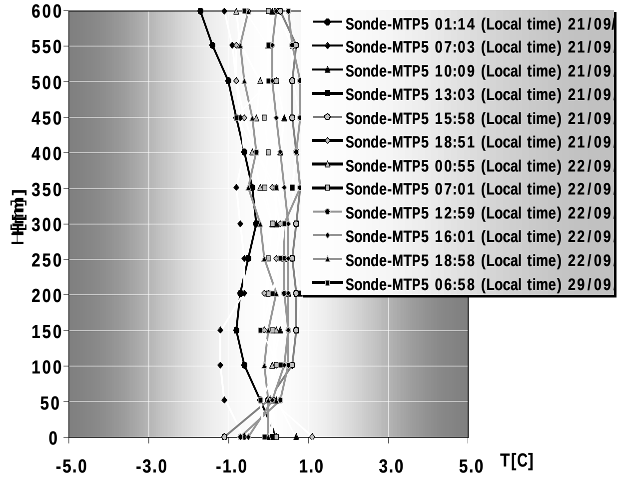

Fig. 3 Some results of comparison MTP-5 data and radio sonde data

4. RESULT OF MEASUREMENTS

One of the advantages of the 5-mm radiometric data is its continuity in time under all meteorological conditions, which allows time series and time-height cross sections to be delivered.

In Fig. 4 and Fig. 5 the temperature time-height cross sections derived by the MTP-5 instrument and some statistical parameters of the temperature inversion are presented. For profiles with a temperature inversion, the temperature difference across inversion (MaxInv, [°C], left scale) was estimated as well as the height of inversion base (Height [m], right scale). During the period of observation there were no multi-day inversions. The maximum of temperature difference across the inversion (9,8°C) was observed at 06.10.99 in 05:55 local time with the height of inversion base 350 m.

The Continuous measurements allowed to for estimating the temperature inversion in a mountainous region. A specific feature of temperature inversion in mountainous regions is the fact that the temperature inversion usually starts by a fast reduction of ground temperature at about 16:00 local time thereby inducing a large day-night temperature variation close to

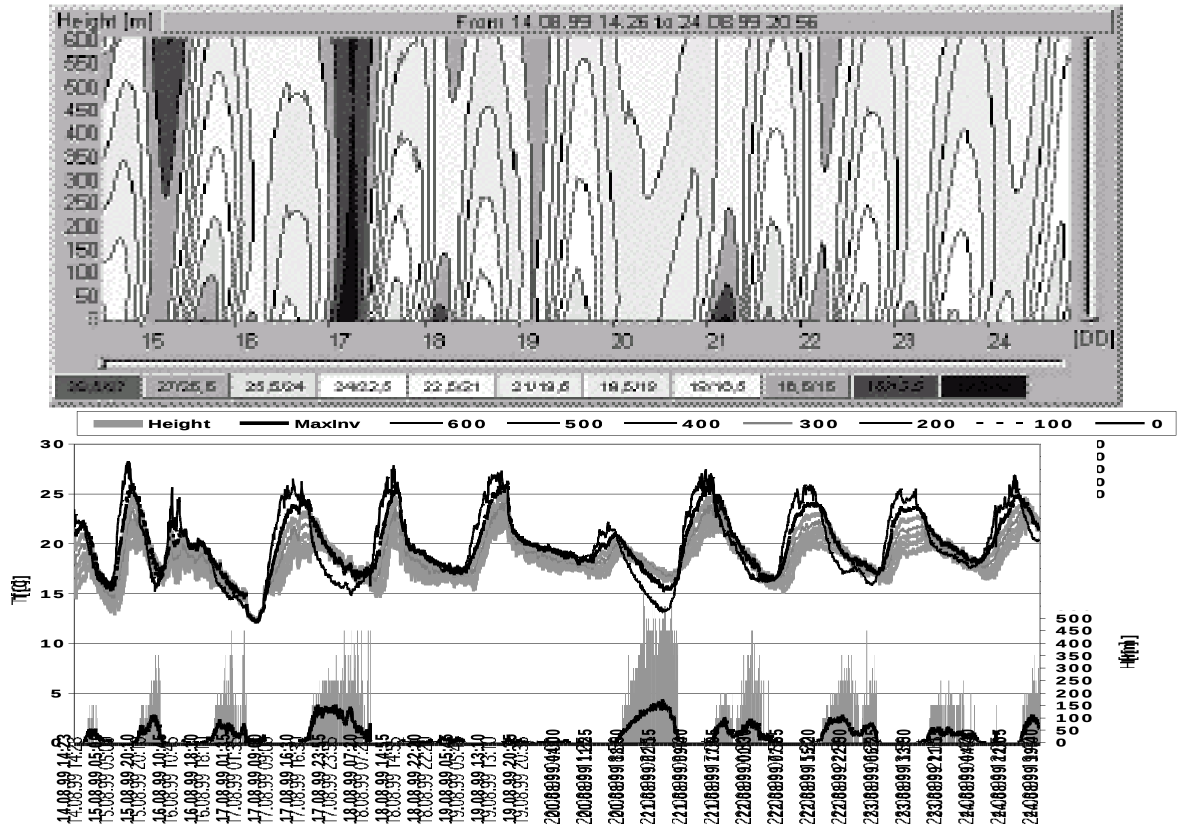

Fig. 4 Temperature time-height cross sections and temperature inversion parameters derived from MTP-5, 14.08 – 24.08.1999

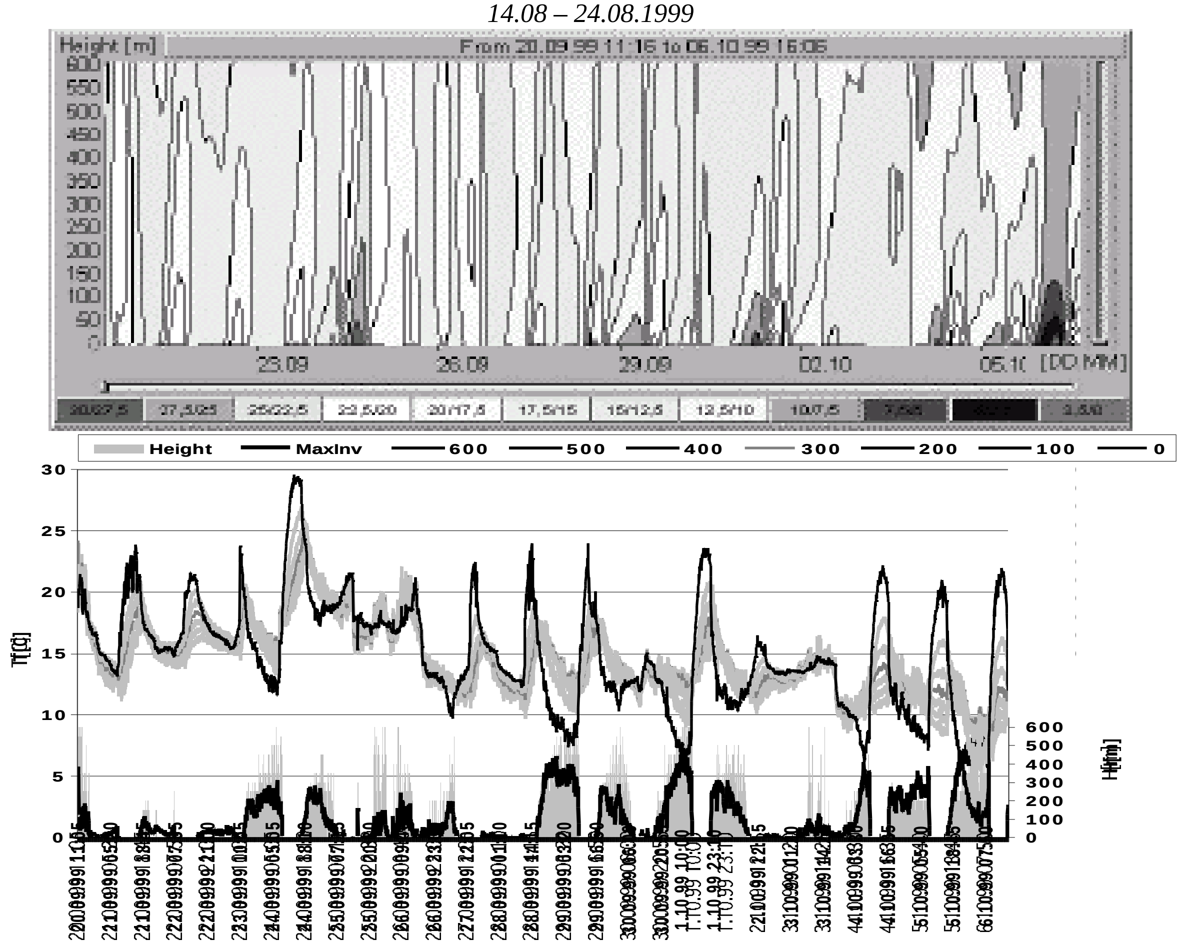

Fig. 5 Temperature time-height cross sections and temperature inversion parameters derived from MTP-5, 20.09 – 06.10.1999

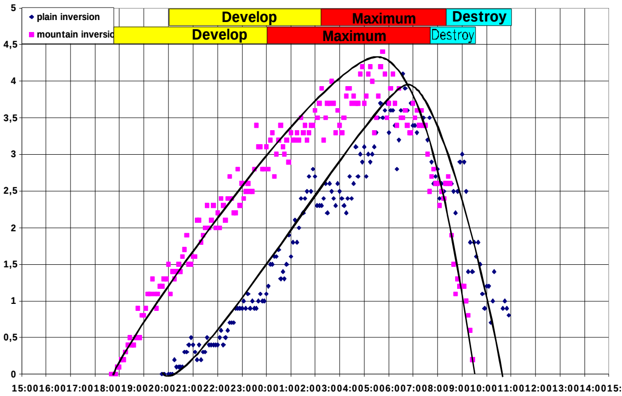

Fig. 6 Differences in temperature inversion dynamic for flat surface and for mountain region.

In Fig. 6 the difference in temperature inversion dynamics between a mountainous region and a flat surface is presented on the basis of MTP-5 data. The reason may be in inflow of cold air mass from the slopes to the valley when the zenith angle of the sun becomes large [5].

In Fig. 7 the temporal evolution of such a night time inversion (from 19:00 local time 20.08 up to 09:30 local time 21.08) is shown. The maximum temperature difference across the inversion was 4.4^{o}C and the height of the inversion base (or inversion point) was 500 m (21.08.99 05:45).

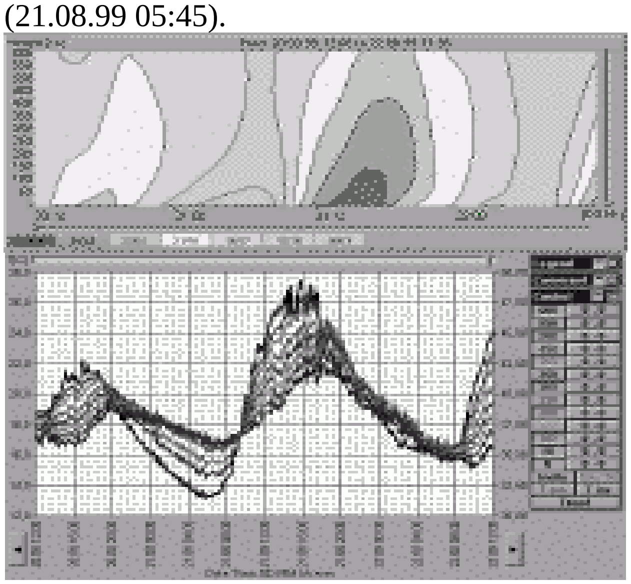

Fig. 7 Example of the temperature profiles dynamics for the observation period 20.08 – 22.08

The continuous measurements gave the possibility to calculate the total distribution of average temperatures at different heights, as well as the minimum and maximum temperatures (Fig. 8, a, b). The minimum value of temperature for all the heights was at 17.08.99 during an event of heavy rain when the

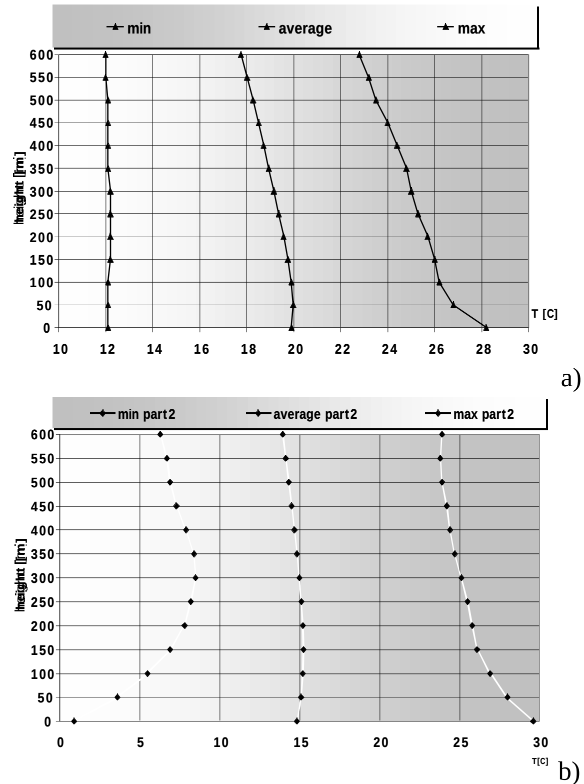

Fig. 8 Stratification of temperature calculated from MTP-5 data for the period of observation 14.08 – 24.08.1999 (a) and 20.09 – 06.10.1999 (b)

5. CONCLUSION

Continuous data of the thermal structure taken during periods of substantial change in the ABL temperature structure within a valley atmosphere were obtained by a microwave remote sensing temperature profiler. The data of this new instrument agree well with radio sonde data. The data set also includes simultaneous and co-located data from sodars and in situ sensors from a meteorological tower and will be useful for the validation and improvement of high-resolution numerical weather prediction and coupled models in mountainous terrain, which was one of the scientific objectives of MAP.

REFERENCES

1. Gajkovich K.P.; Gromov V.D.; Kadygrov E.N.; Kosov A.S. and Troitsky, A.V.: 1993, *Trans. Geosci.and Remote Sens.*, **31** No 1, 116-120.
2. Kadygrov E.N., Pick D.R.: 1998, *Meteorological Applications*, **5**, 393-404.
3. Westwater, E.R.; Han, Y.; Irisov, V.G.; Lenskiy, V.; Kadygrov, E.N. and Viazankinv, S.A.: 1999, *J. Atmosp. Oceanic Technol.*, **16**, No 7, 805-818.
4. Matsui I.; Sugimoto N.; Maksyutov Sh.; Inoue G.; Kadygrov E.; Viazankin S.: 1996, *Jpn.J. Appl.Phys.*, **35**, N 4A, 2168-2169.

7.4 Tethered balloon vs. rawinsonde and tower

7.4.1 Tethered balloon vs. tower

On 2 October 1999, a direct comparison was made between a temperature sensor and sonde 1 and sonde 4, all located at the same height (1.25 m). The result is shown in Figure 7.4-1.

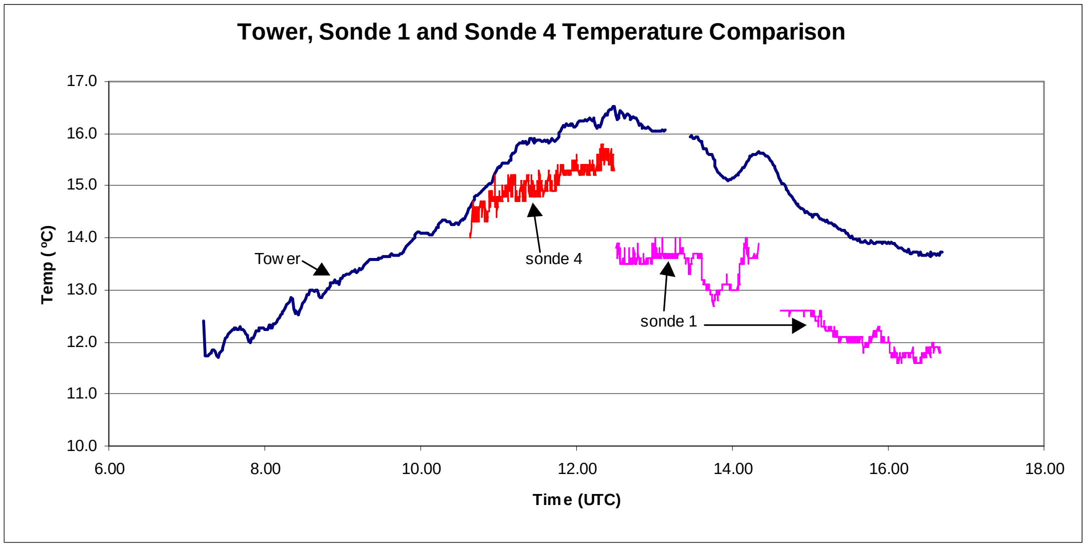

Fig. 7.4-1 intercomparison tower and sonde 1, sonde 4.

7.4.2 Tethered balloon vs. rawinsonde

A comparison between the tethersonde and rawinsonde was carried out on several occasions when the rawinsonde was released on the road near the farm (see Figure 4.4-1). The intercomparison is shown in Figures 7.4-2 – 7.4-6 (next pages). Only ascent data of the thethered balloon is shown in the figures. The variables that are compared are temperature, relative humidity, wind speed- and direction.

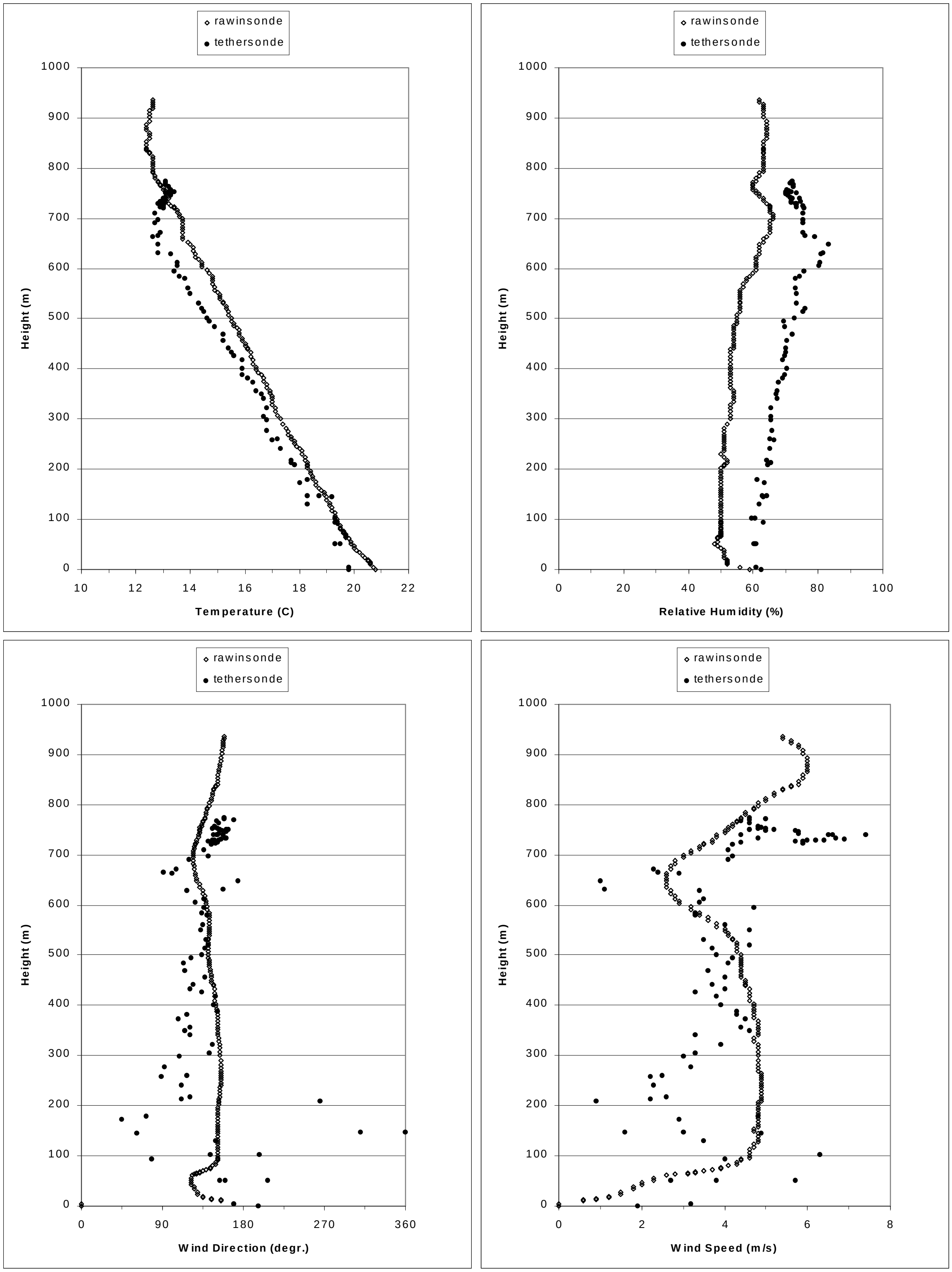

Fig. 7.4-2 intercomparison Radiosonde and Tethered Balloon for 21 September 16:00 LT; **sonde 4**

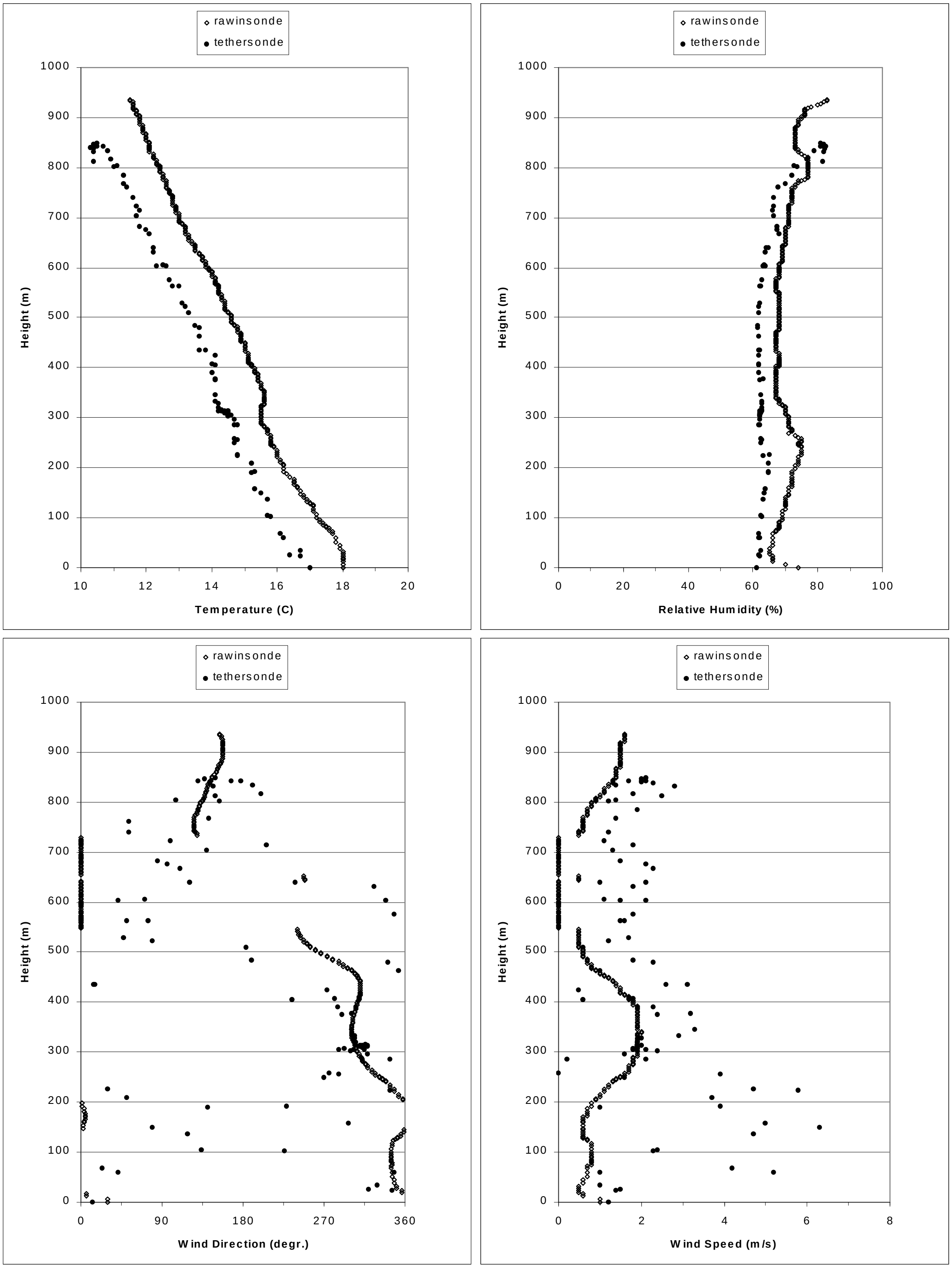

Fig. 7.4-3 intercomparison Radiosonde and Tethered Balloon for 22 September 13:00 LT; **sonde 1**

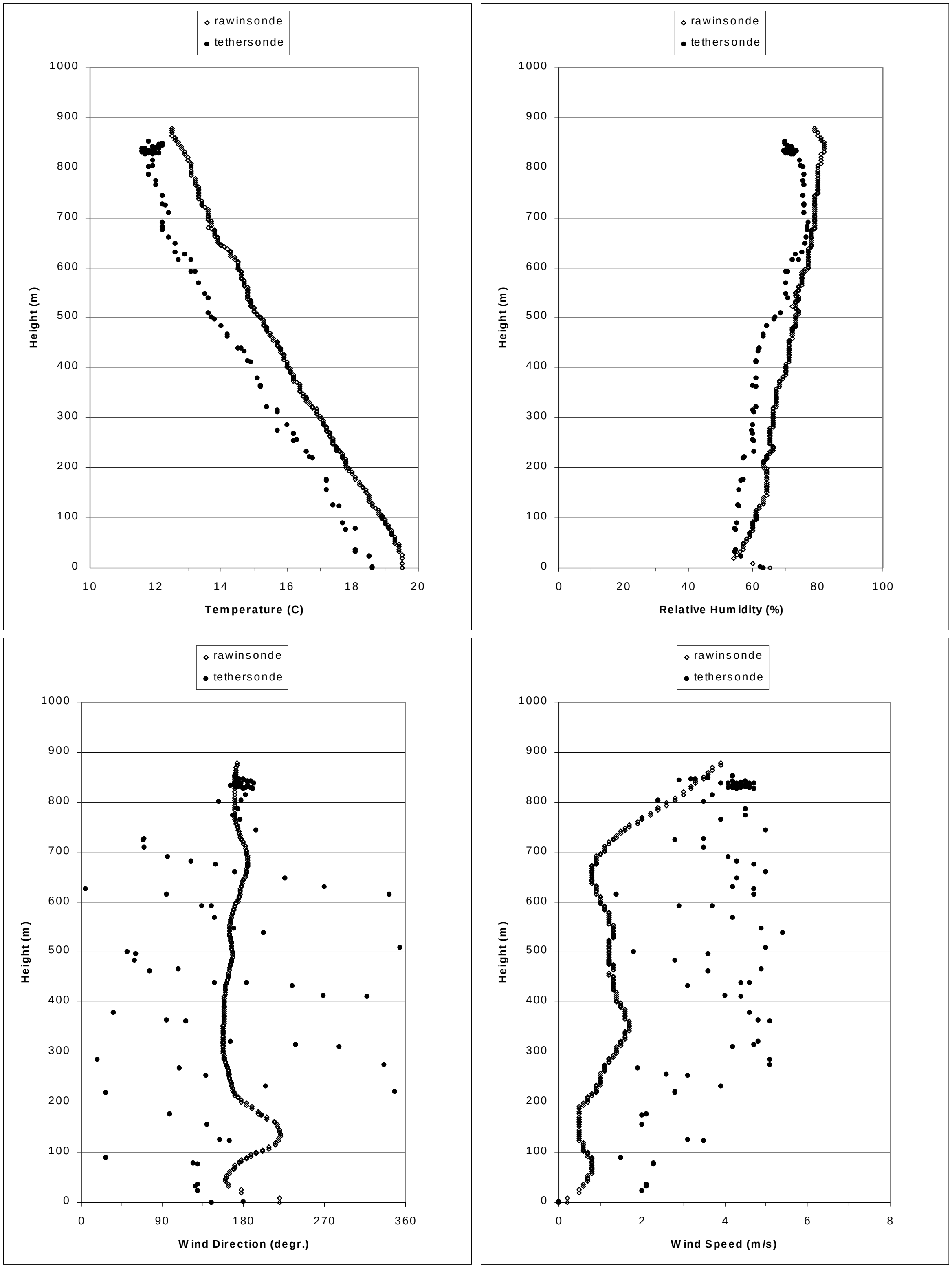

Fig. 7.4-4 intercomparison Radiosonde and Tethered Balloon for 22 September 16:00 LT; **sonde 1**

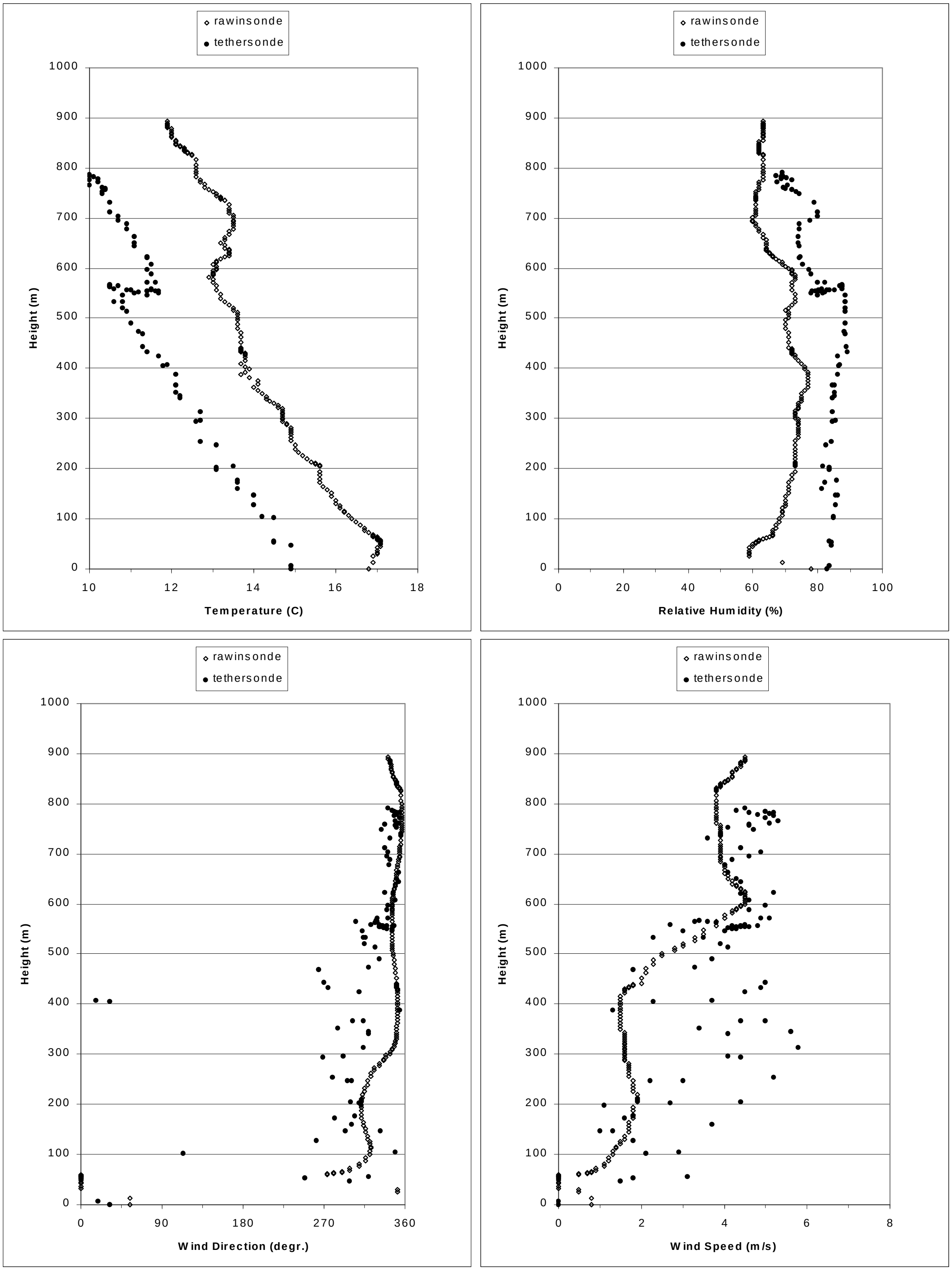

Fig. 7.4-5 intercomparison Radiosonde and Tethered Balloon for 28 September 13:00 LT; **sonde 1**

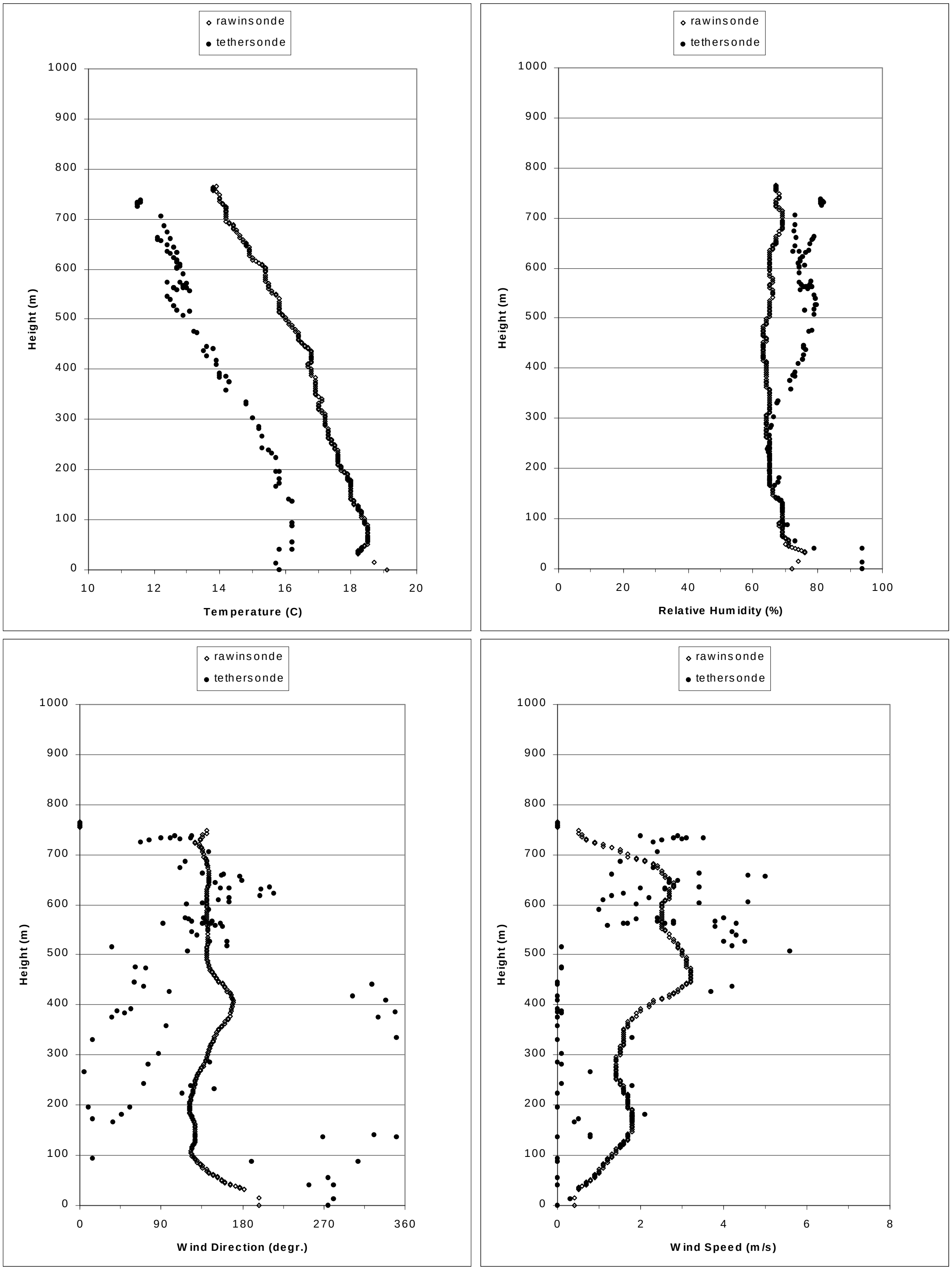

Fig. 7.4-6 intercomparison Radiosonde and Tethered Balloon for 28 September 16:00 LT; **sonde 1**

8 Periods of intensive observations (‘Flight days’)

8.1 Overview

‘Flight Days’ were those days, when the research aircraft (section 5) was available. Usually, a morning and an afternoon flight were performed. Due to reservation requirements for the aircraft the flight days fell into two periods (15 to 31 August and 20 September to 8 October 1999). They are referred to as R-IOP1 and R-IOP2, respectively. The specific days were selected in a way that days with distinctly different boundary layer characteristics should have resulted:

- ‘Fully concetive’ conditions (weak synoptic forcing, clear sky, development of a valley wind system)
- ‘Fully mechanical’ conditions (strong synoptic forcing, overcast).

Some of the flight days indeed correspond to these characteristics (Table 8-II). However, some of the flight days also must be characteriszed as ‘mixed’ (between the two above) or – with respect to boudary layer terminology – as ‘under conditions of forced convection’.

It was made sure that during a flight day as much as possible (usually more than 95%) of the permanent observations (section 3) were active. Furthermore, all the ‘special observation systems’ (section 4) were operating at least during the periods of actual flights (e.g., some noise impact problems prevented the operation of the SODARs during the night before and after the actual flight day). Details on operating times of the various special observation systems are given in the respective subsections of section 4. During R-IOP1 radio sondes were lounched every three hours according to the timetable as given in Table 8-I. Because of the fact that during R-IOP2 additional soundings were performed in support of other projects of MAP (e.g. during heavy precipitation events), release times were scheduled one hour earlier.

A summary of the eight flight days is given in Table 8-II. A total of 14 flights with approximately 45 hours of data was realised. Some mean weather characteristics during the flight days are given in the next sub-section.

	R-IOP1	R-IOP2	
Day X-1	2 pm (12 am UTC)	1 pm (11 am UTC)	RaSo #1
	8 pm (6 pm UTC)	7 pm (5 pm UTC)	RaSo #2
Day X	8 am (6 am UTC)	7 am (5 am UTC)	RaSo #3
	11 am (9 am UTC)	10 am (8 am UTC)	RaSo #4
	2 pm (12 am UTC)	1 pm (11 am UTC)	RaSo #5
	5 pm (3 pm UTC)	4 pm (2 pm UTC)	RaSo #6
	8 pm (6 pm UTC)	7 pm (5 pm UTC)	RaSo #7
	11 pm (9 pm UTC)	10 pm (8 pm UTC)	RaSo #8
Day X+1	2 am (0 UTC)	1 am (11 pm, Day X, UTC)	RaSo #9

Table 8.1-I Approximate release times for the radio sondes for **Day X= flight day** during R-IOP1. *For all the R-IOP2 soundings release times were 1 hour earlier* (so that the sonde would reach the tropopause around 0/6/12/18 UTC.

date	Flight day #	Type of day	Flight times UTC	realized patterns	failures, data coverage
21/8/99	1	~convective	7:21–10:31 14:34–17:00	T-B-A-B-T T-B-A-B-T	Full, expt H_2O Full expt H_2O
22/8/99	2	~convective	7:36–10:10 11:36–15:54	T- A-B-T T-B-A-B-A-B-T	Wind?, expt H_2O Full expt H_2O
25/8/99	3	convective	6:49–9:42 11:12–15:41	T-A-B-A-B-T T-B-A-B-A-B-T	Full Full
21/9/99	4	Mechanical	7:16–9:05 11:17–15:10	T-B-A-B T-B-A-B-A-B-A-T	Full No wind
22/9/99	5	Mechanical	6:58–9:25 11:15–13:02	T-A-B-A-T-B T-B-A-B-A-B	Full Low res. Wind
28/9/99	6	Mixed, transition from rainy period	12:02–16:14	T-B-A-B-A-B-T	Full, H_2O low quality
29/9/99	7	Convective morn. Mixed, aftern.	7:22–9:45 11:56–15:53	T-B-A-B-T T-B-A-B-A-B-T	Full Full
1/10/99	8	convective	10:33–14:09	T-B-A-B-A-B-T	Full

Table 8.1-II Summary information on the flight days. The flight patterns are described in section 5.

8.2 Meteorological conditions during Flight Days

To gain a general impression of the meteorological conditions during the 8 flight days, daily means or sums for a few parameters as observed at station Magadino (swiss topographic coordinates 711’160, 113’540; geographic coordinates 8^o 53’, 46^o 10’, altitude 197 m.a.s.l.), MeteoSwiss (the former of the Swiss Meteorological Institute), are presented in Tab.8.2-I. Symbols are as follows:

p : mean pressure
T : mean air temperature
RH : mean relative humidity
Gl : mean global radiation
ssd : sunshine duration
N : average cloud cover (all clouds)
Nh : average cloud cover (low clouds)
ff : mean wind speed

Table 8.2-I: Meteorological conditions at Magadino.

date	21.08	22.08	25.08	21.09	22.09	28.09	29.09	01.10
GPS in rs available	no	no	yes	yes	yes	yes	yes	yes
p [hPa]	991.1	992.7	995.6	986.2	993.4	986.1	990.1	986.4
T [C]	20.9	21.0	22.3	15.6	16.6	16.1	14.5	14.4
RH [%]	75	75	80	82	86	83	79	79
Gl [Wm^{-2}]	252	234	227	121	76	149	134	177
ssd [hrs]	10.6	8.4	9.6	2.8	0.1	7.0	4.8	10.4
N	0.36	0.59	0.40	0.73	0.93	0.67	0.38	0.20
Nh	0.28	0.40	0.28	0.57	0.33	0.47	0.20	0.02
ff [$m\ s^{-1}$]	1.9	1.5	1.3	1.1	1.0	2.3	1.2	1.2

In addition, daily courses of meteorological parameters as observed at the site A1, Bosco di Sotto, are presented in Figs. 8.2-1 to 8.2-8 (Note, however, total cloud amount refers to observation at the MeteoSwiss station of Magadino).

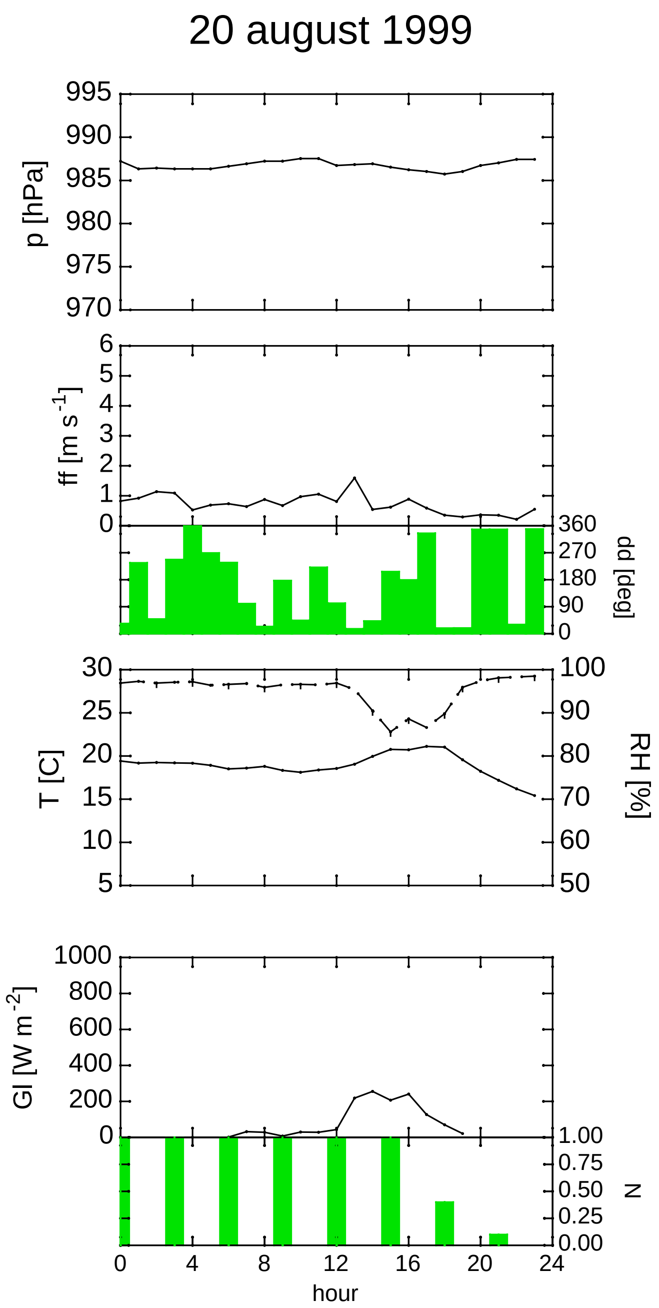

Fig. 8.2-1: Daily course of meteorological parameters at site A1, Bosco di Sotto, on August 20, 1999. p: pressure [hPa]; ff: wind speed [m s^{-1}]; dd: wind direction [deg]; T: temperature [C] (continuous line); RH: relative humidity [%] (dashed line); Gl: global radiation [W m^{-2}]; N: total cloud amount (as observed at the MeteoSwiss station of Magadino).

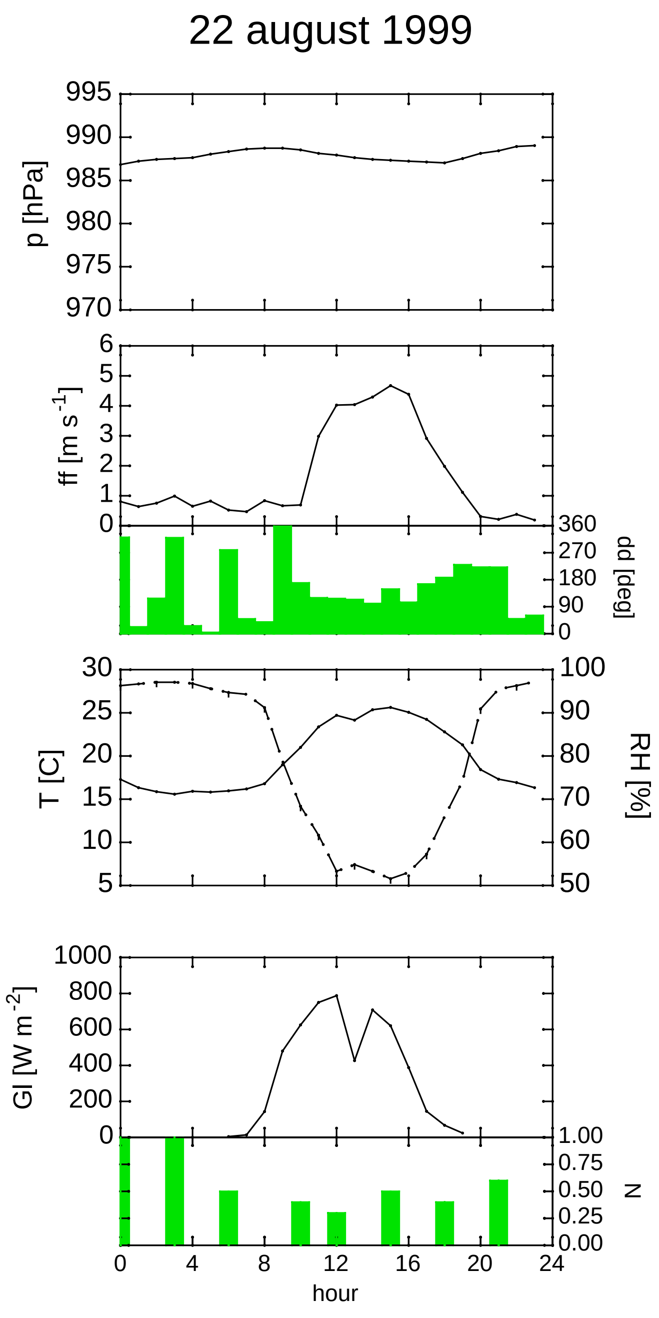

Fig. 8.2-2: Same as for Fig. 8.2-1, but for August 22, 1999.

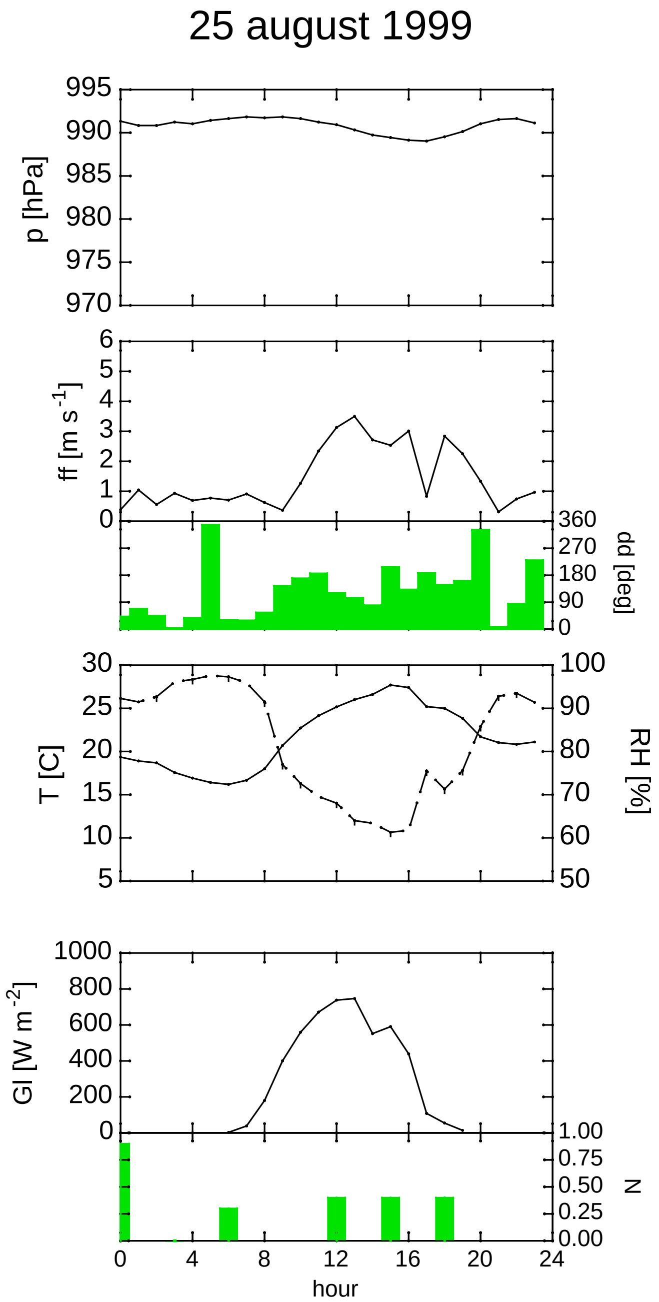

Fig. 8.2-3: Same as for Fig. 8.2-1, but for August 25, 1999.

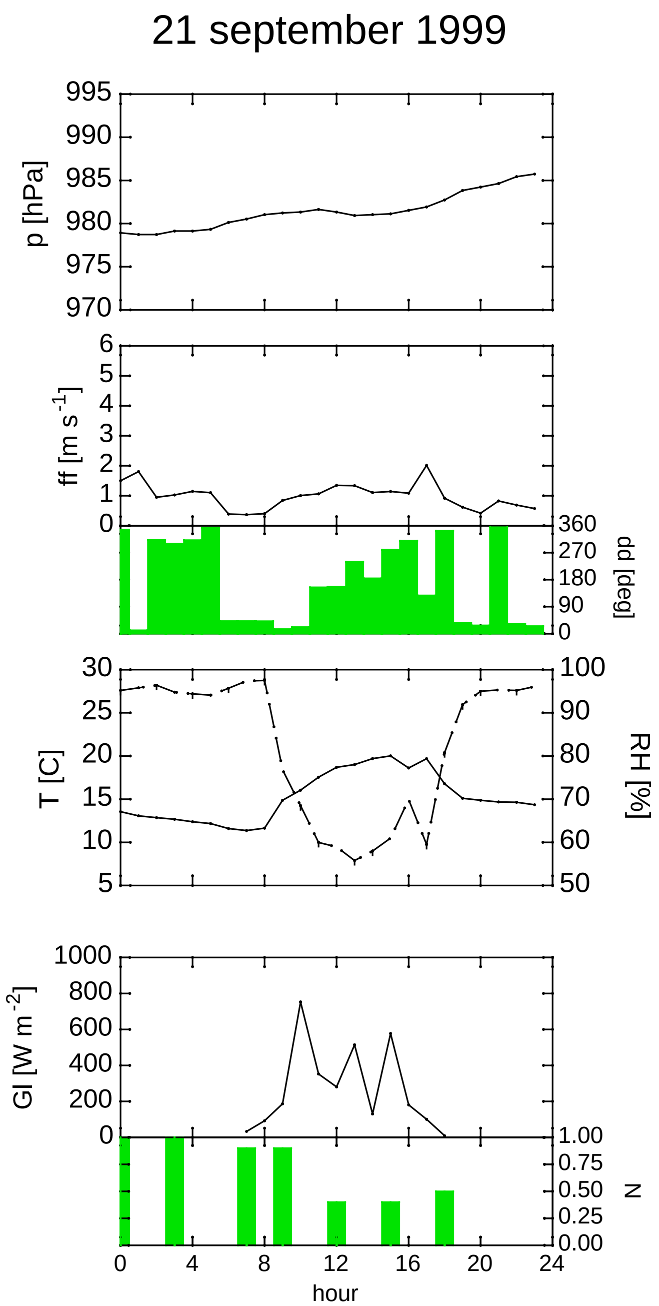

Fig. 8.2-4: Same as for Fig. 8.2-1, but for September 21, 1999.

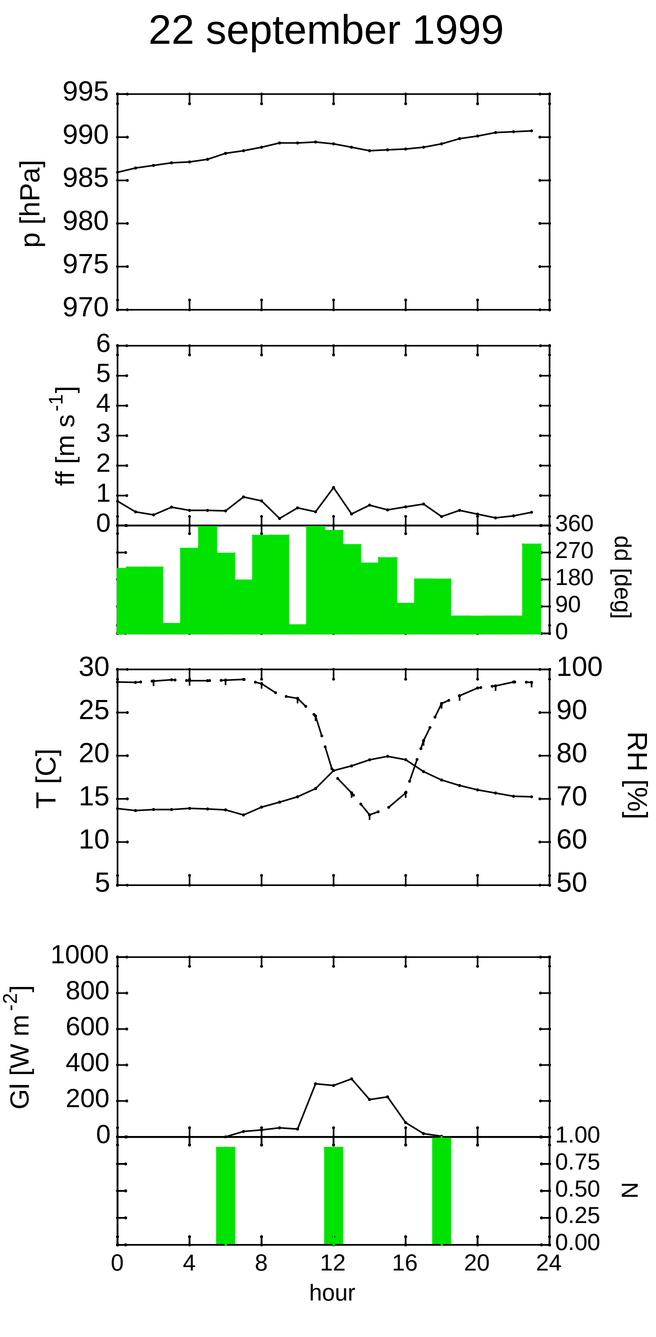

Fig. 8.2-5: Same as for Fig. 8.2-1, but for September 22, 1999.

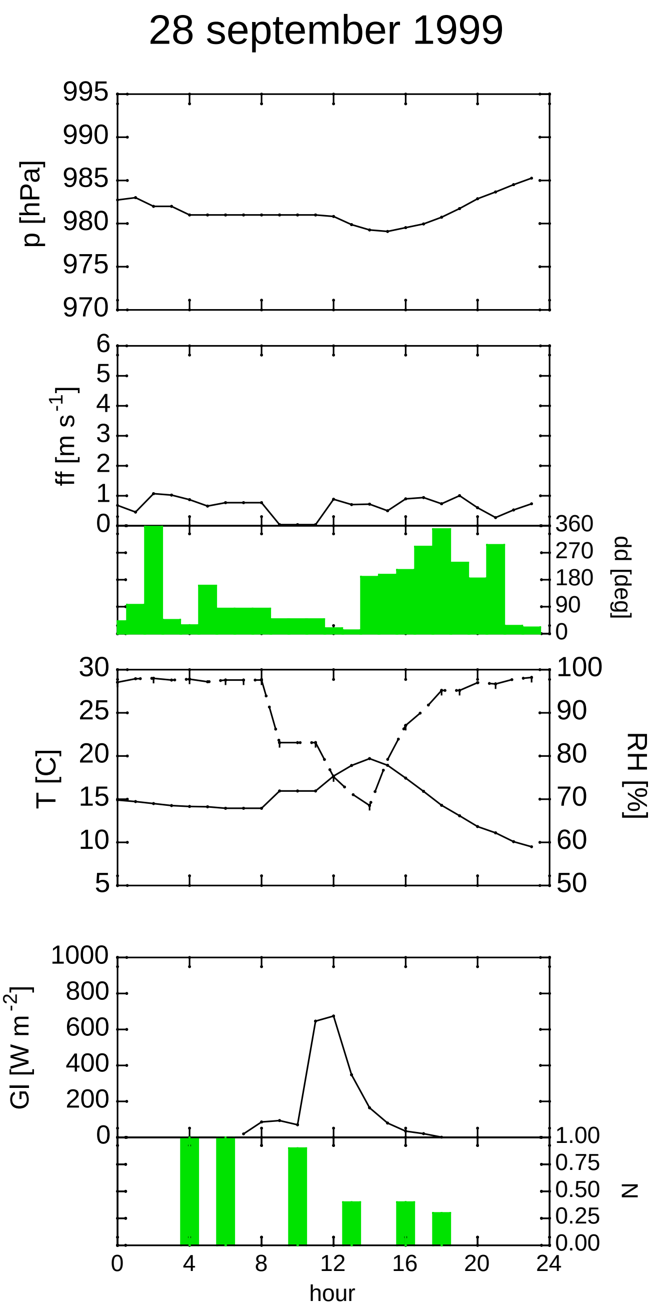

Fig. 8.2-6: Same as for Fig. 8.2-1, but for September 28, 1999.

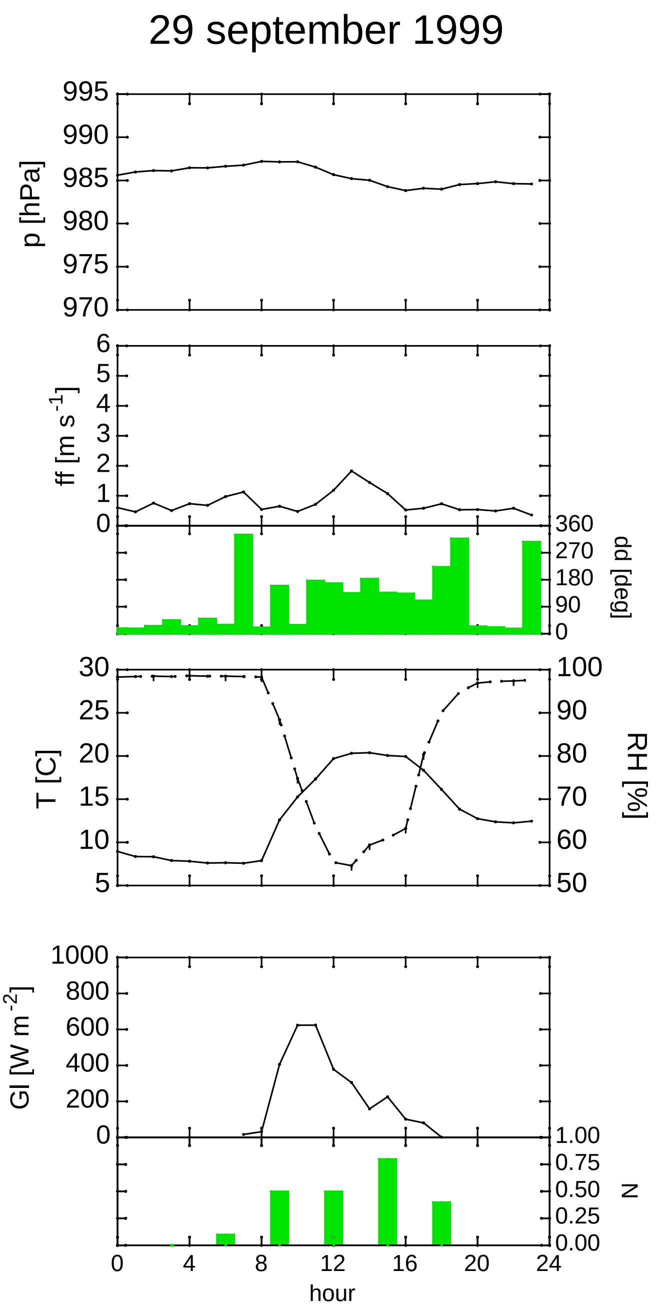

Fig. 8.2-7: Same as for Fig. 8.2-1, but for September 29, 1999.

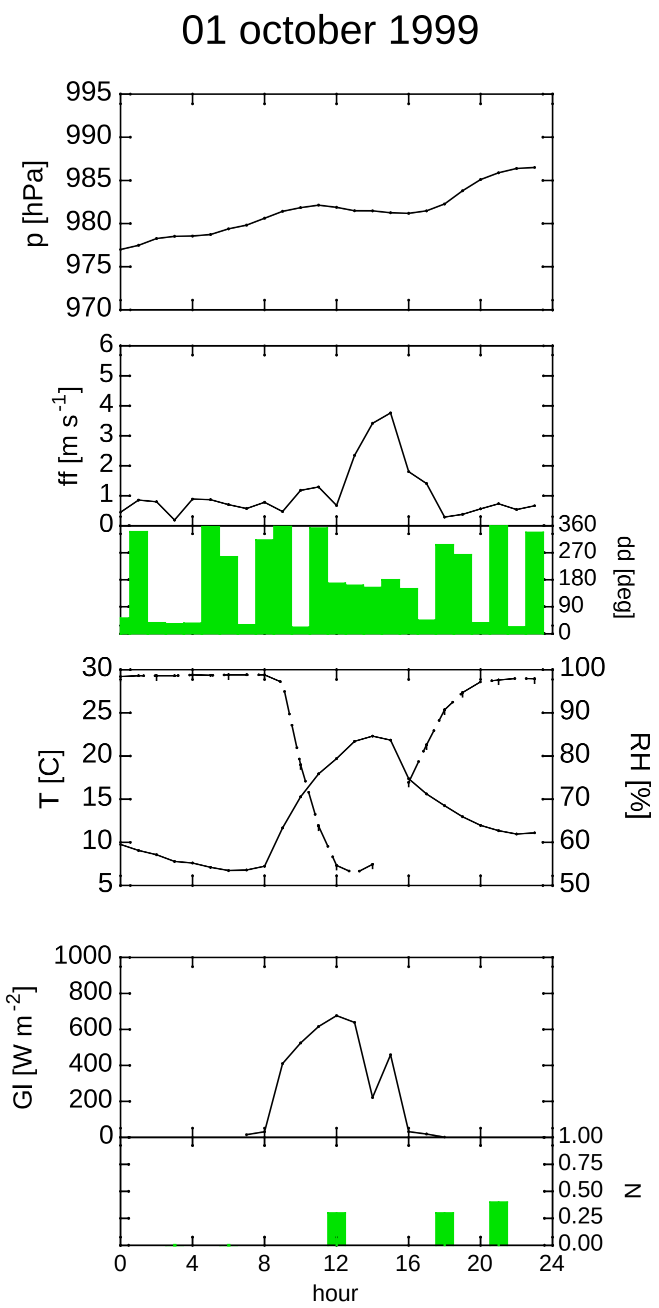

Fig. 8.2-8: Same as for Fig. 8.2-1, but for October 1, 1999.

Acknowledgements

Many individuals and institutions have greatly contributed to the success of the MAP-Riviera project. Funds were available from the Swiss National Science Foundation (grants # 21-54060.98 and 21-55874.98), grants from the Natural Sciences and Engineering Research Council of Canada to D.G. Steyn and the European Joint Research Centre (JRC) in Ispra (I). The support of the local authorities of Claro, Switzerland and in particular Mr. Pellegrini, for their support before and during the observational campaign is greatly acknowledged.

The passive microwave temperature profiler (MTP-5) was made available for the project by *Kipp&Zonen B.V.* (Delft, The Netherlands) through the kind intervention of *markasub AG* (Basel, Switzerland) and *Meteodat GmbH* (Zürich, Switzerland). The possibility to use and test this instrument under field conditions added substantial value to the overall data set. The success of this activity was primarily due to the experts of *ATTEX Ltd.* (Moscow, Russia), the company that has originally developed the instrument.

We are indebted to Forschungszentrum Karlsruhe (Dr. N. Kalthoff) and to Paul Scherrer Institute (Dr. M. Furger) for lending us a number of sonic anemometers.

Karl Schroff and Hansjürg Frei from ETHZ, as well as Valentino Bada and N. Cao from JRC were the key people in the preparation, construction and maintenance of all the countless surface towers, the instrumentation and the necessary facilities. Without their engagement nothing would have been as it was!

Many thanks go to a large number of students and other individuals who helped in the field to operate and maintain the instrumentation, download the data and operate the radio sounding system: Alessia Bassi, Sven Bethke, Shari Carlaw, Martin Dippon, Christian Feigenwinter, Andi Felber, Claudius Heinemann, Sebastian Hoch, Florian Imbery, Peter Keller, Nicolas Matzinger, Eliane Müller, Mathias Müller, Paul Müller (from the workshop of MCR-Lab), Oliver Rahs, Mélanie Raymond, Simone Regazzi, Jan Sedlacek, Sonia Seneviratne, Heidi Weber, Simon Zimmermann.

The good collaboration with MetAir and in particular with Bruno Neininger and Willy Fuchs is highly appreciated and greatly contributed to the success of the aircraft operations during the MAP-Riviera field campaign.

We would like to express our gratitude to the OFIMA SA, to the VERZASCA SA to the FFS and to the AET Bellinzona for sending the daily data of the water level in their storage reservoirs during the whole intensive measurement phase.

Address list RIVIERA project

Climate Research ETH
Swiss Federal Institute of Technology (FAX) +41 1 362 51 97
Winterthurerstr. 190
CH – 8057 Switzerland

Mathias Rotach	rotach@geo.umnw.ethz.ch	+41 1 635 52 22
Pierluigi Calanca	calanca@geo.umnw.ethz.ch	+41 1 635 52 22
Achim Gurtz	gurtz@geo.umnw.ethz.ch	+41 1 635 52 28
Marco Andretta	andretta@geo.umnw.ethz.ch	+41 1 635 52 42
Alexandra Weiss	weiss@geo.umnw.ethz.ch	+41 1 635 52 08
Massimiliano Zappa	zappa@geo.umnw.ethz.ch	+41 1 635 52 27

UBC (University of British Columbia)
Department of Earth and Ocean Science (FAX) (604) 822-6150
1984 West Mall
Vacouver B.C.
CANADA V6T 1Z2

Douw Steyn	douw@geog.ubc.ca	+604 822 64 07
Stephan de Wekker	dewekker@geog.ubc.ca	
Magdalena Rucker	rucker@geog.ubc.ca	(604) 822-2663

JRC (European Joint Research Centre)
Environment Institute (FAX)+39 0332 78 54 66
Commission of the European Communities
21020 Ispra (VA)
Italy

Giovanni Graziani	giovanni.graziani@jrc.it	+39 0332 78 92 95
Stanislaw Cieslik	stanislaw.cieslik@jrc.it	
Richard Conolly		+39 0332-78 53 53

MCR-LAB
University of Basel (FAX) +41 61 272 69 23
Spalenring 145
CH – 4055 Basel

Roland Vogt	vogt@ubaclu.unibas.ch	+41 61 272 65 64
Eva van Gorsel	Eva.Gorsel@unibas.ch	
Andreas Christen	andreas.christen@unibas.ch	

MetAir (GmbH)

Bruno Neininger	metair@zugernet.ch	
phone and FAX		+41 41 755 38 04